FOG

Freiberg Online Geology

FOG is an electronic journal registered under ISSN 1434-7512

2008, Volume 20



Cornelia Härtig

Mobilisation of Arsenic in the low-flow regime of groundwaters in Bangladesh

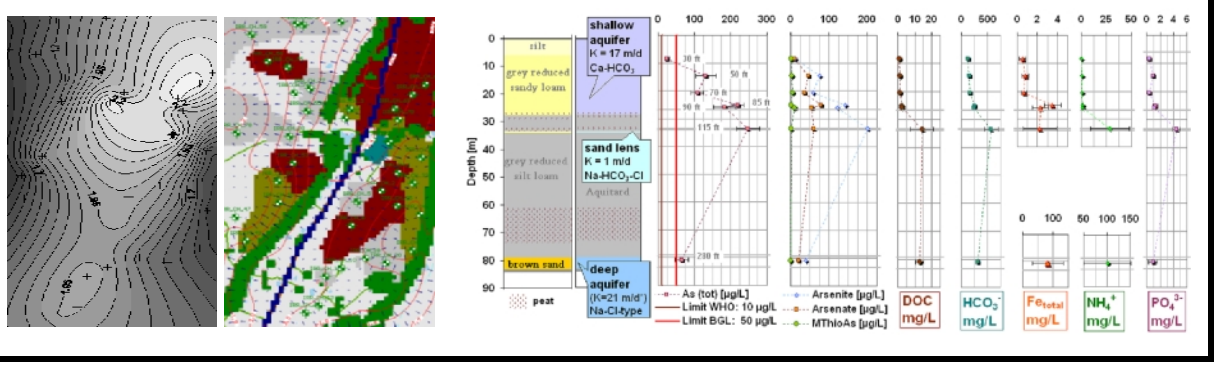

150 pages, 89 figures, 26 tables, 50 references

ACKNOWLEDGEMENTS

First of all I would like to thank my supervisors Prof. Dr. Broder J. Merkel and Prof. Dr. Britta Planer-Friedrich to enable my stay in Bangladesh, where I gained a lot of hydrogeological field experience, but concurrently came in touch with a another culture. Consultations during field work as well as the collaboration whilst data analysis and interpretation was very supportive at any time.

Further, I have to thank Prof. Dr. Md. Qumrul Hassan and Prof. Dr. Mahmood Alam, who supervised me and supported my work during my stay at Dhaka University in Bangladesh. I am deeply indebted to the geologists Md. Rashe Dun Nabi, Md. Baharul Alam Biswas, Md. Arifeen Hossain, and Masud Khan for their support during field work and equipment arrangement, as well as to Md. Shah Alam from the hydrogeological laboratory at Dhaka University for providing distilled water and other needy equipment. Special thanks goes to Anwar Zahid, who established the contact to engineering and survey companies and provided other supportive information. Thanks to Mr. Monir and his staff for managing equipment during pump tests and to Mr. Rahman and his staff for performing the levelling. I have to thank the caretakers at the hospital, Amim and Shadjahan, for allowing the over-night stay in their flat since middle of September 2007. Thanks to Dr. Hrob, who offered a lockable flat for housing and equipment storage at Titas health complex since middle of October 2007, which distinctly facilitated field work. Thanks to Thorsten Oertel, who faced much trouble with tracking the replenishment packages, which got stuck in in the customs office. Special thanks to Rashed and his whole family, Bahar, Smruti, Sven, Darren, Laura, Towheed, Thani, and Chompa, for many enjoyable moments together in Bangladesh.

I much appreciate the help of Dipl. Chem. H. J. Peter and Dr. Sascha Kummer during analysis work at the laboratory of the Hydrogeology Department, Freiberg University. Thanks to Heidi Lissner and Jörg Steinborn for providing their data and countless brainstorming sessions during data interpretation. Thanks to Elke Süß, who gave good hints for data handling and analysis.

Special thanks to my dear companion Sven Sieber, not only for fully supporting my decision to perform the master thesis in Bangladesh, but also for visiting me there and all his good hints, love and patience whilst I wrote down the results. Last but not least, I thank my dear family, in particular my parents and Wilhelm Peters, for supporting me over the entirety of my studies.

TABLE OF CONTENTS

LIST OF TABLES

LIST OF FIGURES

LIST OF APPENDIXES

APPENDIX A – FIGURES AND TABLES (HARDCOPY)

APPENDIX B – EXPERIMENTAL DATA (DIGITAL)

APPENDIX C – OTHER DATA SOURCES (DIGITAL)

APPENDIX C1 Results Steinborn (2008)

APPENDIX C2 Results Lissner (2008)

APPENDIX C3 Climate data

APPENDIX C4 Photometry (HACH manuals)

LIST OF ABBREVIATIONS

A	area, e.g. [m^2]
AET	actual evapotranspiration, calculated [mm/year]
EVT	evapotranspiration, as input parameter in Visual Modflow [mm/year]
ASD	absolute standard deviation
BD	Bangladesh
BGS	British Geological Survey
BP	before present, the year 1950 represents the origin of this age scale
DPHE	Department of Public Health and Engineering, Bangladesh
EC	electric conductivity [µS/cm]
Ed	Editor
Eds	Editors
GSB	Geological Survey of Bangladesh
K	hydraulical permeability, e.g. [m/s], [m/d]
MQ	"Milli-Q" = purified water
PE	potential evaporation, calculated
Q	flow rate per time interval, e.g. [m^3/s], [L/s]
RSD	relative standard deviation [%]
RCH	recharge, as input parameter in Visual Modflow [mm/year]
US EPA	United States Environmental Protection Agency
USDA	United States Department of Agriculture
V	volume, e.g. [m^3], [L]
WHO	World Health Organisation

ABSTRACT

Investigations regarding hydraulical properties of the subsurface and a two-weekly monitoring of the hydrochemistry at seven piezometers at Titas/Daudkandi, Bangladesh, were carried out between September throughout December 2007 in the framework of a project founded by the German Research Foundation (DFG). The subsequent data analysis moreover includes results of sedimentary analyses and monitoring data of two preceding surveys executed between February throughout July 2007 at the Titas's test site wells.

At Titas, a shallow grey reduced sandy aquifer down to 28 m depth is separated by a huge clay-rich grey reduced aquitard, from a leaky to confined deeper aquifer below 81 m depth. The latter showed partially reddish-brown sandy sediments, indicating they had undergone oxidative weathering in the past. Total Arsenic concentrations detected with ICP-MS exceeded the WHO guideline value (10 µg As/L) in all seven piezometers, but varied distinctly with depth. Arsenite, Arsenate, and even Monothioarsenate were detected with AEC-ICP-MS, whereas the more mobile and most toxic Arsenite represented the predominant species in all depths. Highest As values were detected in the deeper shallow aquifer wells near to and in a sand lens encased within a peat-bearing aquitard layer. The occurrence of high dissolved Fe and Mn concentrations, and significant positive correlations of As with Fe, P, DOC, TIC, H_2CO_3, NH_4^+ over depth in the Ca-HCO_3-type groundwaters of the five shallow aquifer wells indicate reductive dissolution of iron (hydr)oxides during organic matter degradation as major process, triggering As-release to groundwater. Nevertheless, results from the sand lens point out that dissolution of As and Fe may be decoupled.

On-site P-spike experiments, reaching maximum added concentrations of 2.3 mg PO_4^{-3}/L in groundwaters, showed that no Arsenic could be released by competitive sorption with the connatural Phosphate anion from sediments in 25 m depth. Also positive significant correlations between As and P indicate a common underlying release mechanism.

Modelling with Visual Modflow emphasized that evapo(transpiration)ration mainly controls water table decline after monsoon season. Thereby, irrigation activities significantly enhance, whereas artificially elevated village and street basements distinctly inhibit direct evapo(transpi)ration from groundwater.

High potential hydraulical permeabilities of 17 m/d in the shallow aquifer were calculated, indicating that recent intense water withdrawals have the potential to significantly alter and accelerate water exchange processes in a natural low-flow aquifer system. Accelerated intrusion of waters during dry season led to distinctly decreasing mineralisation of 115 ft-waters, accompanied by an increase in As-concentrations.

The distinct depth-depending co-increase of As and DOC within groundwaters, related to peat-deposits below 27 m depth, indicates that an accelerated shift of young organic carbon to deeper strata may not play a significant role for As-mobilization at Titas. But, it may indicate that As and organic Carbon were co-deposited.

A seasonal, slight increase of As was detected during the first half of the year for four of the monitored wells. This may be an indicator for seasonal variation trends. Nevertheless, reliable conclusions only can be achieved by continual long-term monitorings over several years.

Slightly acidic pH, extremely high Fe, NH_4^+, elevated DOC, As and P concentrations in the deep aquifer groundwaters appear to be linked to reductive dissolution processes in the huge peat deposit within the overlying aquitard layer. Relatively low As-concentrations compared to dissolved Iron in the deep groundwaters indicate that As after its release, partially may be re-adsorbed on pH-dependent surface-sites of kaolinite detected within the aquitard, or on solid reddish-brown iron hydroxides within the deep aquifer.

Altogether, everything points on predominantly natural causes behind Arsenic mobilization. At Titas irrigation eventually may worsen the situation by enhanced shift of As-polluted waters to more shallow strata.

1 OBJECTIVES AND DELIVERABLES

1.1 Objectives

Hydraulical considerations:

- Detecting the temporal fluctuations and screen-depth dependent variations of water tables at the test site, as well as the spatial variations of hydraulic heads at the investigation area Titas/Daudkandi
- Establishing a conceptual model of the aquifer system and its features at the test site
- Establishing a digital flow model of the subsurface that describes hydraulical conditions at the investigation area Titas/Daudkandi and gives information about factors controlling groundwater flow and water table subsidence in the post-monsoon season.

Considerations regarding groundwater chemistry in relation to Arsenic:

- How do the chemical conditions at the test site vary with depth regarding Arsenic mobilisation?
- Are there significant seasonal changes or trends observable for Arsenic and other water quality parameters in different depths at the test site.
- Evaluation of the influence of Phosphorus on Arsenic chemistry.
- What effect do short time water withdrawals show on water chemistry?

1.2 Deliverables

Hydraulical Investigations:

- Conducting regular water table measurements at the test site, as well as positioning and levelling of well heads and water tables at irrigation and test site wells at Titas/Daudkandi.
- Conducting pumping tests at test site wells for evaluation of transmissivity and hydraulical permeability in different aquifer strata

- Calculating hydraulical permeabilities based on grain size distribution data from Lissner (2008)
- Evaluating litholog data regarding the subsurface structure at the test site
- Establishing contour maps of land surface and water table elevation, as well as feature maps of the land surface at Titas/Daudkandi (TNTmips 2007-73, Surfer8)
- Estimation of the flooding conditions in 2007 and of seasonally changing climate factors like precipitation, potential evaporation, and actual evapotranspiration.
- Establishing the digital flow model (steady state) with Visual Modflow 3.0, based on the afore encountered information.

Investigations regarding general groundwater chemistry and arsenic mobilisation:

- Regular chemistry monitoring of the test site wells in Titas/Daudkandi, which included the measurement of on-site parameters (pH, E_H, EC, O_2, T, alkalinity, acidity, Fe(tot), Fe(II), Mn(tot), Mn(II), S^{2-}, NO^{2-}, NO^{3-}, NH_4^+), and the collection of water samples for ICP-MS (As/P-totals), AEC-ICP-MS (As/P-species), IC (cations, anions), TIC/DOC.
- On-site injection spike test with Phosphorus at one test site well.
- Analysis of water samples (except As/P-totals/-species) at the laboratory of the department for hydrogeology at TU Freiberg, peak detection (OriginPro7.5, WinPeak) and calculation of the concentrations of all determined water constituents.
- Calculation of the ionic balance error (PhreeqC), conductivity check and evaluation of errors that might have occurred during sampling and the consecutive analyses
- Determination of groundwater types as well as interpretation of the data, mainly regarding controls behind Arsenic mobilisation

2 INTRODUCTION

2.1 General overview on the Arsenic crisis in Bangladesh

The groundwaters in widespread areas of Bangladesh show a severely high load of Arsenic. Partly the concentrations are far exceeding international (WHO) and national guide concentrations set at 10 respectively 50 µg As/L. Approximately 30 to 35 million people in the country are exposed to this health hazard called Arsenicosis that can lead to severe skin cancers and skin disorders like keratosis and pigmentation changes. The left map in Figure 1 demonstrates which areas are effected most (Smedley and Kinniburgh, 2001).

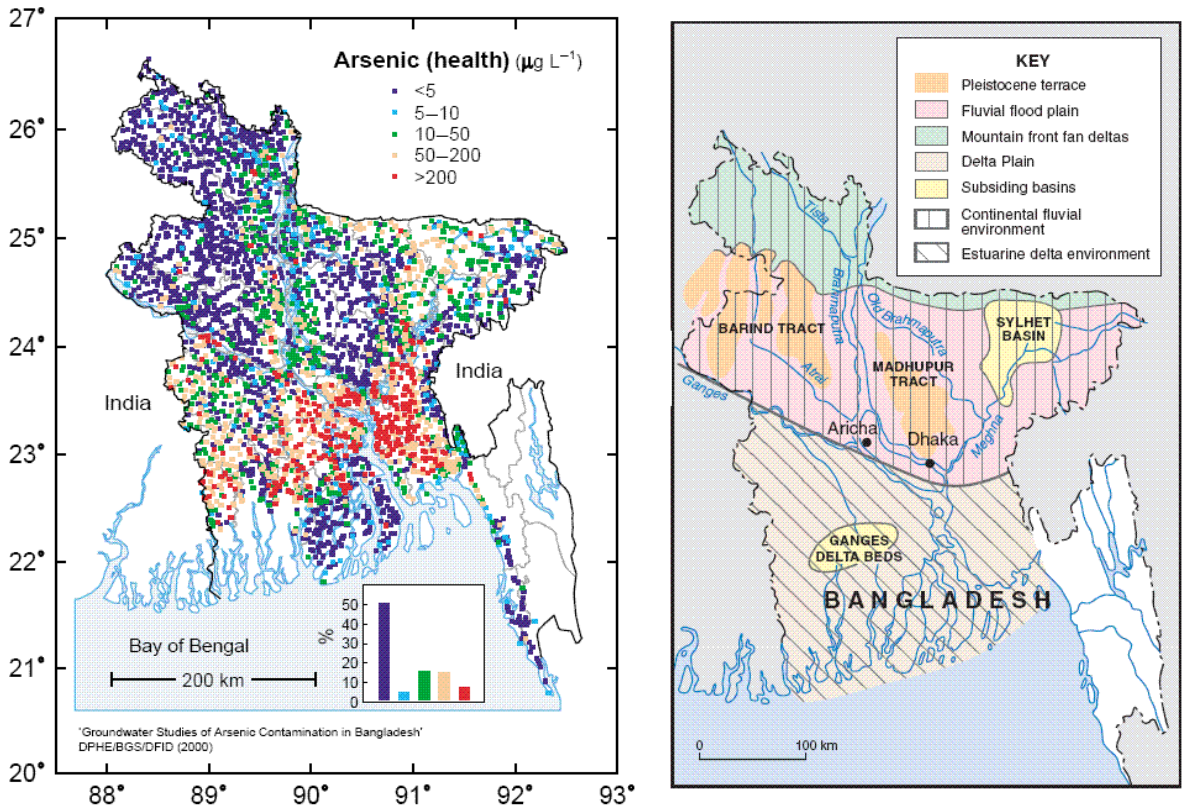

Figure 1 *left: Map showing the concentration of arsenic in groundwaters, based on the DPHE/BGS hydrochemical survey. Class divisions are chosen on the basis of health criteria in Bangladesh; right: Geomorphologic units of Bangladesh (Kinniburgh and Smedley, 2001)*

The utilization of groundwater for public water supply first developed since the 1970's, serving as alternative for pathogenous contaminated surface waters that caused cholera and dysentery (Burgess and Ahmed, 2006). Arsenicosis-related health problems were identified in Bangladesh around 1993, but earlier in West Bengal (India) in the 1980's. This points out that high Arsenic

loads in groundwater constitute a primarily unforeseen problem, occurring in the entire Bengal Basin, where nowadays humans heavily rely on groundwater for public and private water supply (Smedley and Kinniburgh, 2001).

2.1.1 Arsenic in the (hydro)geological and (hydro)geochemical context

The Bengal basin forms one of the worlds largest sedimentary basins and has accumulated a great thickness of Tertiary and Quaternary clastic sediments that underlie the floodplains of the Ganges-Brahmaputra-Meghna river system. The sediments have their origin either in the Himalayan catchments or derived from basement complexes in the northern (Shillong Plateau) and western (Indo-Burman Ranges) parts of Bangladesh.

The right map in Figure 1 shows a top view of the principal geomorphologic units of Bangladesh, mainly consisting of Holocene age mountain front fan deltas in the north, fluvial plains in the central part and delta plains in the south. Mentionable exceptions within the fluvial plains are the remnants of uplifted blocks of Pleistocene age that existed during sea-level low stands, namely the Barind and Madhupur tract. The section through north-east Bangladesh in Figure 2 shows that the Madhupur clay is underlain by the Plio-Pleistocene Dupi Tila sand aquifer and adjacent to the incised Chandina and Dhamrai Formations beneath the huge river floodplains (Ravenscroft et al., 2001), (Smedley and Kinniburgh, 2001), (Burgess and Ahmed, 2006).

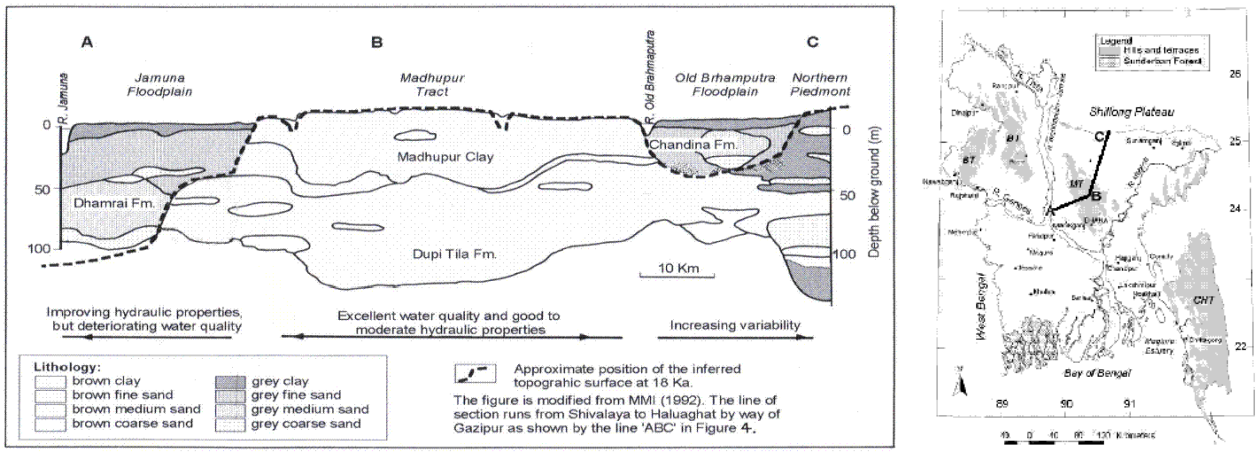

Figure 2 *left picture: Simplified geological section through north-east Bangladesh, right picture: location of the section A-B-C in Bangladesh (Ravenscroft et al. 2001, Ravenscroft et.al. 2005)*

The aquifer distribution and its water quality is strongly influenced by river incision and infilling, which occurred in response to glacial-eustatic sea level changes in the Quaternary. Bangladesh's aquifers in general show transmissivities in the range of 1000 to 5000 m^2 per day, whereas highest

values are found beneath alluvial floodplains. The sediments of Holocene aquifers show high permeabilities of 40 to 80 m/d and a high specific yield, but feature low hydraulic gradients. The Pleistocene Dupi Tila formation is an important leaky-to-confined aquifer, used for irrigation and water supply. In contrast, the Madhupur and Barind clay feature only a low vertical and horizontal permeability and low specific yields (Ravenscroft et al., 2001).

Wells tapping the uplifted Pleistocene Dupi Tila sand aquifer (situated beneath Madhupur Tract, see in Figure 1) show low Arsenic concentrations (< 10 µg/L). Its sediments mainly consist of quartz and plagioclase feldspar and were thoroughly oxidized after their deposition. The efficient oxidation process resulted from relative high hydraulic gradients that allowed an intensive flushing of the sediments. Increasing hydraulic gradients in turn were due to gradually decreasing sea levels in the late Pleistocene age. Lowest sea levels occurred approximately 18,000 years B.P. and exposed Pleistocene and late Tertiary sediments to an extensive surface erosion (Burgess and Ahmed, 2006), (Acharyya et al., 2000). Furthermore, sand aquifers deeper than 150 to 200 meters feature generally low As concentrations (< 5 µg/L) too. Burgess and Ahmed (2006) assume that these sands also were deposited during Pleistocene age. But the assumption could not be proven yet, due to the fact that any age-indicating, formerly overlaying clay aquitards probably were eroded during the aforementioned times of lower base levels (Burgess and Ahmed, 2006).

In contrast, the Arsenic affected aquifers, namely the Chandina and Dhamrai Formation, are generally shallow, i.e. their depth is less than 100 to 150 m. They are composed of recent alluvial or deltaic Holocene sediments, mainly micaceous sands, silts, and clays, accompanied by layers of solid organic matter. The sediments were buried rapidly after their deposition and show a grey to dark grey coloration, suggesting reducing conditions. Due to the low hydraulic gradients in the aquifer it can be assumed that an intensive flushing and oxidation of its sediments accompanied by the mobilisation of adsorbed trace elements did not occur. Aquifer sediments in the most affected areas are confined by a top layer of clay or silt, a fact that additionally benefits the development of reducing conditions (Ravenscroft et al., 2001), (Smedley and Kinniburgh, 2001). On the other side, wells tapping depths of less than 5 m, are commonly Arsenic-free (Burgess and Ahmed, 2006). The aforementioned variations of the Arsenic concentrations with depth demonstrates Figure 3.

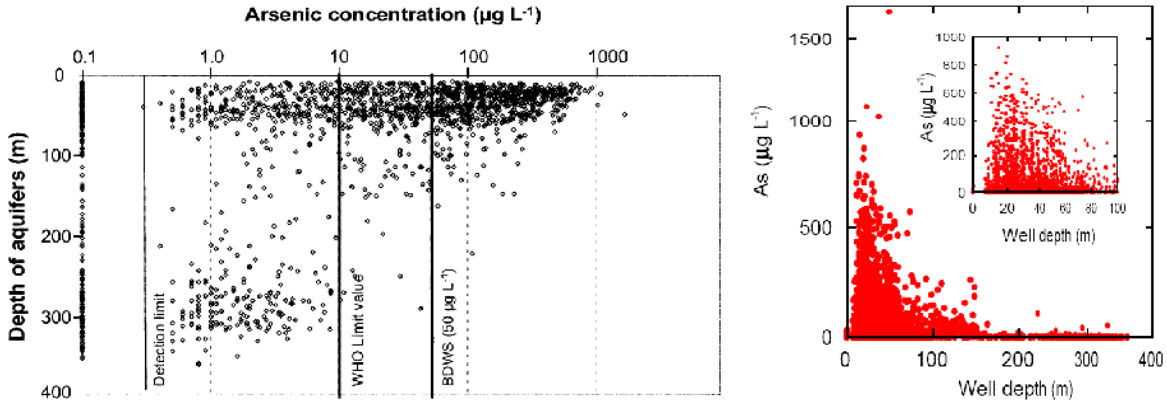

Figure 3 *Distribution of As in groundwaters in relation to the depth. The left picture is taken from Ahmed et al. (2004), modified after Ravenscroft et al. (2001), the right one derives from Kinniburgh and Smedley (2001)*

The typical composition of Arsenic contaminated groundwaters in Bangladesh is presented in Table 1. The near neutral waters show relatively high, but variable contents of Fe(tot), Mn(tot), HCO_3^- and P, in contrast to low Cl^-, SO_4^{-2}, NO_3^- and F^- values. The cations Ca^{+2}, Mg^{+2}, Na^+ and K^+ are present in quite variable amounts. The redox potential ranges from mildly oxidizing over moderate to strongly reducing conditions. Arsenate is prevalent in some wells, but mostly Arsenite is the dominant species, making up 67-99% of total Arsenic (Ahmed et al., 2004), (Smedley and Kinniburgh, 2001).

Table 1 *Characterization of typical Arsenic rich Holocene groundwaters in the Bengal basin*

Parameter	(Smedley and Kinniburgh, 2001)	(Ahmed et al., 2004)	Parameter	(Ahmed et al., 2004)
pH value	close to or greater 7	6.5 – 7.6	**Ca**	21 – 122 mg/L
E_H	typically < 100 mV	+ 594 to -444 mV	**Mg**	14 – 41 mg/L
As (tot)	0.5 – 3,200 µg/L	2.5 – 846 µg/L	**Na**	7 – 150 mg/L
Fe (tot)	> 0.2 mg/L	0.4 – 15.7 mg/L	**K**	1.5 – 13.5 mg/L
Mn (tot)	> 0.5 mg/L	0.02 – 1.86 mg/L	**type of water**	**generally:** Ca-HCO_3, Ca-Mg-HCO_3
HCO_3^-	> 500 mg/L	320 – 600 mg/L		
P	often > 0.5 mg/L (as P)	up to 8.75 mg/L (as PO_4^{3-})		
Cl^-	< 60 mg/L	< 60 mg/L		**locally:** Ca-Na-HCO_3, Na-Cl
SO_4^{2-}	< 1 mg/L	< 3 mg/L		
NO_3^-	< 1 mg/L	< 0.22 mg/L		
F^-	< 1 mg/L	-		

The total Arsenic content of Holocene alluvial sediments from West Bengal and Bangladesh averages to 15.9 mg As/kg. For the Meghna river values between 1.3 to 5.6 mg/kg are reported. These are not excessively high values, compared with the earth's crust average of 1.8 mg/kg (Burgess and Ahmed, 2006), (McArthur et al., 2004). Hence, the sediment background values alone can not explain the high As content of the groundwater. Apparently, Arsenic is accumulated in detrital grain coatings and fine particulates, consisting of Iron oxyhydroxides. For example grain coatings in West Bengal contained over 2000 mg As/kg (Burgess and Ahmed, 2006). Thus, the consideration of the complex interactions between sediment surfaces and the percolating groundwater will be the key to a better understanding of Arsenic mobilization.

2.1.2 Mobilisation of Arsenic

Nickson et. al. (2000) found a strong correlation of As with Fe within the sediments, indicating that dissolution of Iron oxyhydroxides under reducing conditions must contribute to the Arsenic release. Also, Ravenscroft et. al. (2001) as well as Kinniburgh and Smedley (2001) stated that the reduction of Iron oxyhydroxide (FeOOH) is an important mechanism that leads to the release of the Arsenic sorbed on its surface. This release process probably is microbiologically mediated. Initially, microorganisms degrade organic matter (OM), which is present within the sediments as peat deposits. But also young dissolved OM might be available for the microorganisms, which derives from the surface, e.g. from excrements in latrines, drawn down due to intensive irrigation, as Harvey et al. (2002) suggests. Organic matter acts as electron donator and Carbon source, whereas Oxygen in general serves as electron acceptor. But, when all Oxygen is consumed and organic matter still is left in excess, like in BD aquifers, then – in this order – Nitrate, Manganese- and Iron-hydroxides as well as Sulfate will serve as acceptors, accompanied by the release of the reduced species NO_2^-, Mn^{2+}, Fe^{2+} and S^{2-}. Another general by-product of organic matter degradation is Carbon dioxide gas that dissolves in water. Depending on pH it mainly transforms into Bicarbonate (HCO_3^-) and to less extent into H_2CO_3 (Matthess, 1994). High Ammonium and Phosphorus concentrations in groundwaters are also reported as by-product of peat degradation (McArthur et al., 2001). It's a fact that besides reducing conditions, both, very high Bicarbonate (can indicate extensive organic matter degradation) and high dissolved Iron concentrations (indicating reduction of Iron-oxyhydroxides) are found in the Holocene groundwaters (see Table 1). Often are high Arsenic concentrations associated with high Iron concentrations in BD groundwaters, nevertheless only seldom good correlations were found between both parameters. So it must be assumed

that either the reductive dissolution of Iron oxyhydroxides is not the only/main release mechanism for Arsenic or the partial re-precipitation of Iron and/or partial re-adsorption of Arsenic evokes low correlations (Smedley and Kinniburgh, 2001), (Ravenscroft et al., 2001). Another study found that the release of As under reducing conditions partly is linked to the transformation of predominantly Fe(III)-oxyhydroxide coatings on sand particles into Fe(II) or mixed Fe(II/III) solid phases, such as siderite, vivianite, or magnetite. Thus, the release of Arsenic to groundwater must not necessarily be linked to a congruent release of Iron, which would explain low correlations between As and Fe in BD groundwater, too (Horneman et al., 2004).

Former suggestions the Arsenic contamination primarily originates from the oxidation of detrital Arsenic-bearing pyrite, triggered by massive water abstractions in the recent past, are unlikely. First of all, no spatial correlation was found between the distribution of Arsenic and the irrigation intensity. Further the sediments at the surface of shallow aquifers that are exposed to atmospheric Oxygen, should show highest Arsenic contents with regard to the pyrite theory, but they don't. No correlation was found between Arsenic and sulphur in the groundwater. Further pyrite in general is rare in the sediments and shows framboidal form, indicating its development by diagenesis under reducing conditions through consumption of dissolved Sulphate. Framboidal pyrite is stable under present reducing conditions, thus it is unlikely that it serves as a source for Arsenic (Burgess and Ahmed, 2006), (Nickson et al., 2000), (Ravenscroft et al., 2001).

Another theory considers the competitive exchange of Arsenate by fertilizer Phosphate from FeOOH-surfaces, because both, As and P, form connatural anions that show similar sorption behaviour on Iron oxyhydroxides (Acharyya et al., 2000). This assumption is unlikely, because groundwaters in regions of Bangladesh where irrigation and fertilizer application is most intense, were generally free of both, Arsenic and Phosphorus (Ravenscroft et al., 2001). Only poor correlations were found between Arsenic and Phosphorus in groundwaters (Ravenscroft et al., 2005), (Burgess and Ahmed, 2006). Another study showed that a concentration of 5 mg/L Phosphate, matching to the maximum concentrations in BD, only leads to a desorption of 2 µg/L of Arsenic (Manning and Goldberg, 1996). Thus PO_4^{-3} can only play a minor role for mobilization of As.

Besides the widely accepted geochemical control behind Arsenic mobilization, there are reasons to assume that Arsenic release to groundwater might be controlled hydrological too. The team around Polizotto et al. (2008) investigated a 50 km^2 area in the Mekong Delta, which is geologically comparable to the Bengal Basin. But, additionally it represents pre-disturbance groundwater-

conditions, i.e. only negligible antropogenous influence on the aquifer hydraulics exists. The study found that As is released naturally under reducing conditions preferential from near surface river-derived wetland sediments. Then, due to low hydraulic gradients, it is transported through the underlying aquifer back to the river in a centennial time scale (200 – 2,000 yr). The Arsenic influx from fresh sediments into the aquifer and the As-efflux from the aquifer into the river are in approximate balance. Against this background, it can be assumed that activities like intensive irrigation, changes in agricultural practices, levee construction, sediment excavation, and upstream dam installations will alter the hydraulic regime and the As-source material. In turn, this may have influence on arsenic mobilization (Polizzotto et al., 2008). Further investigations on this field of study are necessary to estimate its actual contribution to arsenic release.

2.1.3 Arsenic speciation in groundwater

Arsenic is found in the environment in the oxidation states –III, 0, +III and +V. In natural groundwaters generally the inorganic trivalent Arsenite (H_3AsO_3) besides the pentavalent Arsenate (H_3AsO_4) occur, whereas organic Arsenic forms are found in negligible amounts. Also known are three trivalent Thioarsenite species (H_3AsSO_2, H_3AsS_2O, H_3AsS_3) and four pentavalent Thioarsenate species (H_3AsSO_3, $H_3AsS_2O_2$, H_3AsS_3O, H_3AsS_4). The formation of Thioarsenite species is reported from groundwaters with moderate Sulphide concentrations. But Gault et. al. (2005) claims that there is no evidence for significant concentrations of Thioarsenites in groundwaters of West Bengal. The speciation of Arsenite and Arsenate mainly is controlled by pH and redox conditions, as Figure 4 demonstrates. Arsenic shows relatively high mobility over a wide range of redox conditions. It is sensitive to mobilisation also at the pH values 6.5 to 8.5 that are typical for groundwaters.

The ratio [Arsenite/total Arsenic] in reducing Bangladesh groundwaters varies greatly from 0.1 – 0.9, but typically lies between 0.5 – 0.6. This results from the variable abundance of redox-active solids (mainly organic carbon), microbial activity and Oxygen. Arsenite typically dominates in aquifers with a lack of Oxygen, where strongly reducing conditions occur, due to the reduction of Fe(III) and Sulphate (Smedley and Kinniburgh, 2001).

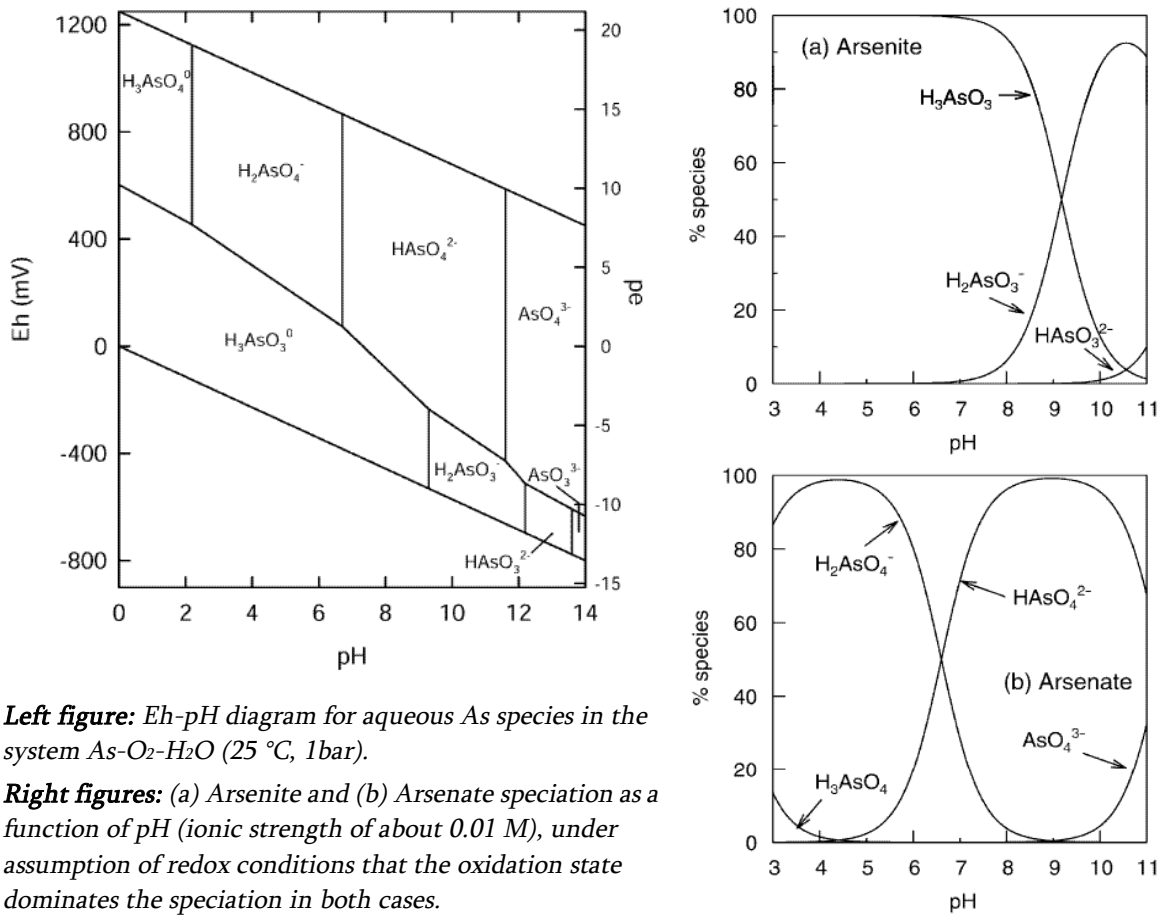

Left figure: *Eh-pH diagram for aqueous As species in the system As-O_2-H_2O (25 °C, 1bar).*

Right figures: *(a) Arsenite and (b) Arsenate speciation as a function of pH (ionic strength of about 0.01 M), under assumption of redox conditions that the oxidation state dominates the speciation in both cases.*

Figure 4 *Redox- and pH-depending As-speciation, after (Smedley and Kinniburgh, 2001).*

2.2 The test site at the Titas hospital complex

The test site area is situated on the property of a Hospital Complex in the village Titas (Daudkandi Upazila, Comilla district), with the coordinates 23° 35,809' N, 90° 47,857' E at an altitude of approximately 5.5 m above sea level. The village Titas lies in a distance of approximately 60 km in south eastern direction from Dhaka, located on the floodplains between the huge Meghna river and the smaller Gumti river, as Figure 5 shows. In February 2007 a core drilling was constructed by rotary drilling and 37 sediment samples were collected at the Titas hospital complex. Based on the findings from the core drilling six individual sampling wells (30, 50, 70, 85, 90, 115 ft, 2 inch in diameter) were drilled with the local "hand flapper" method at the test site, whereas a seventh sampling well (280 ft, 4 inch in diameter) was constructed by manual core drilling. The investigations on this sediment samples were carried out by Lissner (2008) within her masters thesis. The main results will be summed up subsequently.

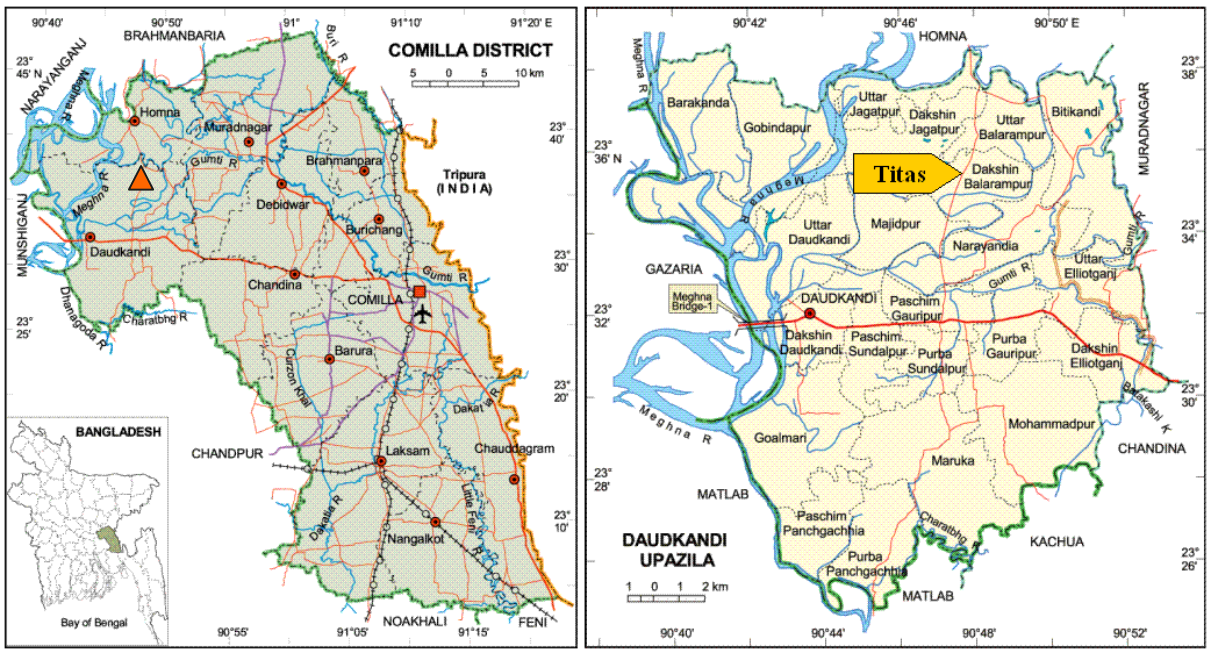

Figure 5 *Location of Titas in Bangladesh (maps taken from Islam (2003), the National Encyclopaedia of Bangladesh, online version: www.banglapedia.search.com.bd)*

2.2.1 Local geology and sediment geochemistry at Titas

The results of the survey on sediment properties and its mineralogy are summarized in Table 2. Lissner ascertained five distinctive sediment units L1 – L5 in the subsurface. The surficial, rather oxidized, silty layer (L1) is underlain by grey coloured sandy loam (L2), indicating reduced conditions, with peat fragments at its bottom. Both form the shallow aquifer. Underneath lays an aquitard consisting of reduced silt loam (L3), featuring a sand lens in its upper and peat fragments in its lower part. Layer L4 is a deeper aquifer with oxidized brown-coloured sand deposits, indicating a high amount of Iron oxyhydroxides probably resulting from oxidative weathering of the sediments before they were buried. Layer 4 is underlain by the less permeable silty layer L5. Mineralogical investigations showed in the aquifer-layers L1, L2, and L4 quartz as the predominant fraction (≥ 51 – 70 %) besides considerable quantities of feldspars (≥ 20 – 29 %), whereas only minor quantities of clay (≤ 6 %) and mica (≤ 8 %) occurred. In comparison, the less permeable layers L3 and L5 have distinctly higher quantities of clay (≥ 25 – 49 %) and mica (≥ 19 – 24 %) besides less quartz (≤ 28 %) and feldspar (≤ 14 %).

Figure 6 represents the data from the own core drilling (277 ft/84.4 m depth) and data from a deep well, situated at the property of the hospital, which was drilled by the hospital building company down to 940 ft (286.5 m) depth. The deep litholog points out that the layer with brown sand (L4)

is a phenomenon, occurring only once in the whole investigated subsurface section, by having a comparatively low vertical extension (< 5 m). Below it lies another thick layer of grey fine to very fine sand, which is interlaminated by two grey reduced clay lenses.

Table 2 *Summary of Lissner's Investigations on sediment samples from the Titas core drilling (Lissner, H., 2008)*

Layer, depth [m]	Description of material in the field	US soil type	Sample depth [m]	Mineralogy major > 15 %	Mineralogy minor ≤ 15 %	HyGeo characterization
L1 3 – 6	sandy silt and brown to grey fine sand	silt	5	**51 % quartz** 28 % feldspar	5 % clay 7 % mica	
L 2 6 – 27	reduced grey fine sand and silt, peat fragments (26 m)	sandy loam	9	**56 % quartz** 24 % feldspar	6 % clay 8 % mica	shallow aquifer
			26	**71 % quartz** 20 % feldspar	5 % mica	
L3 27 – 79	reduced silty clay to clay, lens of fine sand (34 m). peat fragments (61 – 73 m)	silt loam	34	26 % quartz 25 % clay 24 % mica	14 % feldspar	aquitard
			61	**49 % clay** 19 % mica	15 % quartz 8 % feldspar	
L4 79 – 83	oxidized brown, fine to medium sand	sand	83	**60 % quartz** 29 % feldspar	5 % mica 2 % clay	deep aquifer
L5 **> 83**	clay to heavy clay	silt	84	30 % clay 28 % quartz 23 % mica	8 % feldspar 2 % Siderite (Fe-Carbonate)	less permeable lens (or next aquitard?)

feldspars: mainly consist of K-feldspar, plagioclase
mica: mainly consists of muscovite, only traces of biotite in L4
clay: in general smectite, kaolinite and minor amounts of vermiculite, but in L4 mainly kaolinite

Lissner (2008) also explored the sediment geochemistry of the subsurface. The data are listed in Appendix C2. Subsequently the main results are presented and will be considered in detail in section 4 in comparison to the findings of this study.

By leaching sediment samples from different depths with artificial groundwater (AGW) and hot HCl respectively, weakly and moderately bound fractions of As, P, Fe and Mn were determined. AGW released neither As nor P, negligible amounts of Fe (0 – 1.7 µg/g) and only low quantities of Mn (0 – 13 µg/g), thus Lissner (2008) assumed that equilibrium conditions exist between sediment

and natural groundwater. Figure 7 shows the results of hot HCl leach. Fe values range from 4,440 to 23,200 µg/g, Mn from 52 to 476 µg/g, P from 80 to 600 µg/g, and As from 0.3 to 3.8 µg/g.

Figure 8 shows the content of total organic Carbon (TOC), total inorganic Carbon (TIC) determined as $CaCO_3$, the percentage of total Carbon (TC), and the pH($CaCl_2$) of the sediment samples. TOC values range from 1 – 40 mg/g and $CaCO_3$ from 0 – 16 mg/g. The pH lies between 5.7 – 7.1, whereas it reaches lowest values in the peat below 60 m depth. Arsenic, Fe, Mn, $CaCO_3$ and TC reach highest values within the clay-rich layers L3 and L5. TOC follows this distribution as well, but shows another peak near the surface and is especially high in the peat layer below 60 m depth.

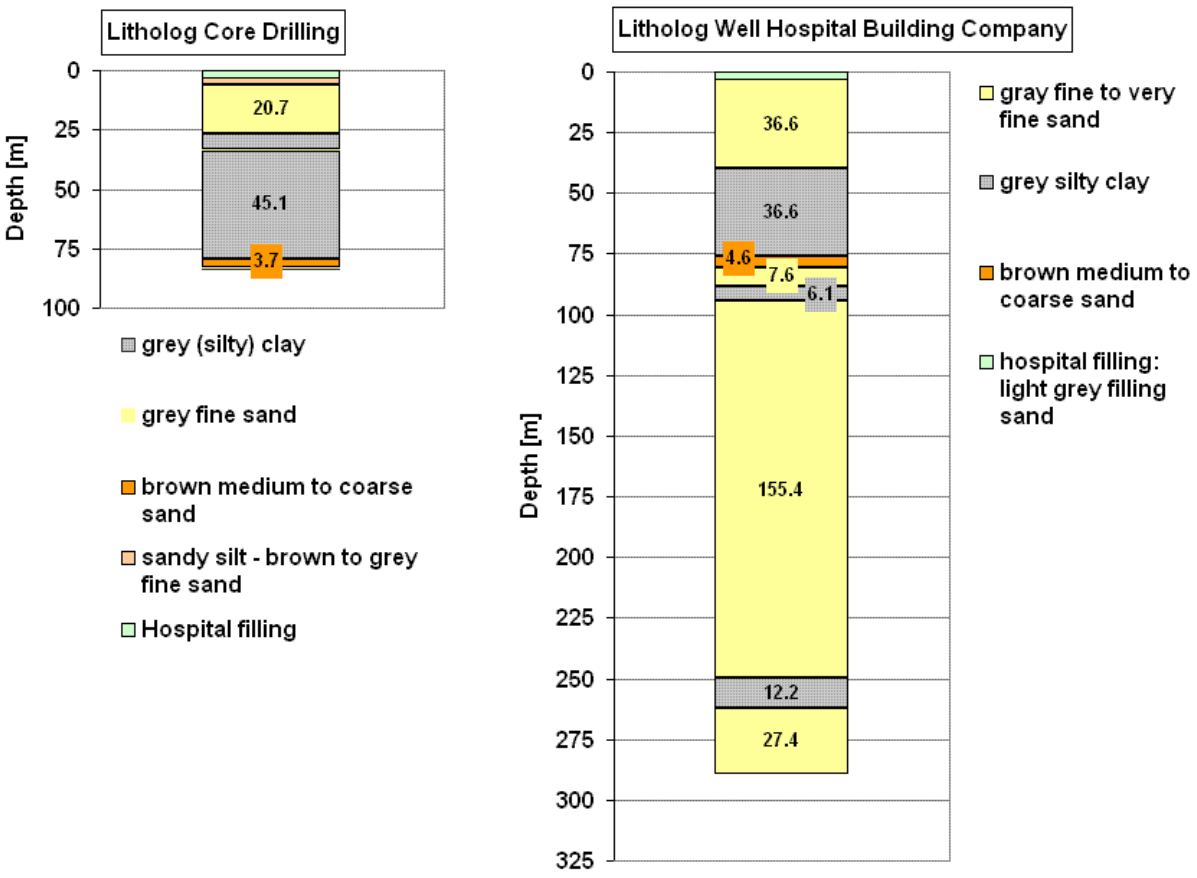

Figure 6 *Structure of the subsurface – visualization of litholog data from the own core drilling (left figure) and of the well data from the Hospital Building Company (right figure)*

Significant (**p <= 0.05**), positive Spearman rank correlations between As and Fe (r=0.883), As and Mn (r=0.745), As and TOC (r=0.700) as well as As and CaCO3 (r=0.813) were found. Phosphorus and Arsenic did not correlate (r=0.033, p=0.92) within the sediments.

Further, As-leaching and -sorption batch experiments with MQ (= pure water, pH 7.1), 0.04 $NaHCO_3$ (pH 8.8) and 0.04 M NaOH (pH 12.3) were done. The 0.04 M NaOH, targeting As on amor-

phous FeOOH and organic matter, induced a very effective leaching of As, quite similar to the results with hot HCl (see Figure 7). Leaching with MQ (0 – 5 µg As/L) and $NaHCO_3$ (0 – 18 µg As/L) released only small amounts of As from the sediments, although Lissner utilized 0.04 M $NaHCO_3$ exceeding maximum Bicarbonate contents in groundwater of the test site (TF115.01 = 0.015 mol/L) and shallow Bangladesh aquifers (0.05 – 0.09 mol/L, (Ahmed et al., 2004)). Thus, Bicarbonate apparently does not contribute much to As-release from Titas sediments.

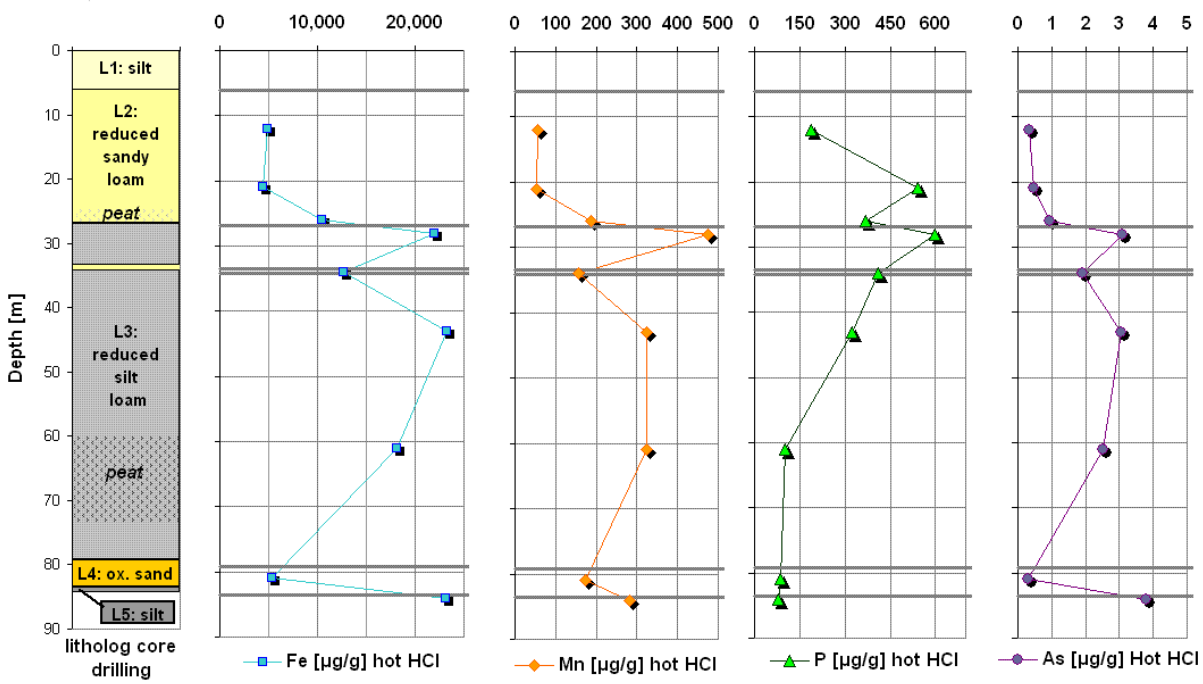

Figure 7 *Results of hot HCl-leach for Fe, Mn, P, As in [µg/g] in the sediment samples in comparison to the stratification of the core drilling at Titas, data ascertained by (Lissner, 2008), basic data listed in Appendix C2.*

On the other side, adsorption of As was most efficient in MQ and $NaHCO_3$, especially in L3, L4 and L5. After spiking the samples with Arsenite and Arsenate, it was almost completely adsorbed. A strong retention of As was noticed in the aquiclude sediments (L3) that feature remarkable higher fractions of clay and mica (see Table 2). The aquifer sorption rates for Arsenic were higher in the brown (formerly oxidized) sand (L4) than in the grey reduced material (L2), what may be due to sorption of As on Ironhydroxides indicated by the brown colour. Moreover microbial oxidation or the contact with oxidative soil compounds like MnO_2 could be factors responsible for the observed partial oxidation of Arsenite to Arsenate in sediment-solution mixtures of the oxidized sand material (L4), whereas spiked Arsenite remained reduced in the reduced sand material (L2).

Another question Lissner dealt with was the competitive exchange between Arsenate and Phosphate in column experiments. Both anions formed stable surface complexes, resulting in a non-exchangeable fraction, whereas Arsenate showed a higher affinity for mineral surfaces than Phosphate. On the other hand Arsenite and Monothioarsenate seem to have weaker bonding structures, because they generally showed a higher mobility through the columns.

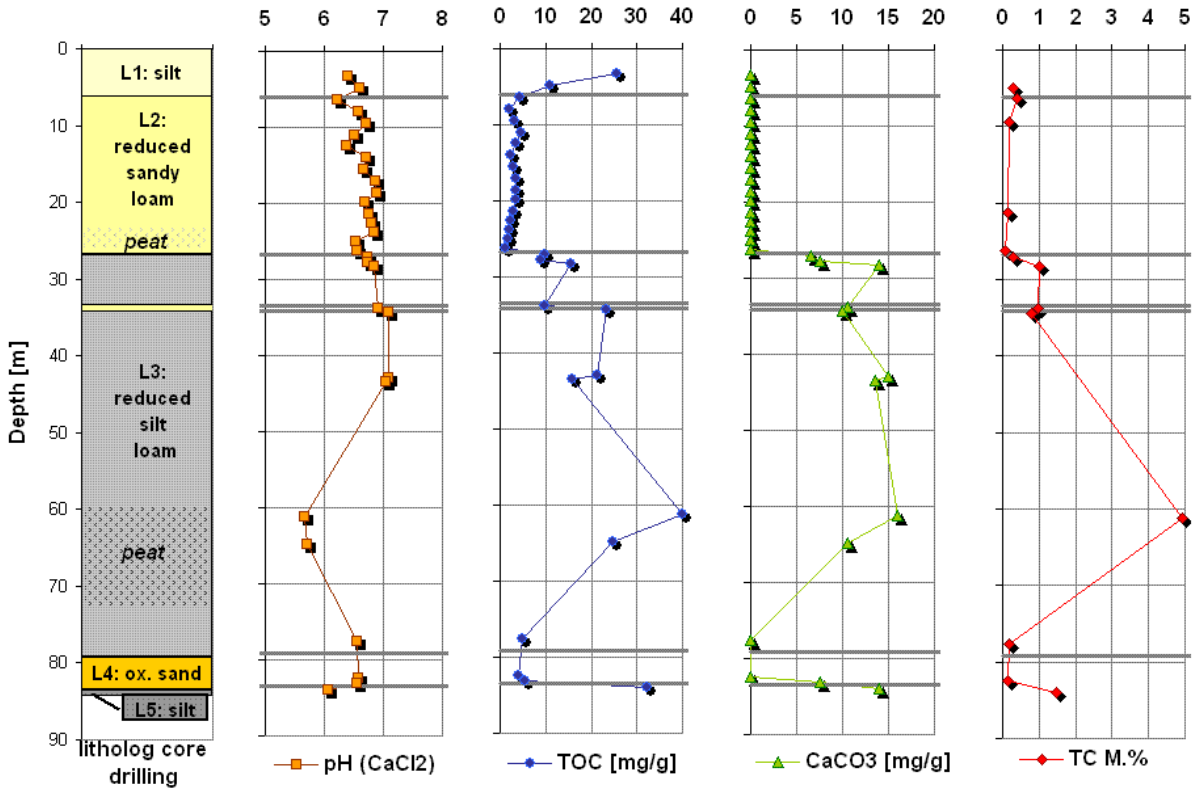

Figure 8 *Results for TOC [mg/g], $CaCO_3$ [mg/g], TC [M%] and pH in comparison to the stratification of the core drilling at Titas. Data were ascertained by Lissner (2008), basic data listed in Appendix C2.*

2.2.2 Local groundwater chemistry and water tables

In the time period February until July 2007 Jörg Steinborn, another masters student of Freiberg University, carried out a weekly chemistry and water table monitoring of the test site wells, but also mapped the location, chemistry, and water tables of several drinking water and irrigation wells in the village and its surrounding agricultural area. The results of the survey are listed in Appendix C1. The data show that Arsenic concentrations in groundwater at Titas span from <1 up to 420 µg/L, whereas 88 % of all sampled wells featured Arsenic contents exceeding the Bangladesh limit of 50 µg/L for drinking water.

As Figure 9 shows, most of the explored wells are used for drinking water supply, but only three wells above 15 m depth and one well situated in a deeper aquifer in 274 m depth (not displayed in the graph) have acceptable concentrations that fall below the WHO limit of 10 µg As/L. Highest average Arsenic contents at the test site were found in the 115 ft well (35.1 m) with 237 µg/L, whereas the lowest values featured the 30 ft well (9.1 m) with 22 µg/L.

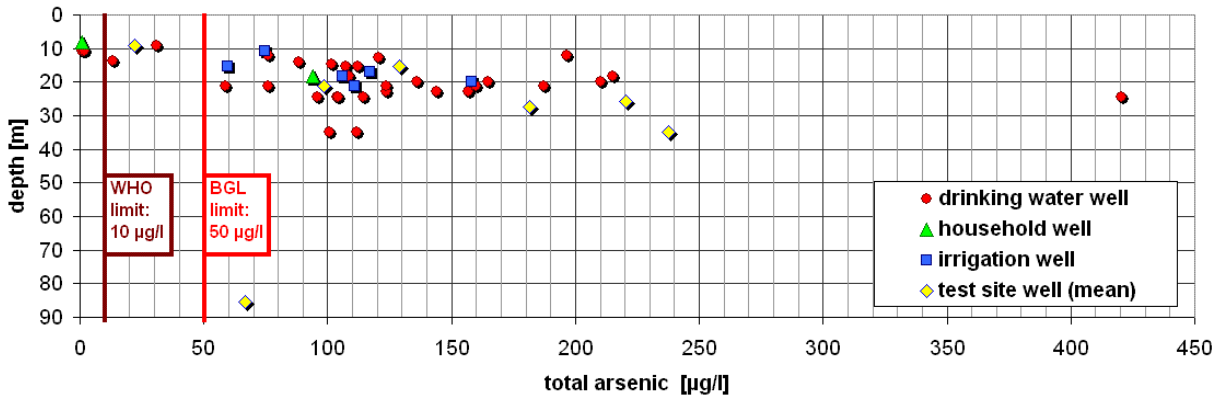

Figure 9 *Total Arsenic concentrations of groundwater samples in µg/L (ppb), collected from 46 wells with known screen depth in Titas by Steinborn (2008) during the time period February until July 2007, measured with ICP-MS at Trent University in Canada. The values represented for test site wells are average values based on 20 single measurements.*

Steinborn's results regarding the general water chemistry are listed in Appendix C1 and will be considered in detail in chapter 4 compared to the own findings in the time period September to December 2007. Remarkable were the extremely high Iron and Ammonium contents at the 280 ft (84 m) test site well, with average values of 111.5 mg Fe_{tot}/L and 124.0 mg NH_4^+/L in the deeper aquifer. Lissner (2008) suggests that peat degradation in Layer 4 is responsible for the high release of Ammonium into Layer L5.

2.2.3 Local climate conditions and the water balance

Bangladesh is characterized by a tropical monsoon climate with three distinct seasons. A cool dry, almost cloudless season from November through February with north-eastern monsoon winds is followed by a transition period, namely the pre-monsoon hot season that comes along with changing wind directions, thunderstorms, and increasing cloud cover from March through May. The least humid months in the eastern areas of Bangladesh are January to March (approx. 60 % relative humidity). Thereafter from June through October the hot and wet monsoon season prevails with south-western winds that bring heavy rainfall, very high relative humidity (> 80 %) and a widespread cloud cover. Information for this general climate description were taken from the National

Encyclopedia of Bangladesh (www.banglapedia.search.com.bd) that references to the publications of Ahmed and Vijnan (1997) and of Barry and Chorley (1998).

At Daudkandi Upazila no meteorological station exists. The next station is Comilla (23°26' N/ 91°11' E) in a distance of 28 km in south-eastern direction from Titas/Daudkandi. Climate data for Comilla are listed in Appendix C3 and were provided by the Meteorological Department of Bangladesh in Dhaka. Figure 10 shows daily recorded precipitation and temperature data in 2007, especially pointing out when heavy rain events occurred, entailing a lowering of the temperatures. Single rain events in March, April and May might be the characteristic thunderstorms of the hot dry season. The Monsoon season started at the end of May and lasted until end of October. Another mentionable single event is cyclone SIDR, devastating Bangladesh at the 15th of November 2007, within the cold, usually dry season.

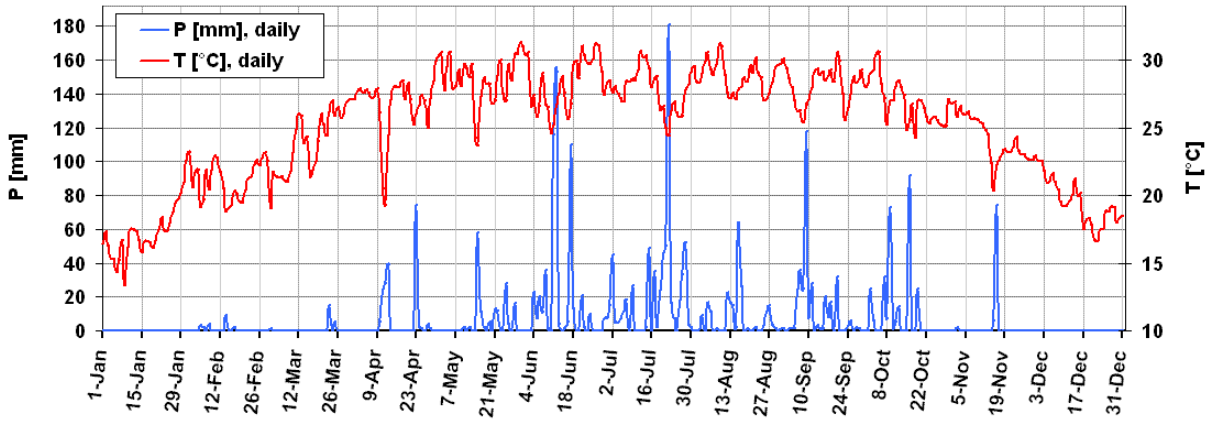

Figure 10 *Daily precipitation and dry bulb temperatures at station Comilla in 2007*

Figure 11 presents monthly total precipitation and monthly average temperatures in 2007 in comparison to the average of these data in the time period 1998-2006. Lowest average temperatures occurred in January 2007 with 17.3 °C, whereas persistent high average temperatures of around 28 °C are found during May until September. The average temperatures of the years 1998-2006 are quite similar. On the other hand the distribution pattern of rainfall shows significant differences. While rainfall in January, March, May, August and December 2007 was lower compared to the average of 1998-2006, the months April, June, July, September, October and November brought distinctly higher precipitation.

In 2007, the monsoon-season from June through October brought 82 % (2,042 mm), the hot dry season from March through May 14 % (353 mm) and the cold dry season from November through February only 4 % (102 mm) of the total precipitation of 2,497 mm. In contrast in the period 1998

until 2006 an average total rainfall of 2,197 mm was recorded, whereas in average 72 % (1,592 mm) fell in the monsoon season, 24 % (531 mm) in the hot dry season and 3 % (73 mm) in the cold dry season. So it can be assumed that 2007 brought distinctly higher-than-average precipitations in the monsoon season, whereas the hot season was dryer than the average. Also the flooding period in 2007 lasted longer than usual, probably also a result of the higher precipitations at Comilla district, but particularly in regions upstream.

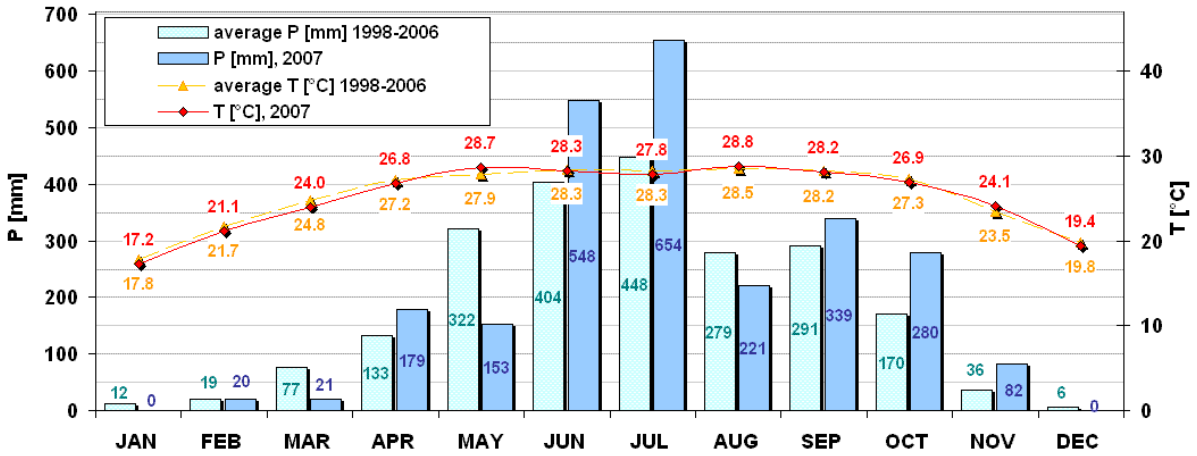

Figure 11 *Monthly precipitation and dry bulb temperatures of the year 2007 vs. the average of 1998-2006 at station Comilla*

For 2007, no daily potential evaporation (PE) data were provided, but for the years 1995 – 2006 Class-A-Pan data were available. In the PE data basis only the years 2001 and 2002 contained a complete data set. For the other years with partially missing values the average monthly PE was estimated by calculating an average daily PE per month from the existing daily data, finally multiplied by the number of days per month. The data were corrected for the oasis effect reported by Haude in 1963 (Blüthgen and Weischet, 1980). It had to be considered that the "true" potential evaporation would make up approximately 66 – 75 % of the measured Class-A-Pan values. Here the factor 0.7 was used, to calculate the corrected potential evaporation PE_c. Figure 12 presents the monthly precipitation of 2007 vs. the average monthly PE_c of 1995 – 2006. The difference between precipitation and potential evaporation (P- PE_c) demonstrates that evaporation from the free water surface of the Class-A-Pan would be much higher than the rainfall per month in 2007. The total PE_c sums up to 9,911 mm in 2007.

The actual evapotranspiration (AET) must be expected to be distinctly lower than PE_c. AET was approximated from the monthly precipitation data and the corrected monthly potential evaporation data with the following formula, which is valid for tropical climate regions.

$$AET[mm] = P[mm]\frac{P[mm]}{\sqrt{1+(\frac{P[mm]}{PEc[mm]})^2}}$$ (Mirza et al., 2003; Pike, 1964)

Figure 12 shows the monthly results for AET and the difference P-AET. The total AET sums up to 2,262 mm in 2007. This value certainly underestimates the real circumstances. Regarding Figure 13, it is obvious that at the 3rd of August 2007 approximately 31 % (44,000 km²) of Bangladesh's land surface were inundated. This area serves as free water surface, where real evaporation actually would correspond to potential evaporation. An enlarged view gives an impression of the flood extent at Comilla district and Titas. From on-site observations can be estimated that during monsoon the inundated land surface at Titas temporarily even exceeded 90 % of the whole land surface. That means, the complete agricultural used land was inundated, whereas only artificially elevated villages and streets remained unaffected.

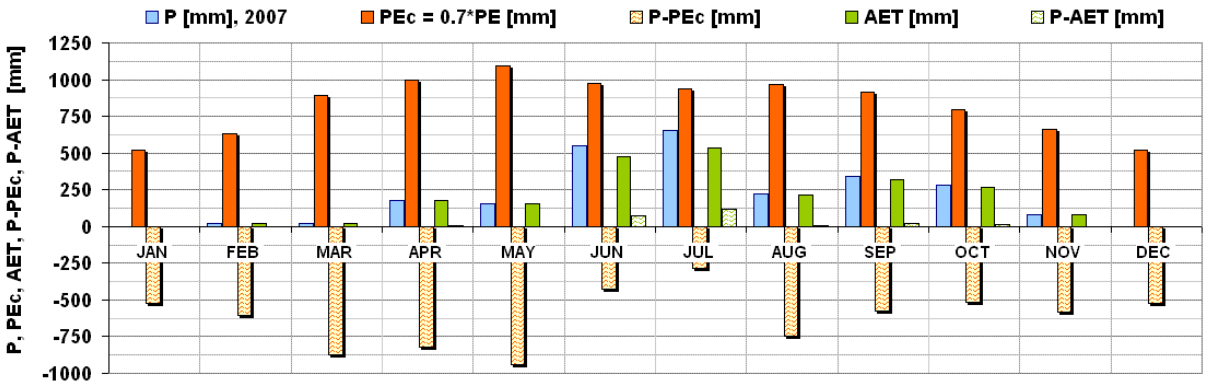

Figure 12 *Monthly total precipitation (P) in 2007 in comparison to the average potential evaporation (PEc, Class-A-Pan) measured from 1995 until 2006 at station Comilla and the calculated actual evapotranspiration (AET) after Pike (1964)*

It is obvious that the flooding at Comilla district is not due to the local monsoon precipitation alone, but rather results from rainwater transported and retained by the Meghna river and its tributaries from northern regions to the south. Thus, a proper estimation of AET can not be done without considering the local temporal and spatial variations of flooded and non-flooded areas besides land use and vegetation cover as well as the influence of irrigation activities.

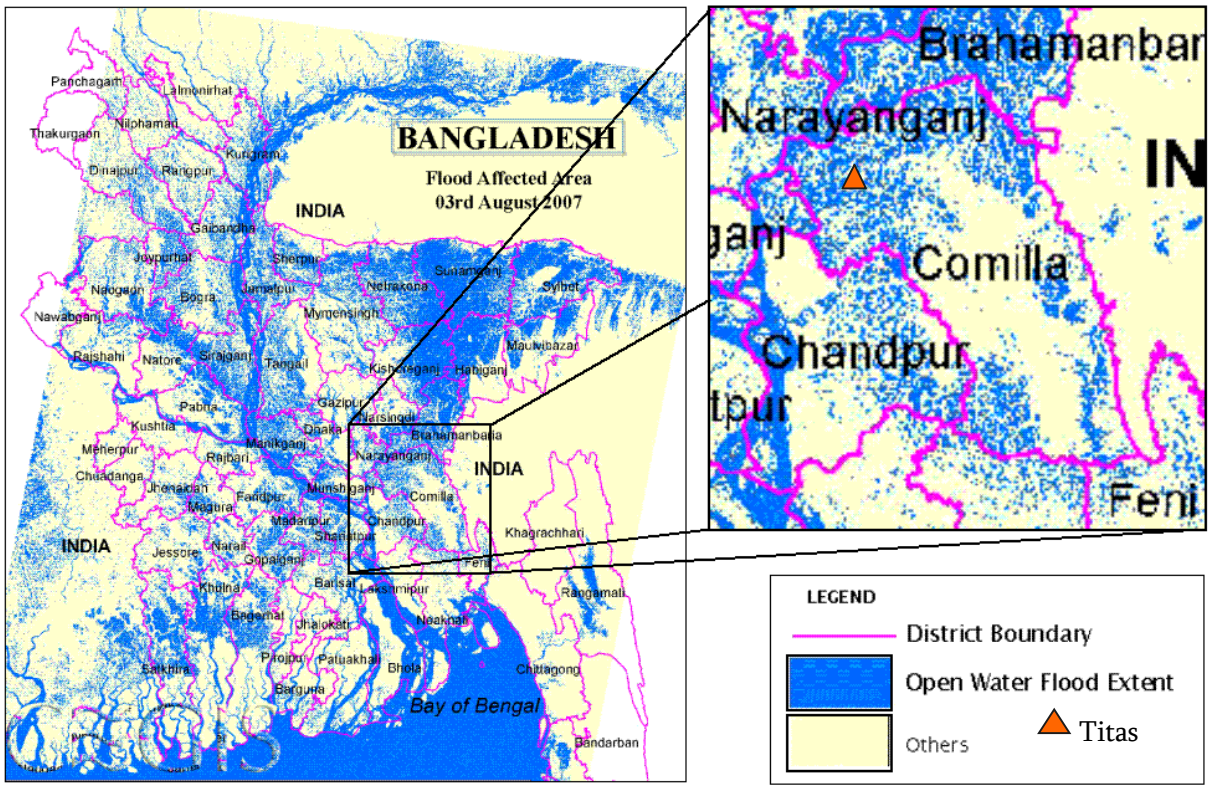

Figure 13 *The map derived from RADARSAT Scan-SAR Wide Beam has a resolution of 100 x 100 m and shows the open water flood extent at the 3rd of August 2007, when approximately 44,000 km² of BD's whole area (144,000 km²) were just flooded. (taken from CEGIS, 2007: http://www.cegisbd.com/flood2007/detailed_map.htm)*

3 METHODOLOGY

The basic work for this thesis was carried out in Titas, Bangladesh between end of August until middle of December 2007. It included two main tasks, on the one hand investigations regarding the groundwater chemistry, in particular the Arsenic contamination, and on the other hand hydraulical considerations concerning the local groundwater flow directions and the survey of hydraulical parameters of the aquifer system.

The first main task was a regular groundwater chemistry monitoring of the seven test site piezometers at Titas/Daudkandi. Besides the electrochemical parameters pH, redox potential, Electrical conductivity as well as Oxygen concentration and saturation the chemistry monitoring also comprised photometrical on-site measurements of total and ferrous Iron, total and divalent Manganese, Ammonium, Nitrate, Nitrite, and Sulphide. Further, alkalinity and acidity were determined by titration. Moreover four distinct water samples were collected from each well during each monitoring, dedicated for the later determination of Arsenic (total and species), Phosphorus (total and species), dissolved organic and total inorganic Carbon as well as the major anions and cations. The hypothesis that Arsenic can be mobilized by higher concentrations of Phosphorus was tested at the 85 ft test site piezometers with an injection spike experiment.

Back in Germany the samples for TIC/DOC, anions and cations were analysed in the hydrogeological laboratory of Freiberg University by the author during the months January – April 2008. The determination of Phosphorus and Arsenic species and totals was carried out by Dr. Britta Planer-Friedrich at Trent University in Canada in November and December 2007.

As mentioned above, besides considerations of the water chemistry also hydraulical field surveys on-site in Bangladesh were of interest. These comprised aquifer tests at the 85, 115, and 280 ft test site piezometers as well as water table measurements and the exact levelling of the altitude and horizontal positioning of the test site and irrigation well heads. The levelling data were processed with the GIS software TNTmips (Version 2007-73) to create a geographical map of the ground surface. Further, digital elevation models (grid-data) of the ground and water table surface were created with the software Surfer8. The aforementioned data, hydraulical parameters calculated from the aquifer tests, estimated parameters that base on Lissner's (2008) granulometry analysis, as well as climate data serve as basis for a model of the shallow aquifer system, which was created

with Visual MODFLOW 3.0.0. The procedures applied in the field, in the laboratory and for data handling are described in detail subsequently.

3.1 Methods in the field

3.1.1 Monitoring of the hydro-geochemistry at test site Daudkandi

From September until beginning of December 2007 seven investigation wells at the test site Titas/Daudkandi were monitored by the author and an assisting student of Dhaka University approximately every two weeks. The investigation wells and litholog data (Figure 6) were introduced in chapter 2.2. The well arrangement at the test site is shown in Figure 15 in section 3.1.3. Steinborn (2008) already proceeded twenty monitorings from February throughout July 2007, so the author continued with the 21st monitoring. The full denotation for each sampling was "BGL" for Bangladesh, "TF" for the sampling location test-field, "well depth" as description for the sampled well and the serial number of monitoring. Thus i.e. the first sampling at the 30 ft well during this survey fully notes "BGLTF.30.21".

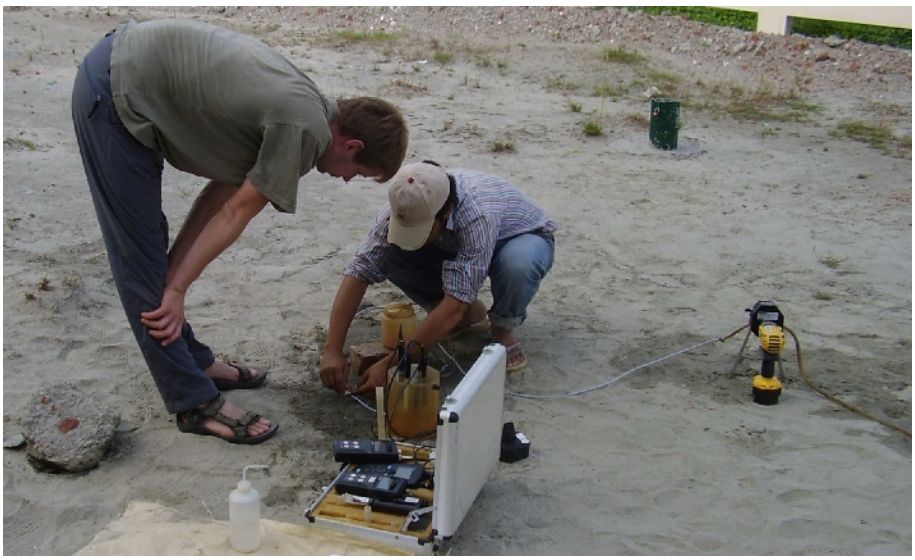

Figure 14 *Baharul Alam Biswas and Sven Sieber preparing the equipment for monitoring the test site wells*

3.1.1.1 Low-flow sampling

Each test site well was equipped with a dedicated sampling system, to prevent carry-over of contaminations from one well to another. The sampling was done as low-flow sampling using a peri-

staltic pump head (Masterflex L/S easy-load, model 75/8-62, Cole Parner), driven by a battery-powered, hand-held drilling machine (De-Walt, Idstein DC980 Type10). Pulse and Barcelona (1996) defined typical flow rates of 0.1 to 0.5 L/minute and pointed out advantages and disadvantages for this sampling method, shown in the box below:

Advantages	Disadvantages
▪ reduced stress on the formation (minimal drawdown) ▪ sampled water corresponds to the screen length (depth-related sampling possible when small screens) ▪ less mixing of stagnant casing water with formation water ▪ reduced need for filtration, in turn reduces sampling time ▪ representative samples for the mobile load of present contaminants ▪ better sample consistency, reduced artificial sample variability ▪ minimal disturbances of the sampling point minimizes sampling of artefacts ▪ smaller purging volume in turn decreases disposal costs and sampling time	▪ higher initial capital costs ▪ greater set-up time in the field ▪ need to transport additional equipment to and from the site ▪ increasing training needs ▪ resistance to change on the part of sampling practitioners ▪ concern that new data will indicate a change in conditions and trigger an action

The time required for purging the well before sampling is independent of well depth or well volumes, but depends on well diameter, the sampling device, hydrogeochemistry, and pump flow rate. To make sure that formation water is sampled instead of stagnant casing water, Pulse and Barcelona (1996) recommend to wait with sampling until the full stabilization of electrochemical parameters such as pH, specific conductance, redox potential, dissolved Oxygen, and turbidity. This purging process requires time and an adequate power supply.

It must be noted that it was not possible to follow this procedure strictly in the field. The pump could not be run with cable energy supply or power supply by a generator. For the internal energy supply of the pump four batteries were available that featured quite low capacities. In average, one battery was running approximately 45 to 60 minutes only. Recharging the batteries in general was possible, but frequent energy cuts occurred in the village. Due to these circumstances a simplified sampling procedure was applied. The water uplifted in the first fifteen minutes after pump start was discarded, assuming that this will abstract the stagnant casing water. After this, the water was

fed into the flow cell. When the flow cell was filled up to the rim, electrochemical measurements and sampling started parallel.

Steinborn told that he used a slightly differing procedure. He purged a full flow cell volume, discarded this water, filled the flow cell again, and then started electrochemical measurements and sampling. It can be assumed that filling the flow cell took more than 15 minutes, in particular in the deep 280 ft well. Thus, Steinborn (2008) probably purged for a longer time interval.

3.1.1.2 On-site measurement of the electrochemical parameters pH, Eh, EC, T, and Oxygen

In time steps of five, ten, twenty, thirty, and forty five minutes after filling of the flow cell measurements of the parameters listed in Table 3 were taken with probes to check their stabilization. The results of the last readings then were utilized in the thesis. Before every monitoring-session the pH-probe was newly calibrated and the Conductivity and redox probes were checked with standard solutions. Calibration of the optical Oxygen sensor was not necessary according to the manual. But to make sure it works properly an aerated water sample that should have 100 % Oxygen saturation, was checked.

Table 3 *Measurement devices for pH, Electrical conductivity EC, electromotive force EMF (redox potential E_H), Oxygen concentration O_{2conc} and saturation O_{2sat}, temperature T*

Parameter	Utilized devices and probes
pH	21st/22nd monitoring: HACH HQ 40 d multi + liquid KCl-filled PHC 301 probe (automatic 2-point-calibration); 24th-26th monitoring: Hanna Instruments pHep® HI 96107 probe (manual 1-point-calibration); 27th-31st monitoring: HACH HQ 40 d + gel filled PHC 101 probe (automatic 2-point-calibration)
EC [µS/cm]	WinLab Data Line Conductivity Meter No. 1525079, Windaus Labortechnik, probe: 9969, EK (check solution: 1413 µS/cm (25 °C)
EMF [mV] (E_H [mV])	WinLab Data Line pH Meter No. 1621038, Windaus Labortechnik + EMC 133 probe from Meinsberger Elektroden (check solution: 212 mV (30°C), 220 mV (25 °C))
O_{2conc} [mg/L] **O_{2sat} [%]**	HACH HQ 40 d multi + HACH LDO 101 optical probe (LDO = luminescent dissolved oxygen)
T [°C]	Ternary simultaneous measurement with the pH-, EC,- and Oxygen-probes

From the three temperature determinations with the pH, EC and Oxygen-probe an average temperature was calculated. The redox potential E_H could not be measured directly in the field. In-

stead the electromotive force EMF in [mV] was determined, which is convertible to E_H with the following equation:

$$E_H\ [mV] = EMF\ [mV] + (0.7443 * T\ [°C] + 224.98)$$

As Table 3 shows, the pH-measurements could not be carried out with the same probe over the whole time, due to a defect of the PHC301 probe. Before a new HACH probe was delivered, the measurements were done with the less accurate pHep from Hanna Instruments. Also with the Win Lab Conductivity probe problems occurred. Checking it with the 1413 µS/cm test solution, often large deviations occurred (absolute standard deviation: ± 43 µS/cm) between measured and the standard control value. In most cases it was not possible, to adjust the probe readings by adjustment of the cell constant. Comparison of measured to calculated conductivity (see section 4.2.1.2 and Steinborn (2008)) confirmed large deviations in several cases. Hence the readings from the pHep and the Conductivity probe must considered with caution.

3.1.1.3 Photometrical on-site measurements of Fe, Mn, NH_4^+, NO_3^-, NO^{2-} and S^{-2}

After the complete filling of the flow cell, also the sampling for and the immediate photometrical determination of the redox sensitive water constituents Iron, Manganese, Ammonium, Nitrate, Nitrite and Sulphide [mg/L] was carried out by means of a HACH DR/890 Colorimeter. Besides the sample volumes and the type of blank solution used for the analysis, Table 4 notes the valid concentration ranges, limits of quantitation, standard deviations, and possible interferences of the utilized methods for each measured parameter. Detailed descriptions of the analysis procedures are accessible in the methodical manuals in Appendix C4.

Before each photometrical measurement the glass-vessels were cleaned with a tissue from dirt and fingerprints. For the determination in general fresh samples were taken directly from the tube, to prevent oxidation by longer air contact. In some individual cases this procedure was not possible, for instance two times the Fe(II)-analysis was delayed due to suddenly occurring rainy/stormy events. Such results are not reliable and will be highlighted separately. The Ammonium analysis was not executable during several monitorings, due to a defect Ammonium-cyanurate reagent. In several cases dilutions were necessary. Before filling the necessary amount of diluted sample in the photometrical vial, it was washed with the diluted sample and shaken to remove residual liquid. For taking small sample volumes quantities an Eppendorf Research® pipette with the volume range 100 to 1,000 µL was used.

Table 4 *On-site parameters measured photometrical with the HACH DR/890 colorimeter listed together with the applied HACH analysis methods, their concentration ranges, quantitation limits (LOQ), absolute standard deviations (ASD) and known interferences (information derives from the HACH-manuals in Appendix C4)*

Parameter [mg/L]	HACH method concentration range LOQ ± ASD	Interferences with other water constituents	Quantity of sample/blank. Type of blank solution
Two valued Iron Fe^{2+}	**1,10-phenanthroline method, 8146** 0 – 3.00 mg/L 0.03 ± 0.017 mg/L	not specified in the manual	25 mL sample/blank blank = sample
Total Iron Fe(tot)	**FerroVer method, 8008** 0 – 3.00 mg/L 0.03 ± 0.017 mg/L	Ca no interferences at $CaCO_3$ < 10 g/L, Mg no interferences at $CaCO_3$ < 100 g/L, Mo no interferences at Mo < 100 g/L, high Iron impedes colour development, Iron oxides require chem. pulping, high S^{-2}, high turbidity, extreme pH values, strongly buffered samples	10 mL sample/blank blank = sample
Two valued and total Manganese Mn^{2+}, Mn(tot)	**PAN-method, 8149** 0 – 0.700 mg/L 0.007 ± 0.013 mg/L	no interferences if Al < 20 mg/L, Pb < 0.5 mg/L, Cd < 10 mg/L, Fe < 5 mg/l, hardness (Mg) < 300 mg/L, Co < 20 mg/L, Cu < 50 mg/L, Mg, Ni < 40 mg/L, Zn < 15 mg/l	10 ml sample/blank blank = distilled water
Ammonium NH_4^+	**salicylate method, 8155** 0 – 0.50 mg/L 0.02 ± 0.02 mg/L	Ca > 1,000 mg/L as $CaCO_3$, Mg > 6,000 mg/L as $CaCO_3$, NO_3^- > 100 mg/L NO_3-N, NO_2^- > 12 mg/L NO_2-N, SO_4^{-2} > 300 mg/L SO_4^{-2}, Fe: interferes in all quantities by lowering results for NH_4^+, S^{-2} intensifies the colour, turbidity/sample colour result in false higher values	10 ml sample/blank blank = distilled water
Nitrate NO_3^-	**cadmium reduction method, 8171** 0 – 5.0 mg/L 0.2 ± 0.2 mg/L	Cl > 100 mg/L results in low NO3-; Fe(III), NO2- and strongly oxidizing/reducing substances interfere in all quantities, strongly buffered samples, extreme pH values	10 ml sample/blank blank = sample
Nitrite NO_2^-	**diazotisation method, 8507** 0 – 0.350 mg/L 0.005 ± 0.001 mg/L	Fe^{2+} and Cu^{2+} lead to low results; if NO_3^- > 100 mg/L small NO_2^- quantities develop during analysis, strongly oxidizing/reducing substances interfere in all quantities, ions of Sb, Pb, Chloroplatinate, Fe(III), Au, Cu, Metavanadate, Hg, Ag, Bi interfere by precipitation	10 ml sample/blank blank = sample
Sulfide S^{2-}	**methylene blue method, 8131** 0 – 0.70 mg/L 0.01 ± 0.02 mg/L	strong reducing agents (Sulphite, Thiosulphate, Hydrosulphite, high Sulphide) restrain the colour development, turbidity	25 ml sample/blank blank = distilled water

From the possible interferences listed in Table 4 the following may have played a role during on-site analysis and will be discussed in detail later. High Chloride values (> 100 mg Cl/L) in the 115 ft and 280 ft piezometers may have caused to low measured Nitrate values. High turbidity/sample colour in the 280 ft well may have interfered the sulphide analysis, but should not have caused to high Ammonium values, because Ammonium samples were diluted (1:100) before analysis. The occurrence of Nitrite has influence on the determined Nitrate values. Iron, especially the extremely high values recognized in the 280 ft well, may have interfered the Iron, Manganese, Ammonium, Nitrate, and Nitrite determination. The assumption that extremely high Iron has influence on measured NH_4^+ -contents was checked additionally in the hydrogeology lab of Freiberg University with Iron values adapted to 280ft-field conditions and delivered slightly decreasing results for NH_4^+, the higher the added Iron (II)-quantity was.

3.1.1.4 On-site titration for alkalinity and acidity determination

The parameters **alkalinity** (content of HCO_3^-) and **acidity** (content of H_2CO_3) were determined by titration with 0.1 molar HCl and 0.1 molar NaOH respectively, using the HACH Digital Titrator. The number of rotations divided by 800 gives the volume of acid or base used for the titration and the equation below the molarity of HCO_3^- or H_2CO_3. To convert the values into the mass concentration [g/L] the results were multiplied by the molar mass of HCO_3^- (61.987 g/mol) or H_2CO_3 (43.980 g/mol) respectively.

HCO_3^-/H_2CO_3 [mol/L] = volume of acid/base [L] molarity of acid/base [mol/L] / volume of sample [L]*

During these measurements problems occurred with the pHep from Hanna Instruments. With its rectangular shape and the size of approximately 1 cm * 2 cm it did not fit in the circular opening (Ø 1cm) in the cap of the titration vessel. Thus, the titration had to be performed with the open vessel, which enabled Carbon dioxide to enter or leave the sample. Due to simple manual one-point calibration that has to be carried out with a screw driver, it must be considered that the pH-measurements were not as accurate as with the HACH probes (see Table 3). Hence, the values determined for alkalinity and acidity may not be reliable and will be highlighted separately in the results. (Therefore HCO_3^- -concentrations in the samples were alternatively determined by calculating them from the measured TIC-values in the lab with help of PhreeqC.)

3.1.1.5 Sampling for laboratory analyses

Four water samples were taken from every well for the subsequent analysis in the lab. All samples were filtered through a 0.2 µm Sartorius cellulose-acetate filter. The sample bottles were washed two times with approximately 20 ml of filtered sample, before they were filled up to the rim with sample and carefully closed. Only the Trent-samples for determination of As-, P-species and -totals were acidified for preservation with 500 µL of 1+1 diluted hydrochloric and nitric acid respectively. Acidification of all samples collected during the day was done generally in the evening, so that individual samples were left filtered, but not stabilized for approximately up to 12 – 14 hours. While the HNO_3-acidified samples for totals are most likely not affected, changes in the speciation might have occurred in the samples for speciation before addition of HCl. Potential effects will be discussed in section 4.2.1.4.

Table 5 shows the sampling conditions in short form. At the test site no refrigerator was available, so for one to two days after each sampling it was not possible to cool the samples. But back to Dhaka the samples were stored in a refrigerator before sending them to Freiberg University, Germany and Trent University, Canada via express mail for analysis.

Table 5 *Sample denotation, sampling conditions and subsequent usage of the water samples, taken during each monitoring*

Sample denotation	Freiberg, IC	Freiberg, TIC/DOC	Trent, ICP-MS	Trent, AEC-ICP-MS
Sample size	50 ml	100 ml	50 ml	50 ml
Bottle type	polyethylene	glass	polyethylene	polyethylene
Filtration pore size	0.2 µm	0.2 µm	0.2 µm	0.2 µm
Reagents used for conservation, their amount and dilution	none	none	500 µL HNO_3 (1+1 diluted)	500 µL HCl (1+1 diluted)
Analysis method	IC	TIC/DOC	ICP-MS	AEC-ICP-MS
Measured parameters	cations (Li^+, Na^+, NH_4^+, Ca^{2+}, Mg^{2+}, K^+), anions (F^-, Cl^-, NO_2^-, NO_3^-, Br^-, PO_4^{3-}, SO_4^{2-})	total inorganic carbon, total dissolved organic Carbon	totals for As, P	speciation of As (Arsenite, Arsenate, Monothio-arsenate), P (Phosphate, unidentified P-species)

3.1.2 Water levels at the test site

The variations of the water tables [m below well head] at the test site piezometers in Titas/Daudkandi were measured regularly with an electric contact gauge (Spohr, Type 733, 50 m cable) during each monitoring over the whole time period from September to December 2007.

3.1.3 Aquifer tests

Pump tests were conducted at the 85, 115, and 280 ft test site wells at the 6th, 7th and 8th of November, to gain knowledge about the aquifer hydraulics.

3.1.3.1 Equipment and set-up of the aquifer tests

The 85 ft well represents the shallow aquifer, the 280 ft well the deeper aquifer, whereas the115 ft well taps the sand pocket within the upper clay aquitard. The well arrangement at the test site is shown in Figure 15. The distance between two directly neighbored wells is approximately 5 m.

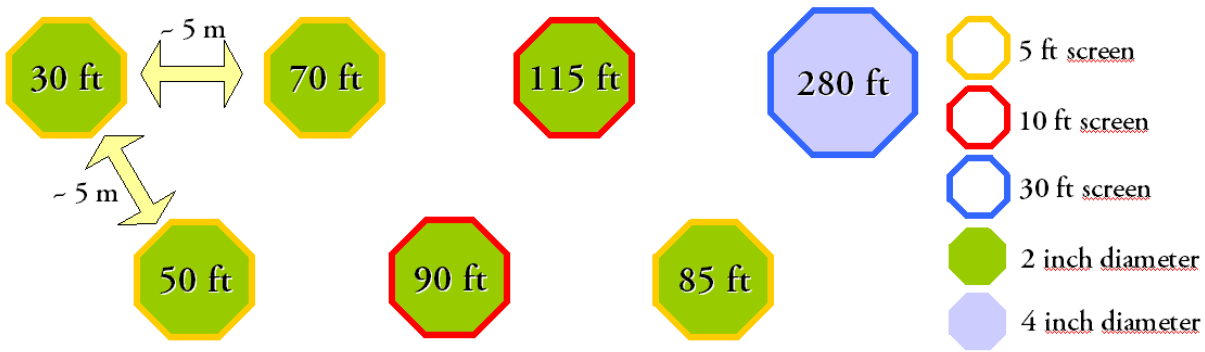

Figure 15 *Arrangement of the wells at the test site, approximate distance, their diameter and screen length*

The 115 and 85 ft wells, both having two inches diameter, were suitable only for the application of a submersible pump. The 280 ft well provided a sufficient diameter of four inches to utilize a more powerful submersible pump. All the necessary technical equipment and technical personnel for the maintenance of the equipment was provided by the M/S. Doyal Enterprise, Dhaka. Table 6 represents the technical data of the utilized pumps. In the evening before each aquifer test the staff installed the pumps and executed a short test run (see Table 6).

Table 6 *Technical data of the utilized pumps*

well	85 and 115 ft: suction pump	280 ft: submersible pump
pump	GRAMEEN shallow tubewell pump,	BIZZI & TEDESCHI,
technical data	Fuan Yongheng Electrical Machinery, China	Campegine (RE) Italy
	Model: SWP 100L	Model: S 200/9, motor type PL4-2M
	Output: 0.75 kW, 1 HP	Output: 1.5 kW, 2 HP
	Q = 70 l/min (= 1.2 l/s)	Q = 80 – 240 l/min (= 1.3 – 4 l/s)
	max head 48 m, max S. head 9 m	H = 5 – 19 m

The pump rate itself was not adjusted or measured directly. Instead it was regulated indirectly by the engine output of the quite archaic diesel generator that in turn was checked with an ampere meter by the technical personnel (see Figure 16). Hence, from this setup a really constant pump rate can not be expected. Data recorded during drawdown have to be considered with caution.

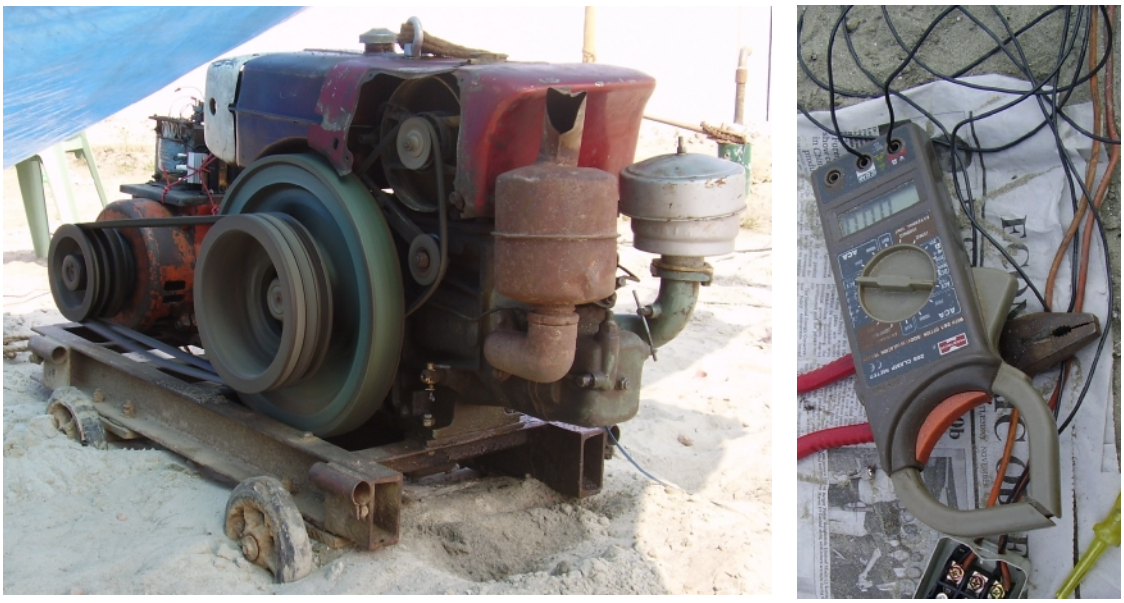

Figure 16 *Left picture: Generator with a diesel engine used for the power supply, Right picture: Ampere meter utilized by the staff to adjust the pump rate by measuring the generated current.*

Figure 17 shows the pumps in action. Obviously disadvantageous during the tests was that pumped water could not be discharged by a tube in some distance from the wells, which would prevent potential direct re-recharge of the aquifer besides the well.

Figure 17 *Pumping tests at the test site, using a submersible pump at the 280 ft well (left picture) and a suction pump at the 85 ft well (right picture). (The left picture shows that the agricultural low-land besides the test site partly still is inundated and overgrown by floating water hyacinths in beginning of November 2007)*

On the other hand, the construction of the hospital base foundation, consisting of several alternating layers of sandy material and plastic sheeting (Figure 18), should prevent quick infiltration of the water during the short time (max. 5 hours) aquifer tests. Most of the water ran off at the surface of the artificially elevated hospital basement area (50 – 100 m) and then discharged to the still inundated low-land.

Figure 18 *Base foundations in Bangladesh, here at the Titas hospital complex and its access road, consist of alternating layers of sandy material and plastic sheeting (the left picture showing the wall around the hospital complex, was photographed by B. Planer-Friedrich in February '07, the right one shows the access road to the hospital, taken by the author in November '07)*

3.1.3.2 Water level measurements

The main task of the aquifer tests was the monitoring of the changing water levels [m] as a function of time during drawdown and recovery with electric contact gauges at all test site wells. Five gauges were available. The Spohr-gauge (Type 733) was used at the pumped well, whereas the

simple (self-made) gauges provided by the MS Doyal Enterprise were utilized a the piezometric wells. As general approach, in the first ten minutes of the drawdown/recovery readings were taken in short time intervals of 0.5 to 1 min in the pumped well and two "primary" piezometers (see Table 7). Then, stepwise 10, 30 and 60 minutes after pump start/stop the reading intervals were stretched to 2, 5 and 10 min. From the outset it was planned to take readings less often in the "secondary" piezometers, due to a lack of staff (only 3) and gauges (only 5). In any case, the exact reading time was noticed per each water table measurement.

Table 7 *Pump-wells, primary and secondary piezometers during pump tests*

Date	Pumped well	primary piezometers	secondary piezometers
11/06/07	280 ft	115 ft, 85 ft	90 ft, 70 ft, 50 ft, 30 ft
11/07/07	115 ft	90 ft, 85 ft	70 ft, 50 ft, 30 ft, (280 ft)
11/08/07	85 ft	90 ft, 70 ft	50 ft, 30 ft, (115 ft, 280 ft)

Per pump test it was planned to pump and measure the drawdown for approximately 5 hours, then stop the pump and take water table readings of the recovery. For the 115 ft and 280 ft test this target could be fulfilled. But during the 85 ft-test the generator broke down after approximately 2 hours pumping time and the recovery measurement was started immediately.

3.1.3.3 Determination of the pump rate

Since for subsequent hydraulical calculations also the knowledge of the pump rate Q is necessary, a 17 litres bucket was used to determine the time needed until it was filled up to the rim with the pumped water. Then Q can be calculated by dividing the volume of the bucket [L] by the time for filling [s]. Per measurement this procedure was repeated three times to get an average pump rate. To notice fluctuations of the pump rate, Q was determined at several time points during each pump test.

3.1.3.4 Checking of water chemistry before, during, and after aquifer tests

To see the effect of higher water withdrawals on the water chemistry of the test site piezometers, one full monitoring preceded the three pump tests (Monitoring No. 27, 4th/5th of November 2007) and one was conducted directly thereafter (Monitoring No. 28, 8th/9th of November 2007).

Moreover, the parameters pH, electrical conductivity [µS/cm], redox potential [mV], Oxygen concentration [mg/L], Oxygen saturation [%] and temperature [°C] were determined in the pumped well water approximately every ten minutes during drawdown.

During each pump test it was planned to take samples for Arsenic species, either with the De Walt pump (after 10 minutes purging) or the running test pump, from all seven test site wells before pump start, before pump stop and after recovery. This worked out well for the 280 ft and 115 ft tests, but during the 85 ft test the generator suddenly broke down before the second sampling was done. An alternative sampling directly after pump stop was not possible, because the water recovery had to be monitored immediately. Thus, only from the 85 ft well a sample, taken for electrochemical measurements some time before the generator broke down was available yet. The 28th monitoring was started directly after the recovery at the 85 ft well was finished. Besides this, a sampling with the De Walt pump during the 85 and 115 ft tests was not possible at the 280 ft well, due to the fact that the submersible pump could not be removed from the well directly after finishing the test. The sampling code during the pump tests was TF(= test site) **.** PT(= pumping test)_pumped_well_depth(ft) . sampled_well_depth(ft) **-** sample_number. I.e. for the first sampling at the 30 ft well before pump start at the 85 ft well the sampling code is TF.PT85.30-1

3.1.4 Water tables at irrigation wells

Water level measurements of irrigation wells in Titas/Daudkandi were performed two times on an area of approximately 3 km². The first survey of water tables was carried out during mapping of 60 irrigation wells at the 1st and 2nd of December 2007. The second survey was done whilst the levelling of 46 irrigation and the seven test site wells at the 10th and 11th of December 2007 (see chapter 3.1.5). The used instruments were a electric contact gauge (Spohr, Type 733) to measure the groundwater table [m below well head] and a GPS-device (Etrex, Garmin) to locate the horizontal well position. Not all irrigation wells were recorded twice, due to difficulties to track them. Most farmers hid the closed well heads beneath a soil layer of up to 30 cm thickness. This prevents clogging of the well with mud when it is not in operation, especially during monsoon time. Figure 19 shows that several parts of the investigated area were still uncultivated or even inundated during the mapping in beginning of December. Often the soil layers above well heads were unscathed and sparsely overgrown by weeds. Only two farmers were found irrigating their fields during the whole survey (Figure 19). Thus, it can be assumed that many of the wells probably was not oper-

ated since beginning of monsoon, due to a still sufficient water yield. It is likely that Steinborn (2008) found a completely different situation, (i.e. many operating irrigation wells, whole area cultivated) whilst mapping of wells and water tables in the dry season from February throughout May 2007.

south-eastern region

south-western region

irrigation in the central-western region

north-western region

Figure 19 *Situation at Titas agricultural area at the 1st of December 2007,*

3.1.5 Well head positions and elevation of the land surface adjacent to wells

To obtain the positions of the irrigation and test site well heads, their exact altitude was determined with levelling tools, contemporary to the horizontal positioning with a Garmin GPS (E-trex). Further the altitude of the land surface neighbouring the mapped wells was levelled too. This work was proceeded from the 9th to the11th of December 2007 by the Land Survey Team, Dhaka in presence of the author.

To gain the absolute elevation above sea level, the leveling started at the Hospital Complex in Gauripur, where the fixed benchmark point BM-6044 of the Geological Survey of Bangladesh

(GSB) is located. BM-6044 has the coordinates 90.70562141760° E and 23.52910568860° N (Date: Kalianpur 1937, Everest Bangladesh) as well as an altitude of 5.348 m above mean sea level.

Figure 20 *Leveling of irrigation wells at Titas/Daudkandi, pictures shot at the 11th of December 2007*

3.1.6 Field injection spike

To check if Arsenic can be mobilized by increasing Phosphorus concentrations, at the 30th of November 2007 an on-site injection spike test was performed at the 85 ft well. Lissner (2008) already did comparable tests in the lab with the sediment samples. Figure 21 shows a simple schematic representation of the input parameters of the on-site test. The volume V_{sc} at the screen is 3 L, calculated with the following equation:

$$V_{sc} = \pi * r^2 * l_{sc} = (0.025\ m)^2 * \pi * 1.52\ m = 0.003\ m^3 = 3\ L$$

Thus, 3 L of the P-solution were pumped down to the filter with the De Walt peristaltic pump. To press the P-solution into the aquifer, immediately after injecting the P-solution 50 L (V_{fl}) water of a nearby hand tube well (HTW) were poured into the well. To get an estimation of the minimum groundwater volume (V_{igw}) influenced by the spike, the radius **x** of the spike plume surrounding the well screen is necessary. It can be calculated from the flushing volume V_{fl} and the surface of the screen casing A_{sc}:

$$A_{sc} = \pi * 2r * l_{sc} = \pi * 2 * 0.025\ m * 1.52\ m = 0.24\ m^2$$

$$x = V_{fl} / A_{sc} = 0.05\ m^3 / 0.24\ m^2 = 0.21\ m$$

$$V_{igw} = (\pi * (x + r)^2 * l_{sc}) = (\pi * (0.21\ m + 0.025\ m)^2 * 1.52\ m) = 0.26\ m^3 \sim 0.3\ m^3 \sim 300\ L$$

It was assumed that approximately up to 300 L of groundwater surrounding the 5 ft well screen will be influenced by the P solution. The calculations for the necessary P-amount base on the

natural As concentrations in the 85 ft well of approximately 0.2 mg/L. From this value derives an equimolar P-concentration of 0.1 mg P/L.

To be sure that a mobilization effect can be noticed, a tenfold excess concentration of 1 mgP/L was assumed. To reach a 1 mg/L concentration in the 300 L groundwater surrounding the filter, finally 300 mg P must be added to the aquifer water. This results in a spike solution concentration of 100 mg P/L. The P-solution was made of Potassium-di-hydrogen-Phosphate (KH_2PO_4, MERCK®). To receive a 100 mg/L concentration, 439.37 mg KH_2PO_4 were dissolved per litre distilled water at the laboratory of Dhaka University. The basic calculations are demonstrated in Appendix B9. Before injecting the P solution in the 85 ft well, samples for P-/As-species and -totals were taken as well as the on-site Parameters pH, E_H, EC, O_2, Fe, Mn, NH_4^+, NO_3^-, NO_2^- and S^{2-} were measured, to get knowledge about the background water chemistry. To be able to infer the influence of the hand tube water, a sampling similar to the 85 ft investigations, was done there too.

To get information about how fast the water infiltrates, well water tables were measured before and after adding the total 53 L to the 85 ft. Then further monitorings were done at the 85 ft well 2, 7, 17, 28, 52 and 71 hours after the P-injection. The sampling code is as follows: TF(=test field).INJ85(=injection_well).sampling _number, i.e., the sampling code for the second sample taken 7 hours after injection is “TF.INJ85.2”. The code for the hand tube water is “TF.INJ85.HTW”

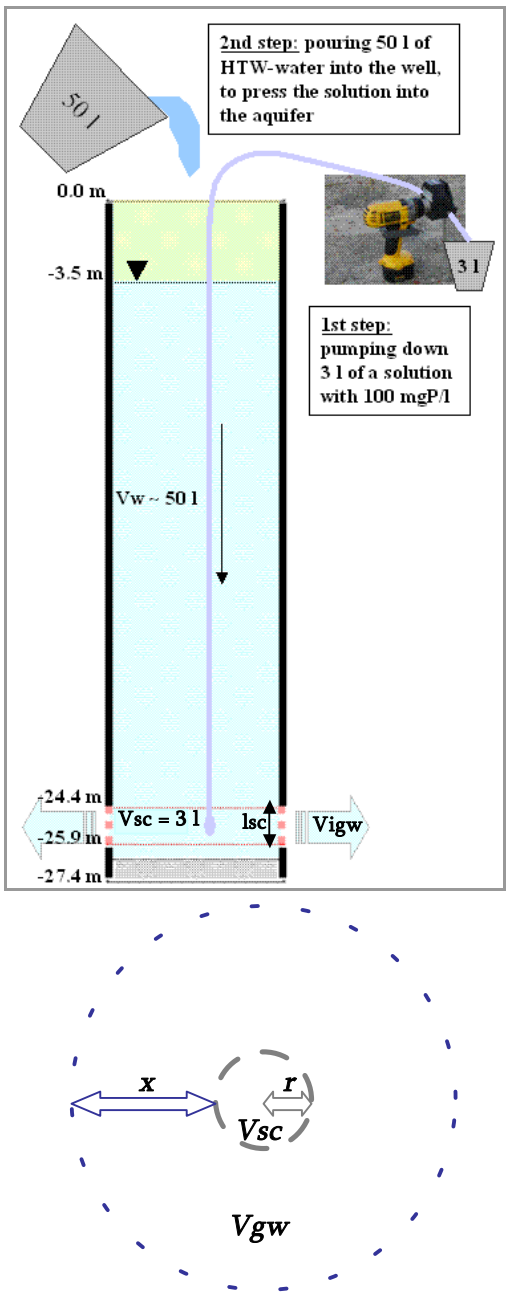

Figure 21 *Schematic diagram of the injection spike test at the 85 ft well and cross section at the screen*

3.2 Analytical methods used in laboratory

3.2.1 Determination of TIC and DOC

The total inorganic (TIC) and dissolved organic (DOC) Carbon content of the non-acidified samples in glass bottles was determined by the author at the laboratory of the Chair of Hydrogeology at Freiberg University, Germany in the time period from 11th until 31st of January 2008 with the Elementar LiquiTOC analyser. For the TIC measurements the LiquiTOC transforms all inorganic Carbon in the sample with phosphoric acid (H_3PO_4) to CO_2 gas, which can be determined with the NDIR-detector. After TIC is severed, DOC is measured by oxidation of all organic substances in solution with Sodium-Peroxy-Bisulphate. The samples were not opened before measurement, to avoid changes of the TIC-content by contact with atmospheric Carbon dioxide. Some TIC values were determined in the previously not opened 50 ml PE IC-samples, because several of the glas bottles were broken. These samples are highlighted separately. DOC values lack in this case, because there was not enough sample left for both – IC and DOC determination. Further organic substances may interact with the surface of the plastic bottles, hence one would measure no reliable data.

To quantify the concentrations in the samples from the peak areas (automatically calculated and printed by the LiquiTOC analyser) calibration curves were calculated by drawing the concentration of measured standard solutions as a function of the peak area. Besides the water blanks, the LiquiTOC measures the blank values of the reagents several times that might slightly change over the whole analysis time and have to be considered for the DOC values. Thus a linear blank correction was performed for the DOC values. In the results the total Carbon content TC [mg/L] in the samples is calculated from the sum of TIC and DOC.

3.2.2 Analysis of anions and cations with IC

In the time period 04th of February until 28th of March 2008 the major anions and cations in the non-acidified samples were determined by the author in the above mentioned laboratory. Ahead of the analysis the samples were filtered through a 0.2 µm Sartorius cellulose-acetate-filter in the lab a second time. For the anion analysis, an Eppendorf Biotronic IC 2001 chromatograph was utilized, working with separating and suppression columns from Frank Gutjahr Chromatography

and a Shimadzu "LC-10As" pump. A strong eluent concentration of 2 mM Na_2CO_3 plus 4 mM $NaHCO_3$, with a flow rate of 1.8 ml/min, was necessary to ensure an adequate temporal segregation of the peaks. The cation analysis was carried out with a Merck HITACHI chromatograph (Metrosep C2 as separating column, Metrosep C2 Guard as pre-column, L-3720 Conductivity Detector, L-5025 Column Thermostat, L-6200A Intelligent Pump, D-6000A Interface). The eluent, with a flow rate of 1 ml/min, was composed of 2 mM Nitric Acid, 1 mM Pyridine-2,6-Dicarbon Acid ($C_7H_5NO_4$) and 0.25 mM Crown Ether.

The peaks were identified by comparing the peak retention times in the samples with those of known standard solutions. Table 8 shows free ions and complexes that were identified in the Bangladesh samples. However, the results of Mn^{2+}, NO_2^-, NO_3^-, NH_4^+ and PO_4^{3-} did not undergo further consideration, because their stability in the non-preserved samples is not likely. Further Manganese and N-species were already measured on-site and Phosphate was determined in the preserved samples with AEC-ICP-MS.

Table 8 *Identified peaks, retention times (RT) with ion chromatography (see Appendix B4)*

Anions	F^-	Cl^-	NO_2^-	PO_4^{3-}	Br^-	NO_3^-	SO_4^{2-}
RT [min]	2.1	5.0	7.4	10.2	11.8	15.7	22.0
Cations	Li^+	Na^+	NH_4^+	Mn^{2+}	K^+	Mg^{2+}	Ca^{2+}
RT [min]	5.3	6.6	7.5	10.0	11.6	14.7	17.5

To quantify the concentrations, peak areas were determined with the analysis software WinPeak (anions) and OriginPro7.5 (cations), respectively. Then calibration curves were calculated by drawing the concentration of standard solutions as a function of the peak area.

The Flouride peaks of the first analyses (30 ft samples) often were overlain by a negative system peak signal. For further analyses the problem was solved by adding 10 µL of a concentrated eluent solution (2ml 1M Na_2CO_3 plus 4 ml 1 M $NaHCO_3$) to 2 ml of the sample or the standard. This led to a better temporal separation of both signals. Further a non-separable overlay occurred in the higher mineralised 115 ft and 280 ft samples between Flouride and another unidentified peak (both together around 2.2 min), so the fluoride concentrations could not be determined for these samples. Finally, dilutions were necessary to determine the high Chloride content and the high Sodium concentrations of the 115 ft and the 280 ft samples.

3.2.3 Flouride determination with an ion sensitive probe

Because the Flouride results with IC were not satisfying, due to negative peak overlay, the Flouride content in the 30 ft samples was additionally measured with a Flouride sensitive probe. Therefore, 25 ml of the sample or the calibration standard was mixed with 20 ml of a conditioning TISAB-solution (total ion strength adjustion buffer). The sensitive probe (WTW F-ISE, F^- 10 66 17) measured the potential E_F of the Flouride activity, while the reference, a probe with 1 M KNO_3 filling, determined the potential E_{Ref} in the solution. The reading potential [mV] was the difference of E_F - E_{Ref}. Finally the Flouride content in the samples was determined from a calibration curve, where the concentration of standards [mg/L] was drawn as a function of the measured potential [mV]. The calculations are demonstrated in Appendix B5.

3.2.4 Speciation and totals of As and P with AEC-ICP-MS and ICP-MS

For Arsenic and phosphorous speciation and the determination of total As and P samples were sent off to Trent University, Peterborough, Canada. Detailed information about the method can be found in Planer-Friedrich, B. et al. (2007) and Wallschläger and Stadey (2007). In brief, the utilized method is as follows: The speciation was done using the HCl-acidified samples in 50 ml plastic bottles by anion-exchange chromatography (Dionex, Sunnyvale, CA, column: IonPac AS-16) coupled to inductively coupled plasma mass-spectrometry (Elan®DRC® II, PerkinElmer, Shelton, CT) using a strongly alkaline eluent (0.1 M NaOH) to preserve potentially occurring Thioarsenate species. Simultaneous ICP-MS on-line detection of Arsenic (as AsO^+, m/z = 91), phosphorous (as PO^+, m/z = 47), and sulfur (as SO^+, m/z = 48) in eluting compounds was accomplished using the dynamic reaction cell (DRC®) technology with O_2 as reaction gas as described previously. Species identification was achieved by retention time match with commercial standards. Arsenite, Arsenate, and Phosphate were quantified using standard solutions made from solids ($NaAsO_2$, J.T.Baker, Phillipsburg, NJ; Na_2HAsO_4, Sigma-Aldrich, Oakville, ON; $NH_4H_2PO_4$, SCP Science, Bale d´Urfé, QC). Due to the lack of a commercial standard, Monothioarsenate was identified via retention time match with a synthesized Monothioarsenate standard (Wallschläger and Stadey, 2007) and routinely quantified using the Arsenate calibration curve. A new phosphorous species was detected with a retention time of approximately 185 s that neither matched the retention times of a Phosphite standard ($Na_2(PHO_3)$ ·5H2O, Riedel-de-Haen. Seelze, Germany; retention time 260 s) nor exactly that of a Hypophosphite standard (H2NaO2P·H2O, Sigma-Aldrich, Oak-

ville, ON; retention time 175-180 s), even though it was close to the latter. Until further identification it is referred to as “unidentified P-species” (abbreviated: “Punid”) in the following. Its quantification is based on the hypophosphite calibration curve.

Arsenic and Phosphorous total concentrations were determined independently from the sum of species by ICP-MS in samples preserved with Nitric Acid. Correction via an internal Rhodium standard (RhCl3·H2O, SCP Science, Bale d´Urfé, QC) was applied in case of longer analytical runs to compensate for instrument sensitivity drift. An analytical reference material (TM-DWS, Environment Canada, National Water Research Institute) was included in each run as standard check..

The peak detection for the species with the software OriginPro7.5 as well as the calibration curves and calculation of the quantity of the totals and species then was done by the author. For the species one standard solution was measured several times, serving as basis for a linear drift correction, whereas for the totals the instrumental sensitivity drift correction was proceeded on the basis of the internal rhodium standard. The mentioned proceedings are demonstrated in Appendix B1 (species) and Appendix B2 (totals).

3.3 Methods of data handling

3.3.1 Error of the analysis and Conductivity check

The percent error of each analysis was calculated with the hydrogeochemical modelling program PhreeqC for Windows, Version 2.15.02, developed by D.L. Parkhurst, C.A.J. Appello, V.E.A. Post. Using the wateq4f.dat database and the ‘spread sheet’-command, the input parameters had to be defined as follows: pH, pE, temp, Fe(+2), Fe(+3), S(-2), N(+5) as NO3-, N(+3) as NO2-, N(-3) as NH4+, Mn, Na, K, Ca, Mg, F, Cl, Br, S(+6) as SO4-2, C(+4) as C, As, and P as PO4-3. All concentrations were given in [mg/L], the temperature in [°C]. C(+4) is the measured TIC-concentration. The mentioned pE-value is a conversion of the redox potential E_H, necessary for calculations in PhreeqC. It’s expressed as the negative common logarithm of the hypothetic electron activity $\{e^-\}$, which is actually not present in water.

$$pE = - \log \{e^-\} = (F \cdot E_H) / (2.303 \cdot R \cdot T)$$

The previous equation contains aside from the redox potential E_H [V] and temperature T [K] also the Faraday constant F (F = 9.648 534 15 · 10^{04} C/mol) and the molar gas constant R (R = 8.314 472

J/(mol·K)). In combination with the WATEQ4F database PhreeqC computes the analytical error of the charge balance with the equation below, wherein the concentrations of cations and anions are given in [meq/L]. An example of the in- and output in PhreeqC is given in Appendix B7.

$$\text{Analytical Error [\%]} = 100^{*} (\Sigma \text{ Cations} - |\Sigma \text{ Anions}|) / (0.5 * [\Sigma \text{ Cations} + |\Sigma \text{ Anions}|])$$

Further, the cause for the analytical error was checked, i.e. the error was compared with the measured and calculated Conductivity, as shown in Table 9. The Conductivity of the samples was measured on-site, but also can be evaluated from the molar concentrations of H^+, OH^-, CO_3^{2-}, HCO_3^-, SO_4^{2-}, Cl^-, NO_3^-, F^-, Br^-, HSO_4^-, Ca^{2+}, Mg^{2+}, Na^+, K^+, Li^+, Fe^{2+}, Fe^{3+} and Al^{3+} in the samples (computed by PhreeqC) and their known equivalent ionic conductances at 25 °C given in literature. The used algorithm for the calculation is demonstrated in Appendix B7. Advanced information can be found in (Rossum, 1975) and (Coury, 1999).

Table 9 *Query structure and conclusion for the analysis*

Analytical error [%]	Electrical conductivity EC [µS/cm]	Conclusion
< 0	calculated EC > measured EC	too many anions
< 0	calculated EC < measured EC	lack of cations
> 0	calculated EC > measured EC	too many cations
> 0	calculated EC < measured EC	lack of anions

3.3.2 Limit of detection (LOD) and limit of quantitation (LOQ)

The limit of detection (LOD) of a given analytical method equals the concentration that represents the smallest measure of an analyte that is significantly higher than the background noise, i.e. still detectable with adequate certainty (Hötzl and Witthüser, 1999), (Merkel and Planer-Friedrich, 2002). It can not be assumed that when no signal was obtained during a measurement, the target value is truly equal to zero mg/L. The true value might lie between the LOD and zero. Thus all values measured in the lab that are lower than the detection limit, "zero" values included, will be substituted by the LOD within the list of the results. During statistical analyses with SPSS16.0 and in graphical presentations all values below LOD will be substituted by the product 0.3 *LOD, which in principal will be rounded up to one last certain digit unequal to zero. This procedure is necessary, because statistical software uses one consistent scale level for all values per variable. SPSS 16.0 can not compute with interval-scaled values (i.e. "0.5") and nominal scaled values (i.e. "< 0.5 ") listed within one variable. Nevertheless, for calculating statistical values that describe the

whole population in Appendix B8 (mean, median, quartiles, standard deviation, maximum, minimum) the values equal or below detection limits and missing values were not included in the calculation as recommended by Hötzl and Witthüser (1999).

The detection limits of the parameters measured in the laboratory were approximated with the help of the 95 % confidence intervals. Therefore the peak areas were drawn as a function of the concentrations determined together with their regression function and the confidence intervals with the software SPSS16.0. First from the intersection of the upper confidence interval with the y-axis a horizontal straight line, parallel to the x-axis was drawn. Then from the point where this straight line intersects the lower confidence interval another vertical straight line, parallel to the y-axis was drawn. Finally the detection limit equals the point on the x-axis that intersects with the vertical line.

From the photometrical field measurements the LOD can not be ascertained by this procedure, but the limit of quantitation (LOQ) was given in the HACH manuals (Appendix C4). This will be used to substitute measured zero values in the list, in analogy to the remarks mentioned regarding to LOD. Table 11 shows the detection limits of the laboratory parameters, together with the calculated values for the product 0.3 *LOD that in principal were rounded up to one last certain digit unequal to zero.

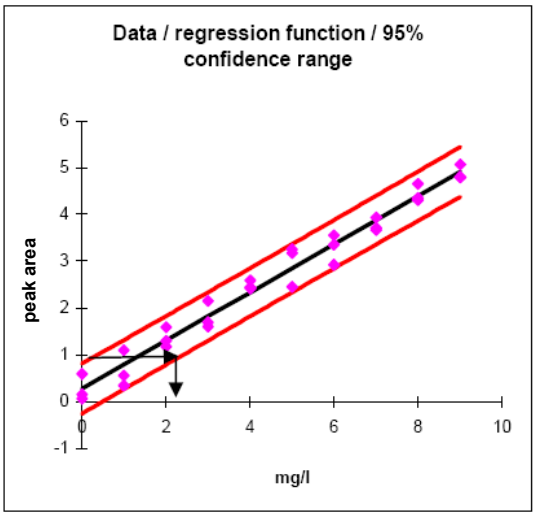

Table 10 *Determination of the detection limit, the graphical representation derives from (Merkel and Planer-Friedrich, 2002)*

Table 11 *Limits of Detection for the laboratory parameters*

Anions	LOD	0.3*LOD	Cations	LOD	0.3*LOD	other	LOD	0.3*LOD
F [mg/L]	< 0.05	0.02	Na [mg/L]	< 0.3	0.1	TIC [mg/L]	< 0.6	0.2
Cl [mg/L]	< 0.4	0.1	K [mg/L]	< 0.3	0.1	DOC [mg/L]	< 0.3	0.1
Br [mg/L]	< 0.10	0.03	Ca [mg/L]	< 0.3	0.1	P tot/spec. [µg/L]	< 0.5	0.2
SO4 [mg/L]	< 0.2	0.1	Mg [mg/L]	< 0.2	0.1	As tot/spec. [µg/L]	< 0.5	0.2

3.3.3 Statistical methods

Statistical data checks and analyses were done with SPSS16.0. The data were checked for outliers. But only outliers that surely were identified to base on measurement errors were excluded from later statistical analyses. Also a consistent scale level was defined per variable. Normality tests were executed with all variables, showing that most variables did not follow a gaussian distribution. Due to this, the coherence between two parameters was checked with the nonparametric Spearman rank correlation. The two-tailed significance level p gives the probability of the error. The value $p \leq 0.05$ was established as level of significance for the whole study. That means, applying the Spearman rank correlation, a statistically significant coherence is assumed to exist between two tested variables, if $p \leq 0.05$. Further information about statistical analyses describes the SPSS-manual from Bühl (2006).

Groundwater types were classified with a hierarchical cluster analysis with SPSS16.0, based on the results for the major cat- and anions per each well. This cluster analysis applies the average linkage[1] between groups by calculating absolute squared Euclidean distances (Bühl, 2006). A Dendrogram display shows the similarities between possible clusters. To check if the clusters (= groundwater types) really belong to different populations (H_a) or come from identical populations (H_0), the results of major cat- and anions were compared with the Kruskal Wallis test. Kruskal Wallis compares three or more independent groups of sampled data.

A possibility to visualize the found groundwater types is the triangular presentation, developed by Piper in1944 (Matthes, 1994), which is based upon the equivalent percentages [meq%] of the major cations and anions. Such diagrams in general allow the comparison between numerous water samples, show outliers, the range of dispersion, and also the effect of mixing between different waters. In 1967, Davies and De Wiest additionally developed a classification system for waters, shown in Figure 22 (Matthess, 1994). It must be noted that a graphical representation with the equivalent percentages of the ions [meq%] does not consider real absolute concentrations.

[1] **Linkage between groups:** The distance between two clusters is the average of the distances of all possible pairs of cases, whereas one case is taken from one, the other case from the other cluster. The information, necessary for the distance-calculation is ascertained from all theoretical possible distance-pairs (Bühl, 2006).

Thus, waters of distinctly different concentrations can look the same in this representation (Matthess, 1994). With the monitoring data such a representation was created with the software RockWorks 7.11. The concentrations [mg/L] of the major cations (Bicarbonate, Carbonate, Chloride, Sulfate) and anions (Sodium, Potassium, Calcium, Magnesium) were entered directly in the program. From this data base RockWorks 7.11 automatically calculates the equivalent molar concentrations and percentages of each ion, and computes the diagram.

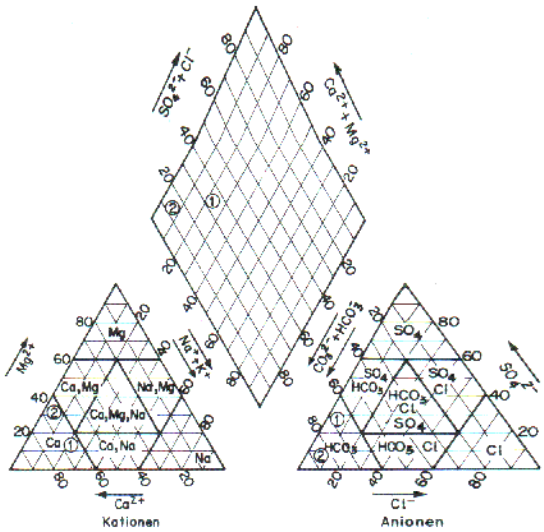

Figure 22 *Trilinear presentation after PIPER (1944) with the classification of water types after Davies and De Wiest (1967). (Matthess, 1994).*

3.3.4 Hydraulical permeability K based on grain size analyses

LISSNER (2008) determined the grain size distribution of 36 samples taken during rotary drilling at the test site, which was used for the calculation of the hydraulical permeability K [m/s]. LANGGUTH AND VOIGT (1980) in detail describe empirical procedures based on granulometry. Here the methods after Hazen (1964) and Beyer (1961) were utilized, which base on the grain diameters that make up 10 % (d_{10} [mm]) and 60 % (d_{60} [mm]) of the sample, the degree of uniformity U = d_{60}/d_{10}, as well as the temperature of the groundwater T [°C]. The values d_{10} and d_{60} were read off from LISSNER'S graphs of log (grain size [mm]) vs. percentage of grain size [%] in Appendix C2. Basic assumptions for both methods are that d_{10} corresponds to the hydraulically effective grain size, and the groundwater generally should show a low mineralisation (< 500 mg/L). The results for K from HAZEN'S equation below are valid only for U ≤ 5.

$$K = 0{,}0116\, d_{10}^2\, (0{,}7 + 0{,}03\, T) \qquad \text{HAZEN (1892)}$$

In BEYER'S equation the parameter C was established that depends on the lithological structure of the sediment and its degree of uniformity U, as shown in Table 12.

$$K = C * d_{10}^2\, (0{,}7 + 0{,}03\, T) \qquad \text{BEYER (1964)}$$

Results for K are valid only in the range $0.006 \leq d_{10} \leq 0.6$ mm and $1 \leq U \leq 20$.

Table 12 *Relation between U and the proportional constant C*

range of U	range of corresponding C values	average C
1.0 – 1.9	(120 – 105) * 10^{-04}	110 * 10^{-04}
2.0 – 2.9	(105 – 95) * 10^{-04}	100 * 10^{-04}
3.0 – 4.9	(95 – 85) * 10^{-04}	90 * 10^{-04}
5.0 – 9.9	(85 – 75) * 10^{-04}	80 * 10^{-04}
10.0 - 19.9	(75 – 65) * 10^{-04}	70 * 10^{-04}
> 20.0	(< 65) * 10^{-04}	60 * 10^{-04}

3.3.5 Transmissivities T and hydraulical permeability K based on aquifer tests

The 115 ft (unconfined, unsteady state) and 280 ft (leaky-confined, probably steady state reached) tests were single well tests. During 85 ft test (unconfined, unsteady state) the drawdown in neighboured wells (90, 70 ft) was to low to consider them as reliable. The complete data and graphical representations can be found in Appendix B10. Most problematic is the fact that single well tests in partial penetrating wells under slightly instable pumping rates had to be analysed. Prerequisite assumptions made for pumping tests are listed in the following box. It is obvious that not all of the general assumptions could be fulfilled. Methods for correction of the drawdown data (Huismann, Hantush, Streltsova) require at least one additional monitoring well (Kruseman and de Ridder, 2000).

General assumptions for aquifer tests ➔ Conclusions for Titas pumping tests
The aquifer has a seemingly infinite aerial extent. ➔ For the area influenced by the test the assumption may be true for 85 and 280 ft test. But, eventually not for the sand lens in 115 ft depth.
The aquifer is homogenous, isotropic. ➔ Unlikely. At Titas peat layers and interbedding of sandy material with clay lenses interfere this thesis.
The aquifer has a uniform thickness over the area influenced by the test. ➔ Unlikely. Layer extensions varied in different well litholog (see Figure 25).
Prior to pumping the piezometric surface is horizontal (nearly), over the area influenced by the test. ➔ Yes.
The aquifer is pumped by a constant discharge rate. ➔ No, the pump rates slightly varied over time.
The well penetrates entire thickness of the aquifer, i. e. receives water by horizontal flow. ➔ No. The wells are partially penetrating, during pumping also vertical flow components must be assumed.
Water removed from storage is discharged instantaneously with decline of head (unsteady state) ➔ Ok.

Due to this, Transmissivities **T**, and so far possible, hydraulical Permeabilities **K** were calculated with Theis's recovery method as quoted by Krusemann and de Ridder (2000). A semi-log graph of the residual drawdown s' vs. the quotient t/t' (= time since pumping/time since pump) stop was plotted, under excluding early data, influenced by well storage. The residual drawdown difference Δ s' per log-cycle was determined.

*Transmissivity T = (2,30 * Pumprate Q) / (4 * π * residual drawdown Δs')*

example: $\mathbf{T_{115ft}}$ = (2,30 * 0.00046 m^3/s) / (4 * π * 0.199 m) = **4.2 E-04 m^2/s**

Hydraulical permeability K = Transmissivity T / saturated aquifer thickness D

example: $\mathbf{K_{115ft}}$ = 4.2 E-04 m^2/s / 32 m = **1.3 E-05 m/s**

Theis's recovery method is a straight line method, valid for single well tests in confined, unconfined and leaky aquifers, provided that the well storage is considered. Partial penetration is negligible, so far pumping/recovery times are long enough (Kruseman and de Ridder, 2000). The prerequisite assumptions and their fulfilment are considered in the following box. Again not all assumptions could be fulfilled. Thus, the results should be considered as rough estimates for the real aquifer conditions.

Special Assumptions for Theis recovery method. ➔ Conclusions for Titas pumping tests
The aquifer is confined, leaky or unconfined, ➔ Ok.
For leaky aquifers the sum of pumping and recovery times should be $[t_p + t'] \leq [L^2S/(20T)]$ (t_p-pumping time, t'-recovery time, T-transmissivity, L-leakage factor, S-Storativity) ➔ Leakage through the aquitard layer may influence all aquifer strata. But, the leakage factor L, to check whether the assumption is fulfilled, is unknown.
For unconfined aquifers only late-time recovery data should be used. ➔ Probably not fulfilled for unconfined 85 ft well, pumping (2h) and recovery times (1h) were very short.
The flow to the well is in an unsteady state. ➔ Ok for 115, 85 ft, possibly not for 280 ft (steady state probably reached)
Storage in the well influences initial drawdown data. The conditions $t_p > 25\ r^2/T$ and $t' > 25\ r^2/T$ must be met. Concurrently minimum times for t_p and t' must be $> 500^*r^2/T$. ➔ Early data, obviously influenced by well storage (they did not fit to later straight line data) were excluded from the calculation of T and K. All time conditions for well storage and minimum pumping/recover time were fulfilled. (see Table 13)
The method for partial penetrated wells is applicable, so far both t_p and t' are $> D^2S/2T$ ➔ The partial penetration condition could not be fulfilled in the 115 ft well (t' to short), see Table 13.

Table 13 *Considering, whether the prerequisite conditions for Theis recovery method are fulfilled. Both, pumping time t_p and recovery time t' must be greater than **$25r^2/T$** and **$500r^2/T$** and **$D^2S/2T$**, respectively (t_p-pumping time, t'-recovery time, T-transmissivity, r-well radius, S-Storativity, Ss-Specific storage, D – saturated aquifer thickness)*

	well bore storage condition				partial penetration condition			measured times	
well	T [m²/s]	r [m]	25r²/T [s]	500r²/T [s]	D [m]	S = D*Ss [m/m]	D²S/2T [s]	t_p [s]	t' [s]
85 ft	6.31E-03	0.0254	3	51	32.0 m	3.14E-02	2,547	6,920	3,070
115 ft	4.20E-04	0.0254	38	768	32.0 m	3.14E-02	38,279	15,411	8,880
280 ft	3.04E-03	0.0508	21	425	12.2 m	1.20E-02	294	22,470	66,600

3.3.6 Actual evapotranspiration in 2007

For the calculation of the actual evapotranspiration (AET) in tropical climates like Bangladesh the following equation was used. Basic climate data, including precipitation (P) and the corrected potential evaporation (PEc) are listed in Appendix C3.

$$AET[mm] = P[mm]\frac{P[mm]}{\sqrt{1+(\frac{P[mm]}{PEc[mm]})^2}} \quad \text{(Mirza et al., 2003; Pike, 1964)}$$

As already referred to in the introduction (section 2.2.3), it's a fact that PE_c (9,911 mm in 2007) definitely overestimates and AET_{Pike} (2,262 mm in 2007) underestimates the real evapotranspiration from Titas agricultural lowland. Monthly PE_c-data seem to fit to the almost completely inundated areas during monsoon season, whereas AET_{Pike} can describe non-flood affected areas. Table 14 lists the factors per month which were used to get a better estimation for the actual evapotranspiration (AET_n) in 2007 with the following equation:

$$AET_n \text{ in } 2007[mm] = \sum_{1}^{12}(a_n * PEc_n[mm] + b_n * AET_n[mm]) = 5{,}225 \text{ mm}$$

Nevertheless, it must be assumed that AET_n gives an estimation only for natural, not anthropogenic influenced environmental conditions. Intense irrigation activities during months with a precipitation deficit (see section 2.2.3) will enhance evaporation from groundwater, resulting in a higher, anthropogenic altered AET_a. On the other side, artificially elevated areas (streets, villages) function as capillary barrier and feature more sparse or no vegetation. This will inhibit evapotranspiration from groundwater in such domains.

Table 14 *Factors for the calculation of real evapotranspiration from Titas agricultural low-land (factors for partial inundation are rough estimates, basing on the field surveys in these months)*

month	J	F	M	A	M	J	J	A	S	O	N	D	∑
situation	no flooding					complete inundation				partial inundation			-
PE_c [mm]	521	629	891	1000	1096	977	937	964	918	796	662	520	9,911
AET_{Pike} [mm]	0	20	21	176	152	478	536	215	318	264	81	0	2,262
a (factor PE_c)	0.0	0.0	0.0	0.0	0.0	1.0	1.0	1.0	1.0	0.7	0.5	0.1	-
b (factor AET_{Pike})	1.0	1.0	1.0	1.0	1.0	0.0	0.0	0.0	0.0	0.3	0.5	0.9	-

3.3.7 Map of Titas geography and irrigation wells

The levelling data (X, Y positions as well as water table) were imported into the GIS-software TNTmips 2007:73 (Micro Images, Inc.), to display their locations on a map. Water table elevations can be highlighted by selecting a well with the cursor. The related datum is Kalianpur1937 and the used projection is BTM (Bangladesh transverse mercator).

Based on the TNTAtlas created by Steinborn (2008) and its basic files that include a satellite image (QuickBird, ID 1010010005888203, Acquisition Date 2007-03-20, 60 cm 4-band PSM RGBI), a geographical feature map of the investigation area was generated. It includes the positions of the irrigation and test-site wells levelled during this survey, the locations of villages, and small ponds as well as the course of streets, important footpaths, and (temporarily dry?) drainage channels of tributaries. It serves as localization map for important features (bitmap formate) in the model.

3.3.8 Contour map of land surface elevation

Land surface elevations are known only beside wells, thus, land surface elevation help points were simulated in TNTmips, based on the geographical feature map. They mark the transition between high and low lying areas, i.e. the artificially elevated surfaces of villages and bituminised streets that suddenly deescalate to the naturally low lying agricultural areas. As elevation for villages, the hospital area, and the street the known average elevation of 5.54 m of the surface besides the test site wells was applied. For agricultural territories an average elevation of 2.67 m was calculated from the known land surface besides irrigation wells. From these data, via Kriging a grid-file of the land surface was generated with the software Surfer8 (Golden Software, Inc.).

3.3.9 Modelling with Visual Modflow

The modelling was done with Visual Modflow 3.0 under steady state conditions. The horizontal extension of the model depends on the positions of the most exterior levelled irrigation wells. The layer extension derives from the litholog data (LCD). A geographical map (bitmap) including surface features and well positions was imported to and georeferenced in Visual Modflow. Further, the land surface elevation was imported as grid-file. The following box lists further important input parameters:

Aquifer properties	Boundary conditions
Conductivity [m/s] horizontal permeability $K_{x,y}$ [m/s], determined from pumping tests and vertical permeability K_z [m/s] = 0.1* $K_{x,y}$ **Storage coefficients** Specific yield $S_{y, \text{fine sand}}$ = 0.23, effective porosity $n_{eff, sand}$ = 0.3, total porosity $n_{tot,sand}$ = 0.4 were estimated from literature values in Krusemann and de Ridder (2000). The value for specific storativity S_s derives from the following formula: $S_s = \rho * g * (\alpha + n_{tot} * \beta) = 9{,}83\ E\text{-}04\ 1/m$ (density of water ρ = 1 kg/m³, gravitational acceleration g = 9.81 m/s^s, compressibility of sand α_{sand} = 1.0E-07 m²/N, compressibility of water β = 4.4E-10 m¹/N, total porosity sand $n_{tot, sand}$ = 0.4, (Kruseman and de Ridder, 2000))	**Model bottom** Q=0, no flow after Neumann **Constant Head H [m MSL]** Q= f(H) after Dirichlet, at the model margin, based on known irrigation well head data **Recharge (EVT) [mm/year]** adapted during calibration **Evapotranspiration (EVT) [mm/year]** based on climate data, but further adapted during calibration

For the calibration of the model the observed heads, location and screen top positions of irrigation and test site wells were utilized. Assumed values for Recharge and Evapotranspiration were adapted during multiple calibration-steps. The stepwise development of the model and concrete values for input parameters are referred to more detailed in section 4.1.6. The model versions and input files are stored in Appendix B12.

4 RESULTS AND DISCUSSION

4.1 Hydraulic properties of the subsurface at the test site

4.1.1 Results of water table measurements at the test site

Repeated water table measurements in 2007 showed that the free water tables of the unconfined shallow aquifer (30, 50, 70, 85, 90 ft) and the sand lens (115 ft) communicated with each other, i. e. groundwaters in those depths are hydraulically connected (see Figure 23).

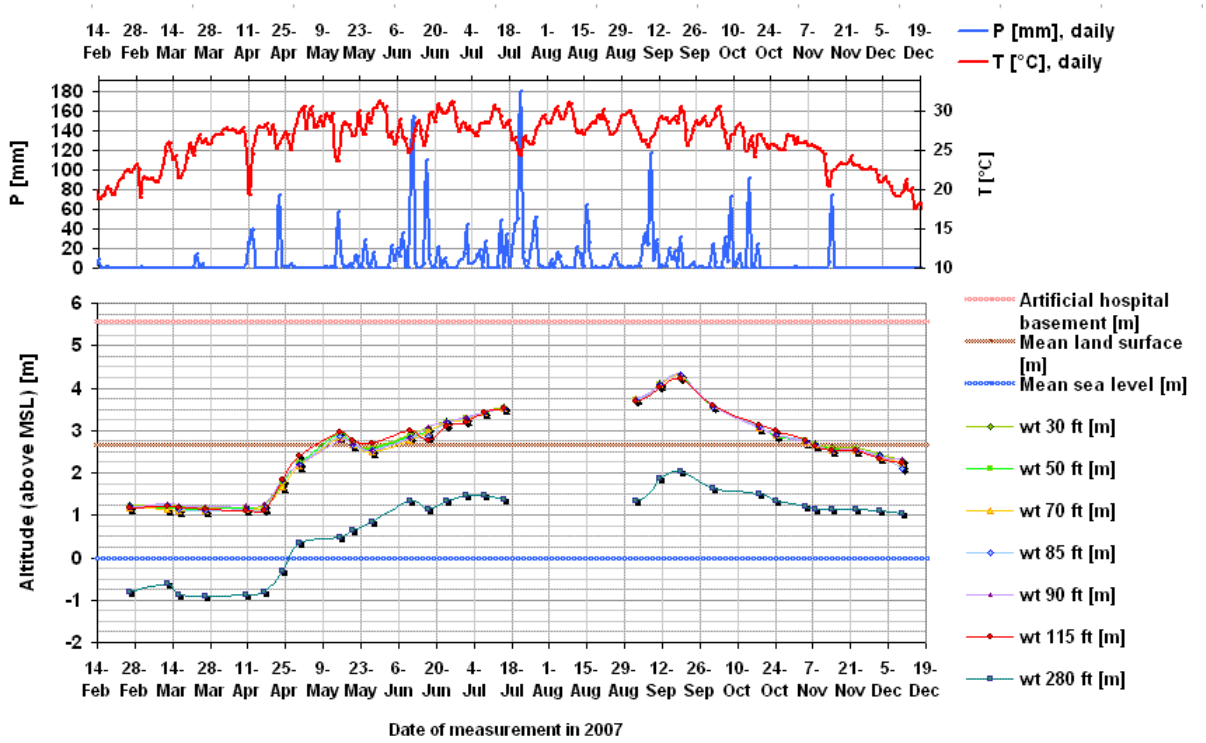

Figure 23 *Temporal variations of water tables (wt) at the seven test site wells in comparison with daily precipitation data in 2007.*

The piezometric head of the confined groundwater in the deep aquifer always lays distinctly below the water surfaces of the other wells and does not communicate directly with them. Nevertheless, the curve progression is similar, which is caused by seasonally changing recharge to and withdrawal from the groundwater. It can be assumed that water in general can move slowly downward through the aquitard, indicated by the lower piezometric head of the 280 ft well, tapping the laky-confined lower aquifer (Zahid et al., 2008).

Highest water tables are linked to the rainy monsoon season (Jun-Sep), whereas the lowest water tables were measured during the dry season (Feb-Apr), when the irrigation activities are most intense due to lacking precipitations, enhancing the direct evaporation and evapotranspiration from groundwater resources.

The line in Figure 23 assigning the average elevation (2.67 m) of the agricultural land surface at Titas, points out that already since beginning of June until end of October parts of the area were persistently inundated in 2007. The flooding did not affect the test site wells, because they are located on the artificially elevated hospital basement that has an average elevation of 5.53 m.

4.1.2 Results of the Aquifer tests

The complete pumping test data and graphical representations are stored in Appendix B10. The pumping tests at the 115 and 280 ft wells did not cause any drawdown in the adjacent wells. The 85 ft pumping test brought very little, almost negligible maximum drawdown of 11 cm and 6 cm in the 90 ft and 70 ft well, respectively. This must be due to the relatively low applied pumping rates in the partially penetrating, small diameter wells (see Figure 15 in section 3.1.3). It can be assumed that, if the application of higher pump rates in 85 ft and 115 ft depth was possible, this would have caused changes of the water tables in both neighbouring wells, because the sand lens and the shallow aquifer are hydraulically connected (see Figure 23). Due to this connection, for both wells the same saturated thickness of the unconfined upper shallow aquifer was presumed, based on the water tables before pump start and the location of the sand lense bottom.

During the 115 ft and 85 ft pump tests, definitely no stationary conditions were reached. The drawdown whilst the 280 ft pumping test appears to become stationary after two and an half hour of pumping. Unfortunately, a sudden water table decline (0.20 m) interrupts the drawdown curve progression, short before equilibrium conditions seem to be reached, making data interpretation difficult. The sudden decline probably is due to an abruptly changing pump rate (see drawdown curve progression in Appendix B10). However, Burgess & Ahmed (2006) report that as a result of leakage, equilibrium hydraulic conditions in Bangladesh aquifers can be reached within a few hours of pumping. Thus, the observations during the 280 ft pumping test may indicate the existence of a leaky-confined aquifer system at Titas.

All wells were only partially penetrating, i. e. featured limited screen lengths and the well base was not positioned in an aquiclude. This would induce higher drawdown in the well than would actually be observable in the aquifer, because turbulent flow conditions build up besides the well screen. Due to the aforementioned reasons and the fact that the pump rate was variable over time, it was reasonable to interpret only recovery data. Regarding the fact that during the 85 ft test no stationary conditions were reached and the drawdown in the neighbouring wells was very low, i. e. relatively uncertain in relation to the variable pump rates, it was reasonable to consider this aquifer test as single well test. The results of recovery evaluation with Theis's recovery method are shown in Table 15. The results for K and T should be seen as rough estimates of the real conditions, because not all prerequisite assumptions could be fulfilled for all the pumping tests, as already described detailed in section 3.3.5.

The calculation of K in the deeper aquifer must be considered with caution, because the aquifer thickness depends on the actual extension of the underlying clay layer, which is not known with certainty. The core drilling litholog only shows 4.3 m extension of the oxidized deeper aquifer layer. The 280 ft well ends within the aquifer layer, occupying 9.1 m of the aquifer sediment thickness. From the litholog of the hospital building company at thickness of at least 12.2 m was derived, by assuming the underlying clay layer (lens or extended aquitard?) to exist at least on a regional scale (see Figure 25). The correctness of this hypothesis can not be verified with the existing data basis. Thus, the result for K in 280 ft depth still remains uncertain.

Table 15 *Results from evaluation of recovery data from the pumping tests at the 85, 115 and 280 ft wells with Theis Recovery Method as described by Krusemann and de Ridder (2000). (The saturated thickness of the deep aquifer (280 ft well) is insecure, thus the result for K is just provisional)*

Pumping well (screen length) [ft]	Duration of pumping	Maximum drawdown [m]	Saturated aquifer thickness [m]	Last Q measured before pump stop [L/s]	Transmissivity T [m^2/s]	Hydraulical permeability K [m/s]
85 (5)	1 h 55 min	1.94	31.98	0.6	6.31E-03	1.97E-04
115 (10)	4 h 17 min	2.79	31.98	0.5	4.20E-04	1.31E-05
280 (30)	6 h 15 min	3.87	(12.20)?	2.5	3.04E-03	(2.49E-04)?

4.1.2.1 Comparison of K from aquifer tests with those based on grain size distribution data

Additionally, K was calculated based on the grain size distribution analyse by Lissner (2008). Strictly speaking, the methods after Hazen and Beyer are applicable only for non-cohesive rocks, i. e. sediments should feature minor amounts of silt and clay (see sediment properties in Table 2 in section 2.2.1). The results are visualized in Figure 24. It shows that the preconditions (as described in section 3.3.4) for the K-calculation after Hazen were not fulfilled in most cases, the results are not reliable. Beyer's preconditions are fulfilled only in the shallow and deep aquifer and the sand lens. But Beyer's K-results for the less permeable clay lenses/aquitards are not reliable either.

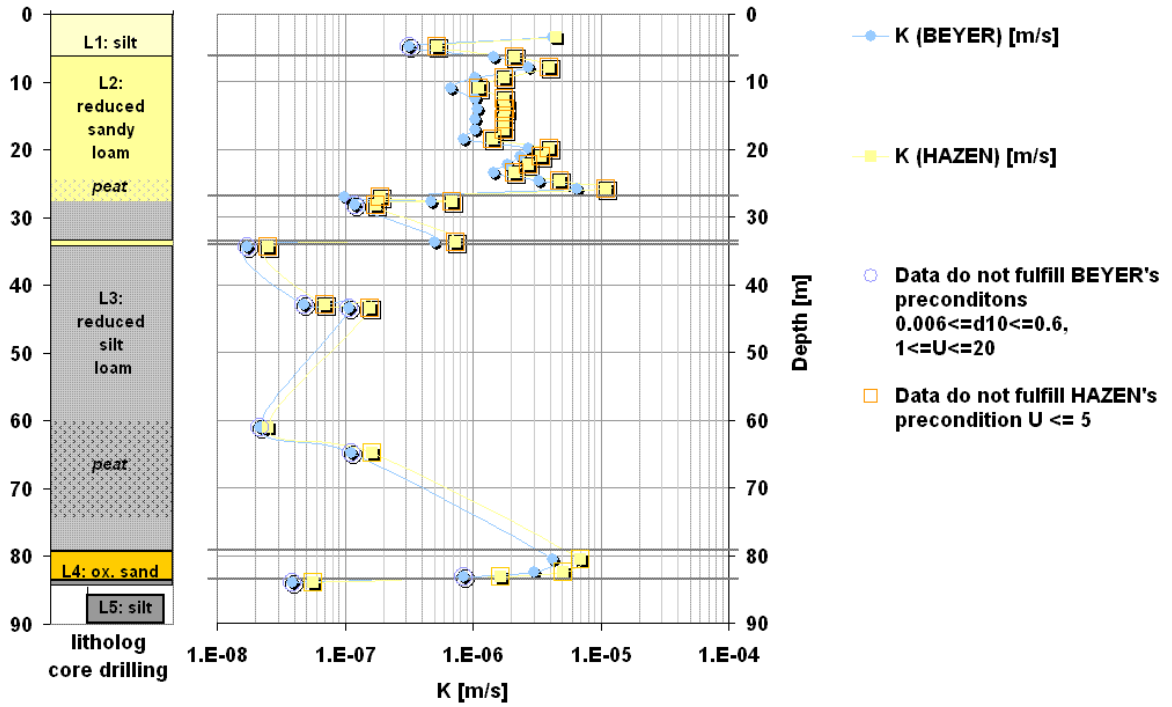

Figure 24 *Hydraulical Conductivities K, calculated from grain size distribution after Hazen (1892) and Beyer (1964), vs. depth and the litholog of the core drilling*

Table 16 compares average K results after Beyer per aquifer layer with the results from the pumping tests. A high discrepancy exists between both values. The average K_{PT} from the aquifer tests is approximately 10 times (sand lens) to 100 times (shallow aquifer, deep aquifer) higher than K_{BEYER}. Causes may be that the method after Beyer only considers primary pore volume that results from the grain size distribution. During a pumping test, the actual, likely heterogeneous texture of the affected aquifer volume is tested. Peat deposits that occur in depths where the screen of the 85 ft well sits (see litholog in Figure 24) definitely will result in relatively high permeabilities. Beyer's K does not consider any anisotropic effects (varying compaction and alignment conditions) or the

organic matter content. Thus, it might be distinctly lower. Average permeabilities of 40 to 80 m/day are reported from other pumping tests in Holocene Bangladesh aquifers (Ravenscroft et al., 2005). These arguments show that K_{BEYER} must distinctly underestimate the real situation. The K_{PT}-values are slightly lower than those reported by Ravenscroft et al. (2005), but seem to be more confidential, by showing a similar order of magnitude. From the shallow aquifer pumping test at Titas transmissivities of 545 m^2/day (6.31E-03 m^2/s, see Table 15) were calculated. Typical transmissivity of the shallow Bangladesh aquifers with 1,000 – 5,000 m^2/day are even higher (Burgess and Ahmed, 2006).

Table 16 *Permeabilities after Beyer (1964) of different identified hydraulical layers in comparision with the results from the 85, 115 and 280 ft pumping tests (PT)*

Permeability based layer description	**Depth [m]**	**K_{PT} [m/s]**	**K_{PT} [m/d]**	**K_{Beyer} [m/s]**	**K_{Beyer} [m/d]**
1rst Aquifer, without sand lense (PT 85 ft well)	3.0 – 26.8	1.97E-04	**17.05**	1.98E-06	**0.17**
Sand lense (PT 115 ft well)	33.5 – 34.1	1.31E-05	**1.13**	5.07E-07	**0.04**
2nd Aquifer (PT 280 ft well)	79.1 – 83.4	(2.49E-04)	**(21.5)**	2.70E-06	**0.23**

4.1.3 Conceptual model of the subsurface

The varying occurrence, differing depth locations and extensions of single hydrogeological structures in the subsurface at the different drilling positions below the hospital property are presented in Figure 25. The litholog data from Lissner (2008) as well as a deep drilling of the hospital building company served as database (see Figure 6).

The shallow, unconfined aquifer, located in the upper 26 to 50 meters, shows non-uniform thickness. The transition range to the underlying aquitard (27 – 45 m thickness) partially is pervaded by only locally occurring sand and clay lenses (see log data of LCD, 280 ft, 115 ft, 90 ft). The sand lens, tapped by the115 ft well, is hydraulically connected to the shallow aquifer, as derived from Figure 23. It can be assumed that the probably leaky aquitard extends on a regional scale, because the water tables of both aquifers did not communicate directly with each other (see Figure 23).

The deeper, semi-confined or confined aquifer, existing between approximately 70 m depth up to minimum 286 m depth, is interlayered by two clay lenses (WHBC). Whether these lenses only exist on a local scale or operate as regionally extended aquitards is unknown.

In deep sedimentary basins like the Bengal delta, an interbedded system of permeable and less permeable layers of non-uniform thickness and varying extensions can be expected, forming a multi layered leaky aquifer system (Kruseman and de Ridder, 2000). The spatially varying layer sequences shown in Figure 25 indicate that such a system also may exist in Titas's subsurface.

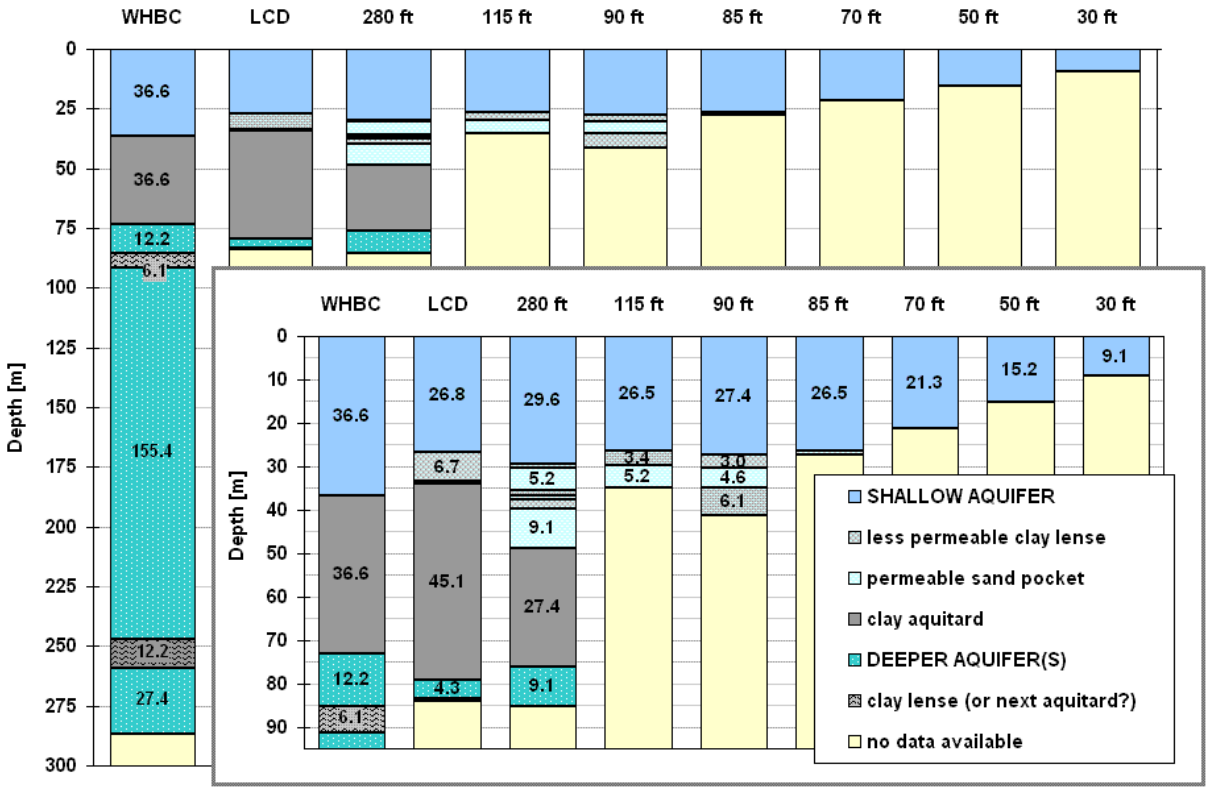

Figure 25 *Hydraulical conditions of the subsurface below the property of the Titas Hospital. The first column shows data of deep drilling for a well constructed by the hospital building company (WHBC). The other data about the subsurface stratigraphy derive from Lissner (2008) (including the litholog of the core drilling (LCD) and data of the test site wells). The numbers present the extension of a layer in [m].*

4.1.4 Levelled water tables at irrigation and test site wells

The positions of levelled wells and the water table elevations at the 11th/12th of December 2007 in m above mean sea level (MSL) are listed in Appendix B12. The water tables were interpolated with Kriging in the contour map in Figure 26. The investigated area has a size of approximately 1400 m x 2000 m. 46 irrigation wells and the 7 test site wells were levelled.

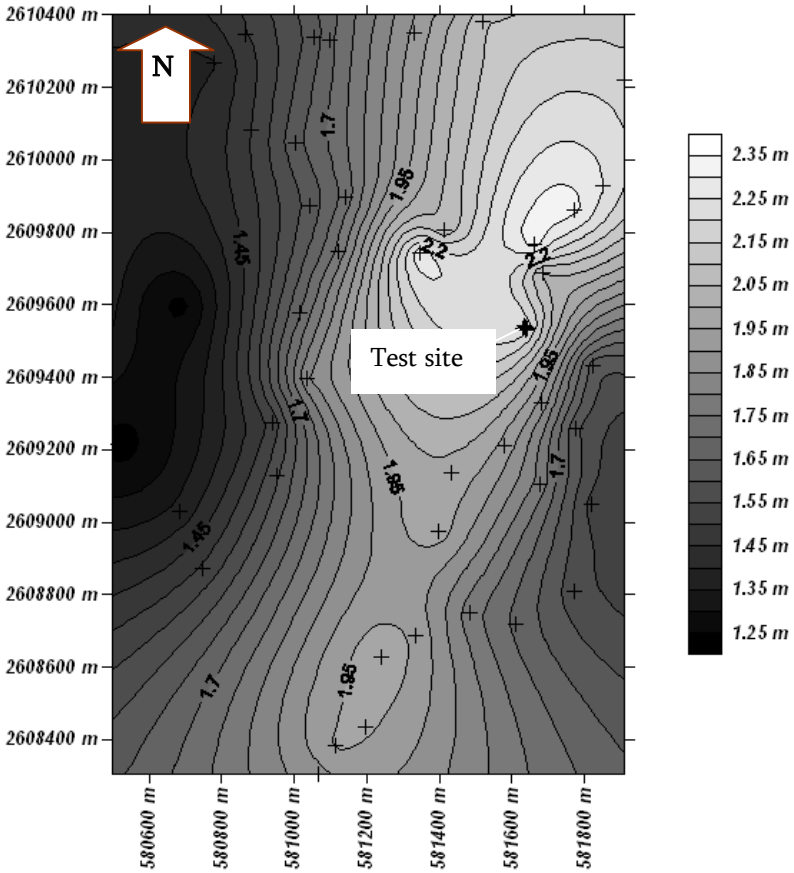

Figure 26 *Contour map of the water tables levelled at 11th/12th of December 2007 (black crosses mark the position of levelled wells)*

It seems that water table elevations are highest (up to 2.32 m MSL) near artificially elevated areas like villages and streets (compare with the left map in Figure 27) and decrease towards agricultural utilized areas (minimum 1.23 m MSL). The average altitude of the agricultural, not artificially elevated land surface is 2.67 m. The natural gradient from Titas to the Bay of Bengal is very low ($\Delta H/\Delta L$= 2.67 m/~100 km = 2.67E-5 m/m), resulting in a correspondingly low hydraulic gradient. From such a low hydraulic gradient high water table fluctuations > 1 m were not expectable. Harvey et al. (2002) assumes negligible natural hydraulic gradients in Bangladesh's aquifers during monsoon season (June-November), too, but states that irrigation pumping largely controls the groundwater flow during dry season, by inducing artificial gradients. However, irrigation activities slowly re-started in the beginning of December (see section 3.1.5) and can not cause these high fluctuations alone. It is possible that direct evaporation and/or evapotranspiration from groundwater play a significant role. In the agricultural areas, with relatively low depths to groundwater, the direct evaporation from groundwater and especially evapotranspiration by crops will be distinctly higher than in the artificially elevated villages or asphalt-sealed streets.

The latter feature up to 3 m thick, additional sediment basements, acting like a barrier for capillary rise from groundwater. Recent foundations even show several horizontal plastic sheetings, acting as additional barrier (see Figure 18 in section 3.1.3.1)

4.1.5 Potential evaporation (PE) and actual evapotranspiration (AET)

The potential evaporation (PE), based on daily class-A-pan measurements, amounts to 9,911 mm/year. With the formula after Pike 1964, based on monthly T and PE data for Comilla district, an actual evapotranspiration value of 2,262 mm/year was calculated (Mirza et al., 2003; Pike, 1964). AET_{Pike} may reflect evapotranspiration from flood-unaffected, artificially elevated areas like villages. But, it must distinctly underestimate the actual evapotranspiration from agricultural lowland, because it can not calculate proper values for the inundated monsoon seasons (see section 2.2.3).

The combination of both, PE and AET_{Pike}, adapted to monthly varying flooding conditions, led to a final AET value of 5,225 mm/year, valid for agricultural lowland. The methodology is described detailed in section 3.3.6. Nevertheless, it hast to be considered that this value only reflects AET due to P and PE in dry-season months and the PE in inundated months. To some extent it may correspond to predisturbance conditions 20 - 40 years ago, before intense irrigation activities started in Bangladesh. However, to which magnitude direct evapotranspiration from groundwater as well as irrigation activities further enhance the actual evapotranspiration, still is unknown.

4.1.6 Stationary flow modelling

Model extension. The model has an extension of 1,425 m in E-W-direction, and 2.100 m in N-S direction. This corresponds to an area of 2,992,500 m^2, i.e. approximately 3 km^2. The model origin is located at E 580,500 m, N 2608290 m (datum: Kalianpur/Everest 1937, projection: BTM - Bangladesh transverse mercator). The geographical surface map used for the model with main features is shown in Figure 27. Further, the land surface elevation, shown in Figure 27, was imported to Modflow as grid-file.

Model layers. Figure 25 showed the conceptual subsurface model. Due to lacking knowledge about the actual location of the bottom of the deep aquifer and only one piezometer in this depth, this strata was excluded from modelling. In the beginning it was planned to implement a less perme-

able, silty soil layer of 0.5 m thickness. But, the strict precondition of Modflow, saying that constant head boundary conditions must lay above the bottom of the layer they are assigned for, could not be fulfilled. This lead to the decision to further simplify the model, by modelling without a top soil formation. Due to lacking knowledge about the exact extension and location of sand and clay lenses in the investigation area, only a simplified one-layer model was created, representing the shallow aquifer and sand lens strata. The one-layer model extends down to 29 m depth below MSL. It corresponds to the boundary between the sand lens bottom and aquitard top, situated in 34 m depth below hospital basement surface (see LCD in Figure 25).

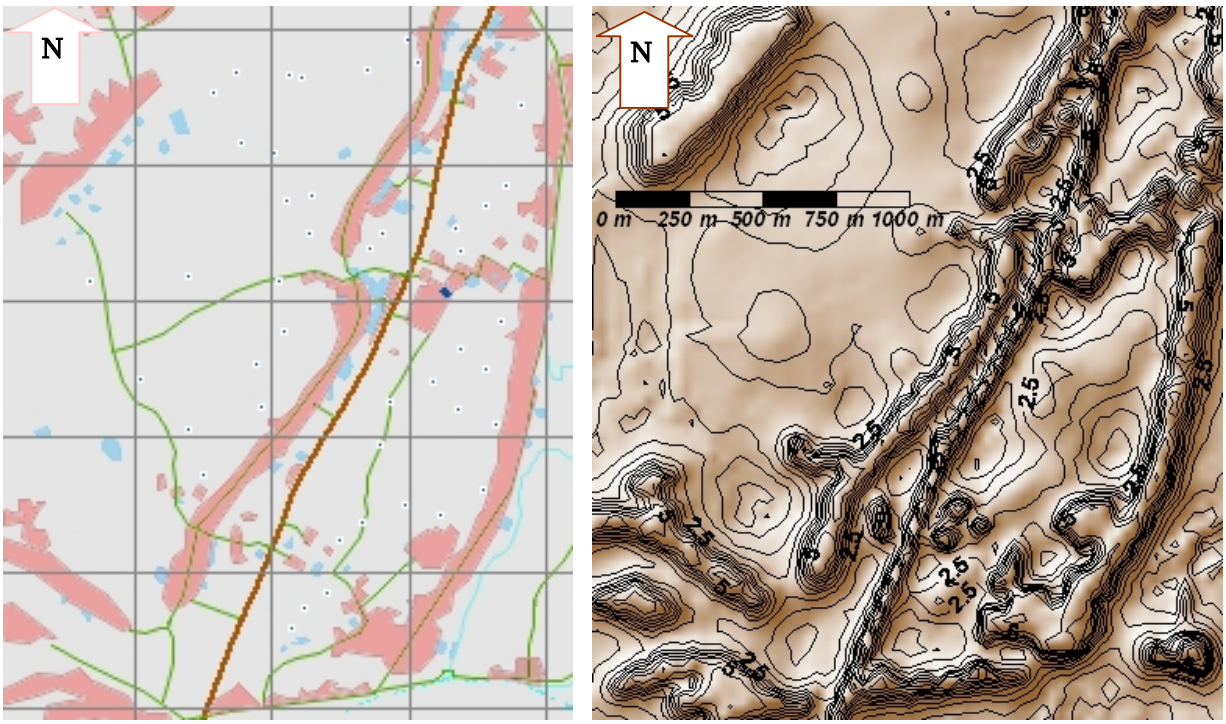

Figure 27 *Left picture:* ***Geographical surface map of Titas*** *(grid size: 500 m x 500 m) generated with TNTmips from a satellite image photographed at 20th of March 2007, including villages (red polygons), asphalt-sealed streets (brown line), footpaths (green lines), small ponds (light blue polygons), tributary channels (light blue lines), agricultural land (grey areas), levelled irrigation wells (white-blue dots), and the test site (dark blue polygon). Right picture:* ***Shaded relief map of Titas*** *with elevation isolines, created from interpolated point data via Kriging with Surfer8 (including positions of known surface elevation at irrigation and test site wells, as well as artificial help points created with TNTmips for streets and villages).*

Constant head boundary conditions. Territory boundary conditions ((Q=f(H), Dirichlet).) for the shallow aquifer on the one hand are constant heads H (marked orange in Figure 28) measured at the irrigation wells determined at 11th/12th of December 2007. Figure 26 pointed out a tendency of increasing measured hydraulic potentials towards the street. Thus, where the street crosses the territory margin, the hydraulic head was set at a reasonable maximum value (see yellow marked constant heads in Figure 28). For the NE, SE, NW and SW corners of the area the constant head

boundary is an estimation, based on measured heads of close irrigation wells (green marked constant heads in Figure 28). Unfortunately, Modflow only offers the boundary condition "no flow" (Q=0, Neumann) for the aquifer bottom, although some flow through the underlying aquitard can be assumed.

a) constant head boundary conditions in [m] above MSL (mean sea level) at the model margins, and position of the imported observed heads (blue crosses):

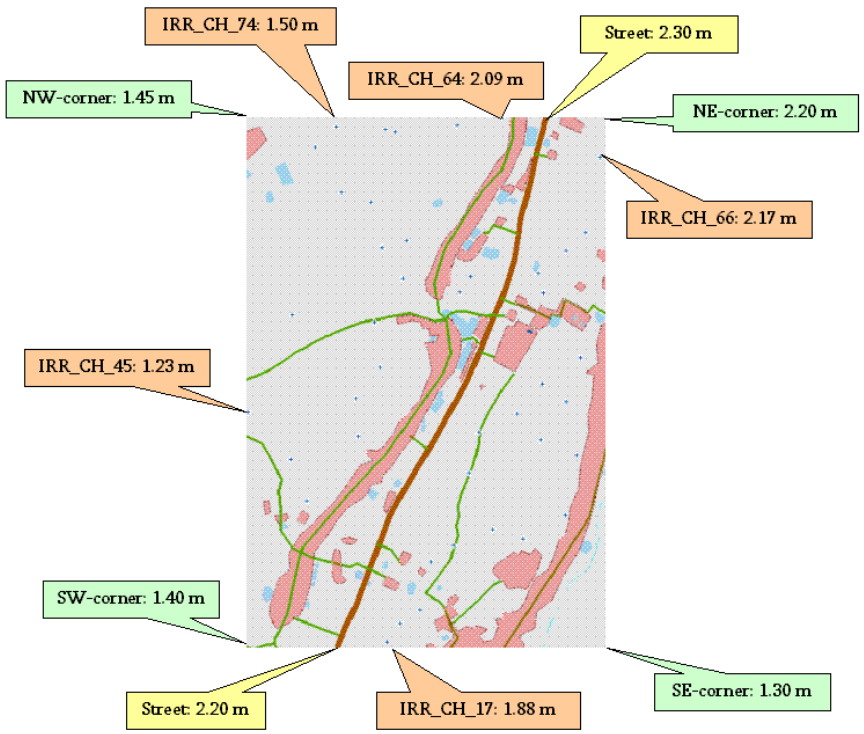

b) further model properties and boundary conditions:

model area: 3 km² (1,425 m x 2,100 m)

layer extension: from –29 up to 6 m MSL

$K_{x,y}$: 1.97 E-04 m/s

K_z: 1.97 E-05 m/s

S_y: 0.23

S_s: 9,83 E-04 1/m

n_{eff}: 0.30

n_{tot}: 0.40

RCH: 5,300 mm/year

EVT, extinction depth: variable (see **Figure 29**)

Figure 28 *Model properties and boundary conditions*

Default conductivity property. The hydraulic conductivity K (1.97E-4 m/s) found during the 85 ft pumping test was set as default horizontal K_x and K_y condition for the whole model. For better numerical stability, the vertical permeability K_z was set one dimension lower (1.97E-5 m/s).

Default storage coefficients. The predominant grain size was fine sand, only in shallow depths some silt was reported from the field-litholog. The specific yield condition for unconfined aquifers S_y (also referred as effective porosity, drainable pore space or unconfined storativity in literature) was set on 23 %, as recommended for fine sands by Krusemann & de Ridder (2000). Unconsolidated sands show a porosity range of 25 – 50 %, whereas silts have 35 – 50 % (Kruseman and de Ridder, 2000). Regarding the aforementioned, the effective porosity n_{eff} (drainable pore space) of the predominant sandy aquifer material was set on 30 %, whereas the total porosity n_{tot} was as-

sumed to be higher (40 %). Even though the shallow aquifer is unconfined, the specific storage coefficient (S_s) has to be added in Modflow. Based on the effective porosity of 30 %, it was calculated to 0.0026 1/m (see section 3.3.9)

Head observation wells for model calibration. For the model calibration the positions, water tables and screen top elevations of the remainder irrigation and test site well water tables, measured at 11th/12th of December, were imported to Modflow. The wells, which were used as constant head boundary condition at the model margin, were excluded from calibration.

Boundaries Recharge (RCH) and Evapotranspiration (EVT). Both, the actual annual recharge due to monsoon precipitations and river afflux, and the actual annual evapotranspiration strongly influenced by irrigation activities and artificial basements, are not known. The monsoon season brought 82 % (2,042 mm) of the annual precipitations, but additionally, an unknown amount of dammed up river waters to the territory, leading to an uniform flooding and feeding of the whole investigation area. The final actual evapotranspiration value of 5225 mm/year (= AET_{final}, see section 4.1.5) does not consider the influence of irrigation or artificially elevated areas on evapotranspiration, but, at least may reflect pre-disturbance conditions (= no antropogenous influence). Thus, it served as start value in the model, to estimate the minimum annual recharge at Titas (Step 1, see Table 17 and Figure 29). Therefore, the recharge-value was adapted until the maximum observed water tables on agricultural land (2.32 m MSL) corresponded to its calculated head at well IRR_CH_68, by assuming this well may reflect best the minimum recharge conditions at Titas. The resulting recharge value of **5,300 mm/year** was maintained throughout the further calibration procedure.

Table 17 *Results during adaption of recharge and evapotranspiration whilst calibration of the model*

	Step 1	**Step 2.1**	**Step 2.2**	**Step 3.1**	**Step 3.2**
Calibration with	all wells	all wells	all wells	all wells	except IRR_CH_ No. 3, 70, 35
Error	46.3 %	34.8 %	11.1 %	5.2 %	3.4 %
Max residual	+ 0.81 m	- 0.64 m	-0.29 m	+ 0.16 m	- 0.14 m
at well No.	IRR_CH_50	IRR_CH_6	IRR_CH_68	IRR_CH_3	IRR_CH_67

Thereafter (Step 2.1, see Table 17 and Figure 29), reasonable EVT-values were assigned for the different surface features street, village, hospital, and agriculture by assuming differing magnitudes of recent irrigation activities and direct evapotranspiration from groundwater. For the sealed

street EVT was assumed to be zero, also for artificially elevated basements a lower EVT (2,262 mm/year = AET_{Pike}, see section 4.1.5) was assumed. For the agricultural land a higher inital EVT (9,911 mm/year) was assigned that equals the potential evaporation value (see section 4.1.5) calculated for Titas. The modelling error became lower (34.8 %). Further optimisation (Step 2.2) led to 7,550 mm EVT/year on agricultural territory and a residual modelling error of 11,1 %.

During the final Step 3 the aforementioned conditions at street, village, and hospital basements were maintained. Only on agricultural area a further adaptation considering the differences between observed and calculated heads was carried out (see legend in Figure 29).The modelling error decreased to 5.2 % (Step 3.2). Further adaptation did not appear reasonable. In particular the wells IRR_CH_No. 3, 70, and 35 showed relatively low water tables, compared to the majority of neighboured wells. This deviation might have its cause in errors during the measurement, or was caused by distinctly higher recent water withdrawals, even though this was not noticed during field work. It is questionable, if tube wells (Hand tube wells, house wells) in close villages may play a role. However, better adaptation of these wells would have required to assign very high local ETV (> 30,000 mm/a), which was considered for not being reasonable. As an experiment, these “outliers” were excluded from calibration in Step 3.2, which led to a slightly better model optimisation result (3.4 %).

Modelling results. No distinct flow direction valid for the whole model area was found. It appears, the locally varying hydraulic gradients at Titas (visualized by velocity vectors in Figure 29) are mainly caused by the variable magnitude of evapotranspiration at the area. On artificially elevated areas smaller evapotranspiration leads to relatively higher heads. In contrast, on the fields irrigation and stronger direct evapotranspiration from groundwater may have caused relatively lower water tables. Higher deviations between observed and calculated heads in the model may have its cause in irrigation activities, which in particular should be highest on areas that dry up early after monsoon. In a tropical climate like Bangladesh irrigation waters almost completely will evaporate or get evapotranspirated by field crops, thus, it appears reasonable to describe water withdrawals provisionally with higher evapotranspiration rates in the model.

a) EVT boundary step 2

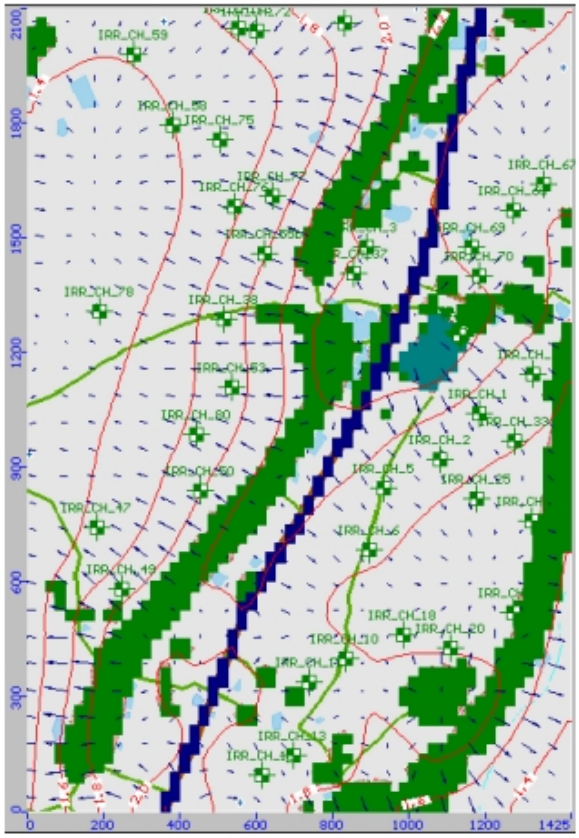

b) EVT boundary step 3

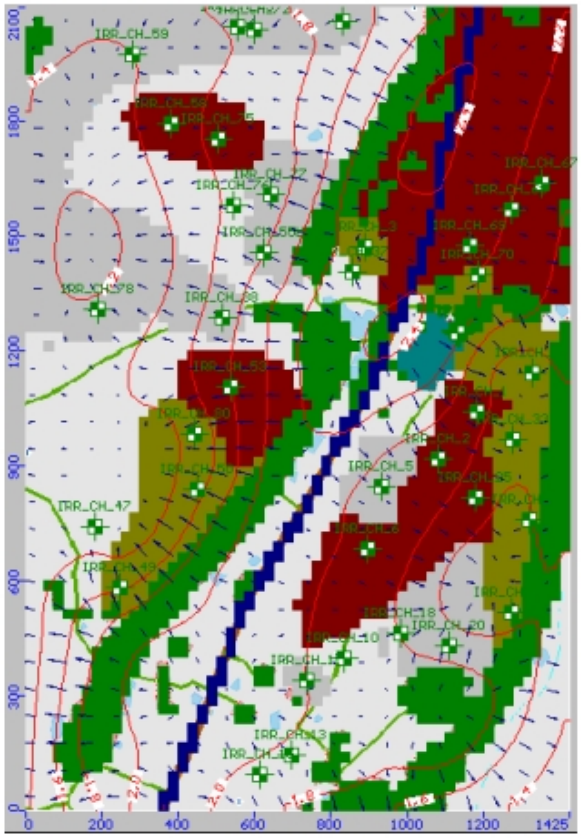

c) Legend

EVT-Symbol	Territory	EVT [mm/a] (Extinction depth [m])			
		Step 1	Step 2.1	Step 2.2	Step 3
	Street	5,225 (3)	0 (0)	0 (0)	0 (0)
	Village	5,225 (3)	2,262 (3)	2,262 (3)	2,262 (3)
	Hospital	5,225 (3)	2,262 (1)	2,262 (1)	2,262 (1)
	Agriculture	-	-	-	5,225 (3)
	Agriculture	5,225 (3)	9,911 (3)	7,550 (3)	6,200 (3)
	Agriculture	-	-	-	9,500 (3)
	Agriculture	-	-	-	13,600 (3)
Other symbols	**Description**				
	Head equipotentials				
	Velocity vectors				
	Observation wells				

Figure 29 *Evapotranspiration (EVT) boundary conditions assigned to the aquifer layer during several modeling steps. Velocity vectors point out the groundwater flow directions, the relative magnitude of groundwater flow, and show locally varying hydraulic gradients, respectively.*

Further, direct evapo(transpi)ration from groundwater (increases the lower the distance to the surface), varying soil properties that lower/enhance capillary ascension, and feeding from shallow, clogged water bodies that contain residual monsoon precipitation waters probably have caused spatially varying water tables. But, measurement errors may have contributed to some extent, too. For water table measurements an error of ± 1 cm can be assumed. The levelling was carried out by professionals (Land Survey Team, Dhaka). Thus, the error of the levelling normally should not exceed 1 cm per 1 km distance.

Seen on this background, the results are consistent with the hypothesis of a low-flow groundwater system. Only higher water withdrawals can trigger higher groundwater water exchange and mixing processes in the subsurface, but, which concurrently are locally limited.

4.2 Groundwater chemistry at the test site

Unless something else is mentioned, both, the data ascertained during Steinborn's (2008) survey from February throughout July 2007 and the own findings from the survey in the time period September until December 2007, will be considered consecutively. A compendium of all single values measured per parameter at the seven piezometers during each of the thirty one monitorings can be found in digital Appendix B8. For a better illustration of these results, in Appendix A1 printed graphical representations of the temporal variations of all measured parameters in 2007 are shown. These data and figures are the basis for the data evaluation in the following sub-chapters.

4.2.1 Quality evaluation of the analyses

4.2.1.1 Analytical error of the electrical balance

The analytical error of the analyses of samples from the time period **September throughout December 2007** was checked with PhreeqC. The results of the analytical error analysis are shown in Appendix B7. For laboratory analyses usually an error of up to ± 2 % is said to be acceptable, those results are marked as **"ok"** in the Appendix. However, considering the fact that the analysis partially was carried out on-site, it must be reckoned with up to ±10 %. This condition generally is fulfilled for analyses where no missing values (pH and/or NH_4^+) occurred in the data and where the pH was measured with the HACH pH meter.

In the 280 ft well the Ammonium content was quite high, thus it can be assumed that the high errors of TF.280.23, TF.280.24 and TF.280.25 mainly must be caused by the missing NH_4^+ values. The pH-value for TF.90.23 is missing, then PhreeqC by default computes with pH = 7, what might result in the higher error. The samples TF.30.24, TF.30.25, TF.30.26, TF.50.25, TF.90.26 also show errors higher than 10 %. Here, the pH-values were determined with the less accurate pHep pH-meter. In contrast pH measured with the HACH device, obviously didn't oscillate much over time per well. Thus, it must be concluded that the measurements executed with the pHep pH-meter are not reliable. This concerns pH determination as well as titration of alkalinity and acidity,

Just to check these assumptions, missing NH_4^+-values in the 280 ft well, and missing or not reliable pH values of all wells, were substituted by the mean of the other reliable measurements and a new run with PhreeqC was executed, resulting in errors lower than ±10 %.

4.2.1.2 Conductivity check

Before considering the results, it must be noted that the conclusions from the Conductivity test depend on the accuracy of the measured conductivities. Due to problems with the probe (overestimation of EC in the field, see section 4.2.1.4) the results and conclusions from the Conductivity check, listed in Appendix B7, must be examined with caution

The Conductivity check showed that most analyses featured a **lack of anions**. Bicarbonate as the main anion could be the reason. PhreeqC utilizes the TIC-values from the lab as basis for the HCO_3^- calculations. Bicarbonate concentrations are strongly pH-dependent, i. e. the pH-values measured in the field determine the proportions of Carbonate species computed by PhreeqC. Some CO_2 may have left the samples before analysis, leading to lower computed HCO_3^- concentrations, than the samples really contained in the field.

Several 280 ft samples showed a **lack of cations**. For TF.280.23/24/25 this might be due to the unknown real amount of NH_4^+ (missing values). The samples TF.115.21 and TF.115.22 had **too many anions**, but after checking the data no coherent explanation could be found.

4.2.1.3 Quality Control

4.2.1.3.1 Triplicates

Repeated triplicate samplings to check the variations between samples taken during the same monitoring at one well were conducted for the parameters TIC, DOC, As/P-totals/-species, and the cation/anion analyses with IC. The calculated average results and standard-deviations per parameter are listed in the digital Appendix B6. For better visualization the results of the absolute standard deviation found per triplicate and parameter are graphically displayed as error indicators in the Figures T – HH in Appendix A1. These indicators can help to evaluate, which temporal changes really are due to natural variations.

4.2.1.3.2 Matrix duplicates for As/P totals/species and matrix spikes for As/P totals

To get an estimation of deviations which might be due to laboratory methodology or instrumentation, one As(tot)/P(tot) sample per piezometric test site well was measured two times, designated as matrix duplicates (md1, md2). Additionally, two doubles of the same sample – designated as matrix spikes (ms1, ms2) – were spiked with a definite amount of **10 µg/L As** and**100 µg/L P,** to see how well the added concentrations are recovered. The whole results are listed in Appendix B6. A graphical visualization of the results is shown in Figure 30. The represented matrix spike results for ms1 and ms2 were already corrected for the spiked As and P quantities.

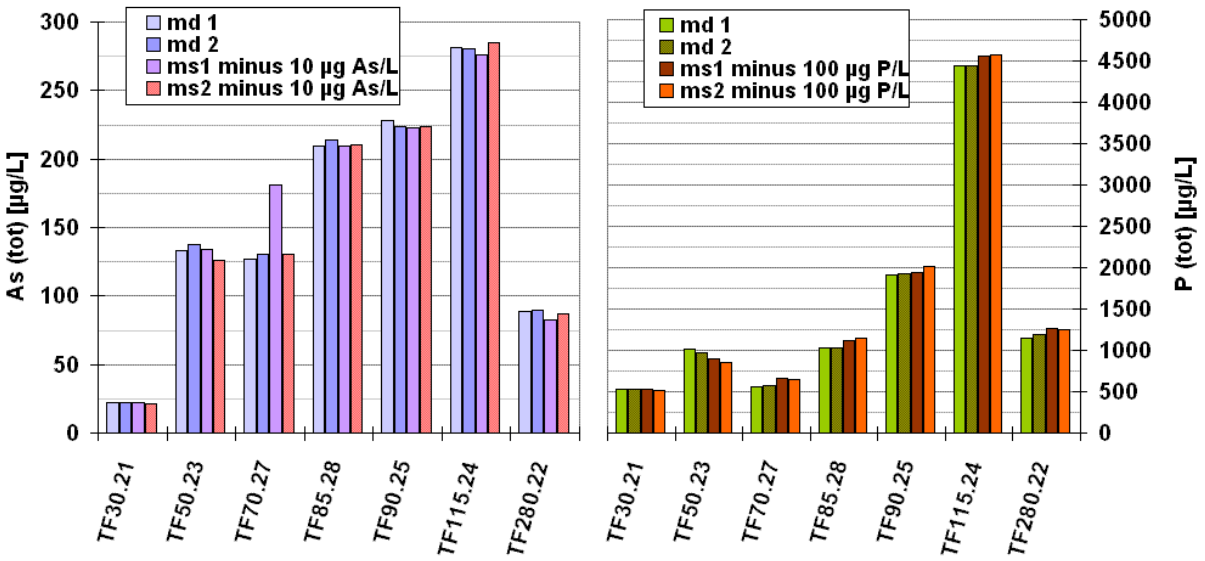

Figure 30 *Total Arsenic results for matrix duplicates (md) and matrix spikes (ms)*

In the low concentration range of sample TF30.21, where no dilution was necessary to apply, the recovery rate for both As and P was best, i.e. absolute standard deviations were minimal. The

highest deviation shows As-sample TF70.27 with RSD=18 %, which is caused by the false higher value of the ms1-sample (see Table 18). Regarding the fact that a comparable high deviation can not be seen in the corresponding P values, it is not likely that this is due to a dilution error or a sudden extreme drift in sensitivity of the ICP-MS. The internal drift correction with a Rhodium standard worked out well during these analyses (Appendix B2).

Table 18 *Average values ± their absolute standard deviations and the relative standard deviations (RSD) calculated from the four samples md1, md2, ms1, and ms2.*

	Sample	TF30.21	TF50.23	TF70.27	TF85.28	TF90.25	TF115.24	TF280.22
As(tot)	Average [µg/L]	22 ± 0.4	133 ± 5	142 ± 26	211 ± 2	225 ± 2	281 ± 3	87 ± 3
	RSD [%]	2	4	18	1	1	1	4
P(tot)	Average [µg/L]	525 ± 6	932 ± 77	612 ± 54	1,081 ± 58	1,949 ± 40	4,506 ± 73	1,213 ± 53
	RSD [%]	1	8	9	5	2	2	4

With exception of the unclear TF70.27 ms1 As-result, it can be concluded that deviations due to laboratory measurements for As samples in general lie below 5 %. Phosphorus, occurring in a higher concentration range than Arsenic, features in most cases correspondingly higher absolute standard deviations. However, deviations due to laboratory methodology and ICP-MS sensitivity should not exceed 10 %.

Figure 31 shows the deviations of matrix duplicate samples for Arsenite, Arsenate, and As(sum). The two measured values md1, md2, and absolute differences |Δ| between both values are listed in Table 19 per parameter. Highest recognized absolute differences between matrix duplicate measurements are 9 µg As(sum)/L (TF70.31, TF85.29), 4 µg Arsenite/L (TF70.29/30) and 10 µg Arsenate/L (TF85.29). Due to the fact that only duplicate measurements were available, the calculation of RSD was not possible, because it is defined for minimum three cases.

In contrast, the deviations between determined values for both species between the simultaneous collected triplicate samples TF85.30 QC are distinctly higher than 4 µg Arsenite/L and 10 µg Arsenate/L (see triplicate sample TF85.30 in Table 19). This means, regarding both As-species, higher than the above mentioned deviations in the determined quantities of simultaneous collected samples mainly will be due to the sampling methodology (e.g. late acidification, inadequate filtration) or even might have natural causes, but only to less extent can result from the laboratory measurements.

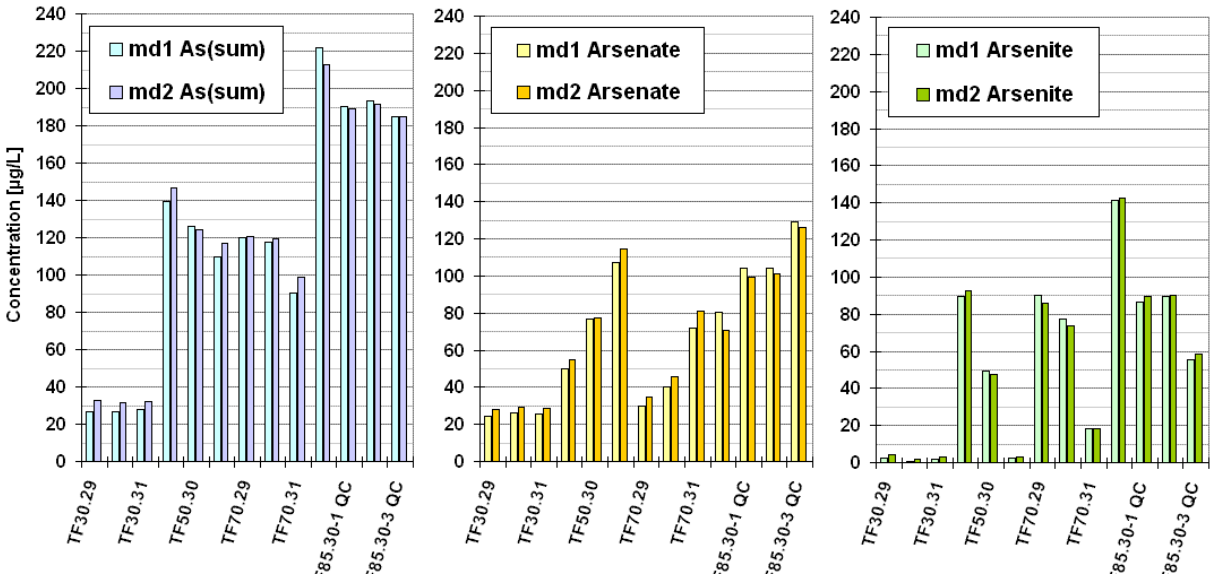

Figure 31 *Results of the matrix duplicate analyses for As(sum), Arsenate and Arsenite*

Table 19 *Results of the matrix duplicate analyses for As(sum), Arsenate and Arsenite and the absolute difference |Δ| between both measurements*

Well		TF30			TF50			TF70			TF85			
Monitoring		29	30	31	29	30	31	29	30	31	29	30-1	30-2	30-3
As(sum) [µg/L]	md1	27	27	28	139	126	110	120	118	90	222	191	193	185
	md2	33	31	32	147	124	117	121	120	99	213	189	191	185
	|Δ|	**6**	**5**	**4**	**7**	**2**	**8**	**1**	**2**	**9**	**9**	**2**	**2**	**0**
Arsenite [µg/L]	md1	2	1	2	89	49	2	90	78	19	142	86	90	56
	md2	4	2	3	92	47	3	86	74	18	142	90	90	58
	|Δ|	**2**	**1**	**1**	**3**	**2**	**0**	**4**	**4**	**0**	**1**	**3**	**1**	**3**
Arsenate [µg/L]	md1	24	26	26	50	77	107	30	40	72	80	104	104	129
	md2	28	30	29	55	77	114	35	46	81	71	99	101	126
	|Δ|	**4**	**3**	**3**	**4**	**0**	**7**	**5**	**6**	**9**	**10**	**5**	**3**	**3**

4.2.1.3.3 As reference material

To check the accuracy of the analyses, during three runs with the ICP-MS the As concentration of a standardized reference material was determined. The original concentration of the reference material was 72.5 µg As/L. The reported dilution for these measurements was 1:10. The value measured during run '071215' of 76 µg As/L shows a deviation of 4 % from the reference value 72.5 µg As/L (Table 20).

Table 20 *Results of the reference material (72.5 µg As/L) check*

data file	assuming 1:10 dilution		assuming 1:5 dilution		additional information
	As (tot) [µg/L]	Deviation [%]	As (tot) [µg/L]	Deviation [%]	
'071215'	**76**	4	-	-	new calibration standards and new reference material solution were utilized, monitorings 29 - 31
'071130'	**128**	43	**64**	13	same calibration standards and same reference material solution were utilized during both runs, monitorings 21 - 28
'071204a'	**136**	46	**68**	6	

The both other runs show extreme deviations regarding the reference value, which are difficult to explain. The values measured for As-samples did not show a sudden deviations per well in this order or magnitude since the last three monitorings (Appendix A1, Graphs HH – KK). Thus, the measured sample values seem to be all right. Yet there is reasonable concern, if the 1:10 dilution really was applied during the runs '071130' and '071204' that base on the same calibration standards and reference material solution. A possible assumption would be that actually an 1:5 dilution was applied in these cases, like during the analysis of the 280, 70 and 50 ft samples in file '071204' (see Appendix B2).

4.2.1.4 Error evaluation

Oxygen and redox potential. Comparisons between Oxygen measurements showed that in the 115 ft and 280 ft groundwaters distinctly lower oxygen contents/saturations were determined during pump tests than during monitorings in the beginning of November (see Figures B, C, D in Appendix A1, section 4.3 and Appendix A2. In contrast, results for the 85 ft well were similar. This suggests that oxygen values/saturations of waters lifted during low-flow sampling with the peristaltic pump might be overvalued and at least may not reflect the actually lower oxygen concentrations of the 115 and 280 ft waters. Astonishing was a straight tendency of increasing O_2-values since end of May in all wells (Figures C, D Appendix A1). In spite of the oscillations, there also seems to be a tendency of increasing redox potential during April until July in all wells, thereafter E_H remains on the July-level (Figure B, Appendix A1). If generally inadequate purging times should be the cause, then it is still questionable, why a similar effect can't be seen for the 85 ft well. Slightly lower purging times are expectable since September, as explained in section 3.1.1,

but O_2 and E_H started to increase since May, although no variation of sampling techniques is reported for this time point.

In the beginning of the year throughout May intensive irrigation activities are assumable that trigger enhanced exchange and movement of the subsurface waters. Then, since June, when monsoon season sets in and concurrently irrigation activities were discontinued, the movement of the subsurface waters becomes minimal, due to very low natural horizontal hydraulic gradients. One would expect that Oxygen can be delivered from the surface only during irrigation season, whereas a lack of Oxygen would develop during rainy monsoon season. It is astonishing, but actually the opposite is visible. A natural explanation for such a contrary process, visible in all wells, is hard to find. One of the disadvantages of the peristaltic pump was that the flow rate could not be adjusted to a certain level during each monitoring. It is questionable, if the definitely decreasing capacity of the batteries for the peristaltic pump may have caused a slowly progressing decrease in the flow rates, in turn resulting in lower discharged water volumes per time interval.

On this background it seems reasonable that in particular seasonal changes of O_2 and E_H, set in relation with Arsenic will not deliver meaningful results. Nevertheless, average values calculated per well for O_2 and E_H may at least reflect relative differences between the wells.

Electrical conductivity. Table 21 shows the deviation of the measured from the calculated average conductivities per well for samples taken between Sep-Dec 2007. The EC measured on-site is generally higher than the calculated value. Also Steinborn (2008), who utilized the same probe, reported this problem.

Table 21 *Average values and standard deviation of measured and calculated electrical conductivities (EC) of samples taken within the time period **Sep-Dec 2007**, the difference $\Delta EC = EC_{measured} - EC_{calculated}$ per well and estimated values for total dissolved solids (TDS = 65 % of EC)*

Parameter	Shallow Aquifer					Sand lens	Deep Aq.
	TF.30	TF.50	TF.70	TF.85	TF.90	TF.115	TF.280
$EC_{measured}$ [µS/cm]	**240** ± 35	**299** ± 18	**298** ± 13	**461** ± 36	**429** ± 29	**1,272** ± 173	**2,503** ± 216
$EC_{calculated}$ [µS/cm]	**190** ± 37	**227** ± 4	**217** ± 5	**310** ± 7	**296** ± 13	**1,163** ± 124	**1,870** ± 149
ΔEC [µS/cm]	51	72	81	152	133	110	633
TDS ($EC_{measured}$) [mg/L]	**160**	**200**	**200**	**300**	**280**	**830**	**1,630**
TDS ($EC_{calculated}$) [mg/L]	**120**	**150**	**140**	**200**	**190**	**760**	**1,220**
ΔTDS [mg/L]	40	50	60	100	90	70	410

Even though the calculated Conductivity is valid for infinite dilutions only, such a high deviation is abnormal. At least an accuracy of 15 % can be expected (Matthess, 1994). Thus, it must be assumed that the probe generally overestimated the values. This should be considered generally when assessing the on-site measured EC values, and the derived TDS-values, found during 2007.

pH-values. The representations of average pH-values vs. depth in Figure 38 and the pH-values vs. time in APPENDIX A1 (Figure A) do not include the values measured with the pH-Hep device, because these values were identified as not being reliable (see Chapter 4.2.1.1).

Temperatures. Even though the flow cell was wrapped up with Aluminium foil during measurements in the time period Sep.-Dec. 2007, heating of the slowly pumped groundwater in the small tube and the flow cell by the sun during low flow sampling is still probable. Thus, it must be assumed that the values measured probably are higher than real groundwater temperatures.

Alkalinity/Bicarbonate. Differences between measured (on-site-titration) and calculated Bicarbonate (TIC, PhreeqC) were observed (see Figure Q, Appendix A1). Calculated HCO_3^- might be lower than the measured Bicarbonate, because some CO_2 might have left the sample and changed the Carbon equilibrium before the TIC-analysis took place. In some cases over-titration may contribute, too. But there also might be natural causes (see section 4.2.2.2.4).

In some cases the alkalinity-values are missing. They lack due to bad weather conditions (TF30.18, TF85.05, TF85.19, TF90.09, TF90.19, TF280.19) or the broken pH-meter (complete monitorings 23, 24). Further, measurements with the pH-Hep device were not reliable (monitorings 25, 26).

Major Cations. A distinct dip of Ca, Mg and Na for sample TF90.13 is visible in the Figures T (8 mg Na^+/L), U (13 mg Ca^{2+}/L) and V (8 mg Mg^{2+}/L) in Appendix A1. The outlier TF90.13 also shows Ca-Mg-Na-HCO_3 type, in contrast to Ca-HCO_3-type in all other 90 ft samples (see Figure 33). This effect might be due to errors during IC-analysis, because the ionic balance for the whole analysis showed an error of – 45 % (see Appendix B8).

Flouride was determined with two measurement-devices. All samples collected from February until Juli 2007 and the 30 ft samples from September until December 2007 were determined with a Flouride sensitive probe. All residual samples collected during September until December 2007 were measured with the IC, which did not deliver utilizable results for the 115 and 280 ft well due to inseparable peak overlay. The stable measurements with the probe generally seem to be more reliable than the fluctuating F^- results found with IC (see Figure AA, APPENDIX A1), probably

caused by partial overlay with the negative system peak. However, both measurement methods found Fluoride values in a similar concentration range.

Iron and **Ammonium.** There is a distinct dip between iron and to a lesser extent also in the ammonium values measured by Steinborn (2008) and during this survey in the 280 ft well (Appendix A1, Figures). Steinborn (2008) reported that his two pipettes probably did not measure precise anymore, since they were overheated once in springtime. They were used for the volume measurements of 1:100 dilutions in the 280 ft well. This may have led to some overestimation. Another cause for lower measured Iron concentrations since Sep. 2007 might be the slightly lower purging times during this survey, as described in section 3.1.1. Particularly in the 280 ft well, where the flow rate was lowest (probably due the longer lifting distance and generally lower water table compared to the other wells) this might have resulted in sampling of more stagnant waters since Sep. 2007, which already lost parts of its initial Iron load due to precipitations. But the fact that both, Iron and Ammonium, in the 280 ft well show relatively similar temporal variations and already relatively low values were determined during March and April points out that the lower values determined since September are likely to have natural causes, too.

Ammonium values are missing during the monitorings 22, 23, 24 and 25, due to a defective cyanurate reagent. Further, it was questionable, if there is any falsifying influence on the measurement due to extremely high Iron in the 280 ft well. The HACH-manual reports interferences from Iron that would lower measured NH_4^+ -contents. This assumption was checked additionally in the laboratory of the Department of Hydrogeology at Freiberg University and delivered slightly decreasing results for NH_4^+, the higher the of added Iron (II)-quantity was. Against this background, it can be assumed that Ammonium to some extent even was under-, but not overestimated. On the other hand, a high turbidity or sample colour can result in false higher values. The 280 ft groundwater featured high turbidity and a brownish colour. But considering the fact that the samples were diluted 1:100 with distilled water before photometrical analysis, this effect might be negligible.

Manganese is very high in the 280 ft well since September. It also might be an artefact from differing sampling/analysis methodologies. But it's a fact that for the determination of Mn(tot) during Sep.-Dec. several times dilutions were necessary, because the HACH®-Mn-method has a limited measuring range of 0 – 0.7 mg Mn/L. That means, higher Mn(tot)-values definitely were observed on-site. The HACH-manual reports that Fe(tot) > 5 mg/L interferes during Mn-measurements. It is

assumable that these interferences are the higher, the more Fe(tot) is found in the sample. This might result in higher determined Mn-results when Fe(tot) is relatively low, concurrently.

Nitrite and **Nitrate.** The presence of Nitrite interferes with Nitrate measurements, because Nitrate is transformed into and determined as Nitrite during photometrical measurements. Considering the fact that Nitrite concentrations were one order of magnitude lower than those of Nitrate in all depths (see Appendix A1, Figures O, N), the interference effect seems to be negligible.

Phosphorus. Referring to the unidentified P-species, (P(unid), see Figure GG, Appendix A1) a measurement artefact seems to occur in the samples from all wells, especially in the late-year data. The relative measured height of the P(unid) values seems to escalate after 3rd of May, decreased after July-measurements, and suddenly increased again after the 8th of November. The samples were measured in several AEC-ICP-MS runs. Probably variable sensitivities occurred regarding the P(unid)-species determination. From this side is known that two serial runs with the same calibration standards include the Monitorings 21-28 and another run with new calibration standards the last three monitorings 29 – 31. About Steinborn's (2008) data no information is on hand. It is assumable that these erratic variations are due to systematic errors. Correlations regarding the seasonal variation of P(unid) with other parameters may not deliver meaningful results.

Referring to the variations of P(sum) over time (Figures EE, Appendix A1), which were calculated on the P(unid) and PO_4^{-3} data, there are striking differences to the temporal P(tot) results (Figure DD) visible in the 115 ft well, especially in the early year data. In the other wells such deviations are not apparent. Possibly higher variations in sensitivity of the measurement also occur for PO_4^{-3} in higher concentration ranges. The influence of the erratic P(unid) values on P(sum) should be negligible here, because these are one dimension lower than Phosphate concentrations.

Slightly lower purging times and/or late acidification seems to show effect in the 280 ft samples, where Phosphate and the P-totals (P(tot), P(sum)) show lower values than during Steinborn's survey. It is assumable that dissolved Iron partially precipitated and Phosphate co-precipitated.

Arsenic. General later acidification of the filtered samples during this survey (Feb.-Jul. 2007), in comparison to Steinborn's (2008) survey (Sep.-Dec. 2007) might have caused advanced transformation of Monothioarsenate into Arsenite, and of Arsenite into Arsenate, due to oxidation by atmospheric oxygen. This may be reflected by lower determined Monothioarsenate and partially Arsenite values. The results must be interpreted with caution. Absolutely implausible species data

generally were not included in further considerations. This especially concerns the species results found during monitorings 27 and 28 and samples taken during pumping tests. These definitely were acidified too late, by showing advanced loss of Arsenite. Species results of the 280 ft samples generally showed complete conversion of Monothioarsenate and Arsenite into Arsenate, which might additionally be promoted by slightly lower purging times since September or probably are due to the high dissolved iron contents. Steinborn (2008) reported to late acidification for monitoring 16. For statistical considerations only the species results of Steinborn (2008) (except monitoring 16) were consulted.

Nevertheless, results for Arsenic totals, and also the sum of Arsenic species in general should not be influenced too much by late acidification, because immediate filtration (0.2 µm) after sampling removed microorganisms and colloidal substances that would trigger enhanced precipitation of As.

As(sum) data seem to show more distinct fluctuations than As(tot) over time. Also error indicators (ASD) from triplicate samples during QC90.15 and QC85.13 were distinctly wider for As(sum). Nevertheless, the results generally have more similar curve progression than results for P(tot) and P(sum).

4.2.2 Depth-dependent variation of the groundwater chemistry

4.2.2.1 Determination of groundwater types

The dendrogram-outputs in Figure 32 are the main result of the hierarchical cluster analysis. Both dendrograms (the unscaled and the scaled) show that the groundwaters in 30, 50, 70, 85 and 90 ft depth resemble each other more, than those in 115 ft and 280 ft depth. The Kruskal-Wallis test showed that these three clusters form significantly different groups (see Appendix B11).

The 115 ft cluster represents the groundwater of the sand lens, the 280 ft cluster the groundwater of the deep aquifer, whereas the cluster including the 30, 50, 70, 85 and 90 ft well can be described as groundwaters of the shallow aquifer. For more detailed considerations a further division of the shallow aquifer into sub-clusters would be possible. Dendrogram A shows two sub-clusters: the upper (30, 50, 70 ft) and deeper (85, 90 ft) shallow aquifer. This clustering is mainly based on the concentrations of the predominant species. From Dendrogram B, which gives equal weight to

all cat- and anions, this cluster segmentation derives: 1st cluster: 30 ft; 2nd cluster: 50 ft, 70 ft; and 3rd cluster: 85 ft, 90 ft.

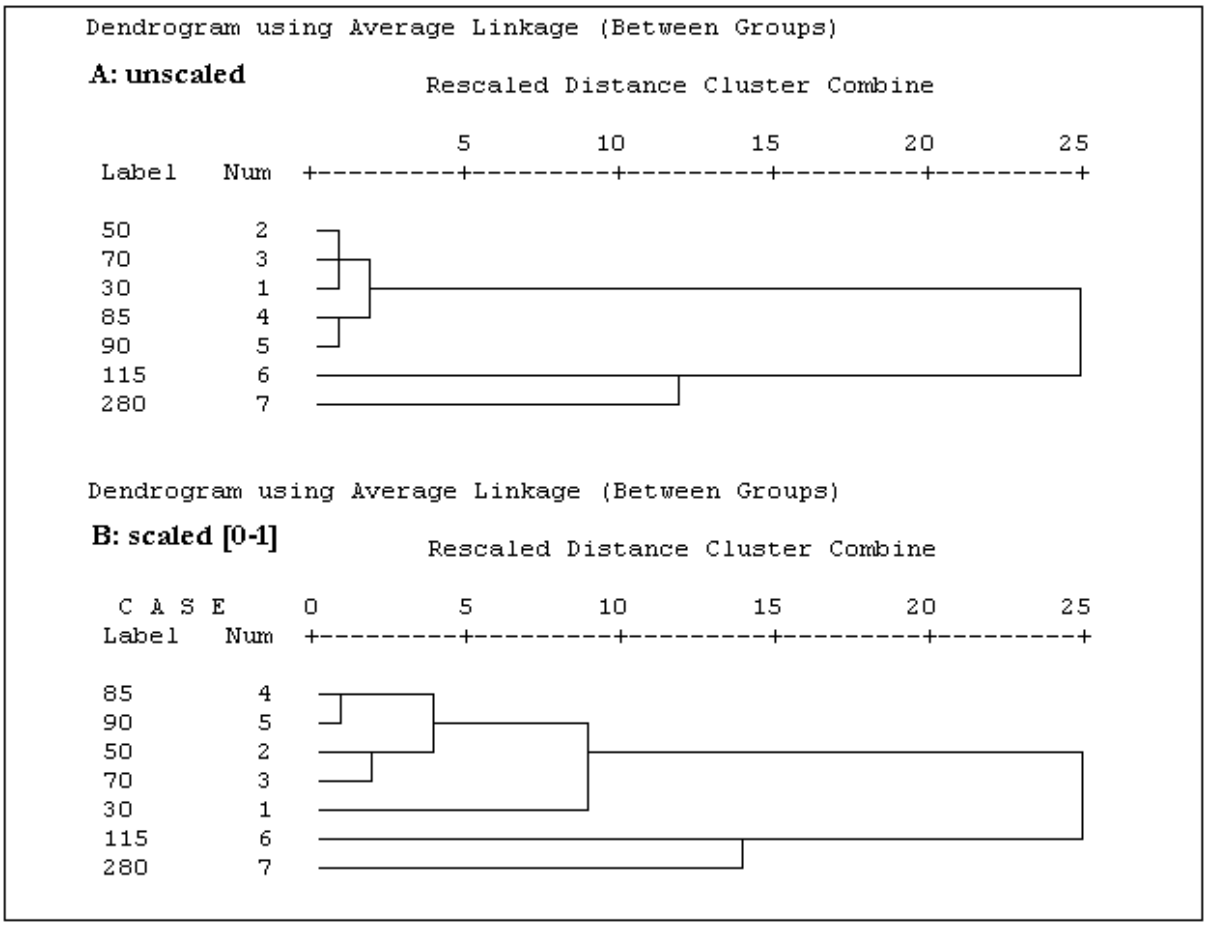

Figure 32 *Dendrogram-outputs of the hierarchical cluster-analysis with the software SPSS16.0. It is based on the median values of the parameters HCO_3^-, Cl^-, SO_4^{2-}, Ca^{2+}, Na^+, K^+ and Mg^{2+} [mg/L] per well. Dendrogram **A** uses the unscaled input parameters, i.e. predominant ions like HCO_3^- or Cl^- have the highest weight during clustering. In Dendrogram **B** all values per input parameter were downscaled to the interval [0-1], giving them the same weight.*

The diagram in Figure 33 points out, which water composition predominates in which depth and highlights remarkable changes of the chemistry that occurred within the investigation period. Table 22 shows the resulting groundwater types for each well, based on the classification scheme of DAVIES AND DE WIEST (1967), (see Figure 33). Summarized it can be concluded that three groundwaters types are distinctly discriminable based on Davies and de Wiest (1967) classification scheme and would refer to the three major groundwater clusters found during cluster analysis. Groundwaters in the shallow aquifer have the **Ca-HCO_3-type** in common, featuring varying influences from Mg and Na. The deep aquifer mainly is characterized by the **Na-Cl type.** The groundwater in the sand lens can be described as **Na-HCO_3-Cl-type** in the beginning of the year. But during the year it remarkably changed its character to a less mineralised water of **Na-HCO_3-**

type. This basic classification constitutes the grouping of wells for considerations in the following chapters.

Table 22 *Detailed description of groundwater types with reference to the sampling depth (= average depth ± length of the screen)*

	Well depth [ft]	Well depth [m]	Average screen depth ± length [m]	Groundwater type
Shallow aquifer	30	9.1	8.4 ± 0.8	Ca-Mg-Na-HCO_3 (tendency to Ca-Mg-HCO_3)
	50	15.2	14.5 ± 0.8	Ca-Na-HCO_3 and Ca-Na-Mg-HCO_3
	70	21.3	20.6 ± 0.8	Ca-Mg-Na-HCO_3 (tendency to Ca-Mg-HCO_3)
	85	25.9	25.1 ± 0.8	Ca-HCO_3 and Ca-Mg-HCO_3
	90	27.4	25.9 ± 1.5	Ca-HCO_3 and Ca-Mg-HCO_3
Sand lens	115	35.1	33.5 ± 1.5	Na-HCO_3 and Na-HCO_3-Cl
Deep aquifer	280	85.3	80.8 ± 4.6	Na-Cl (with tendency to Na-Ca-Cl)

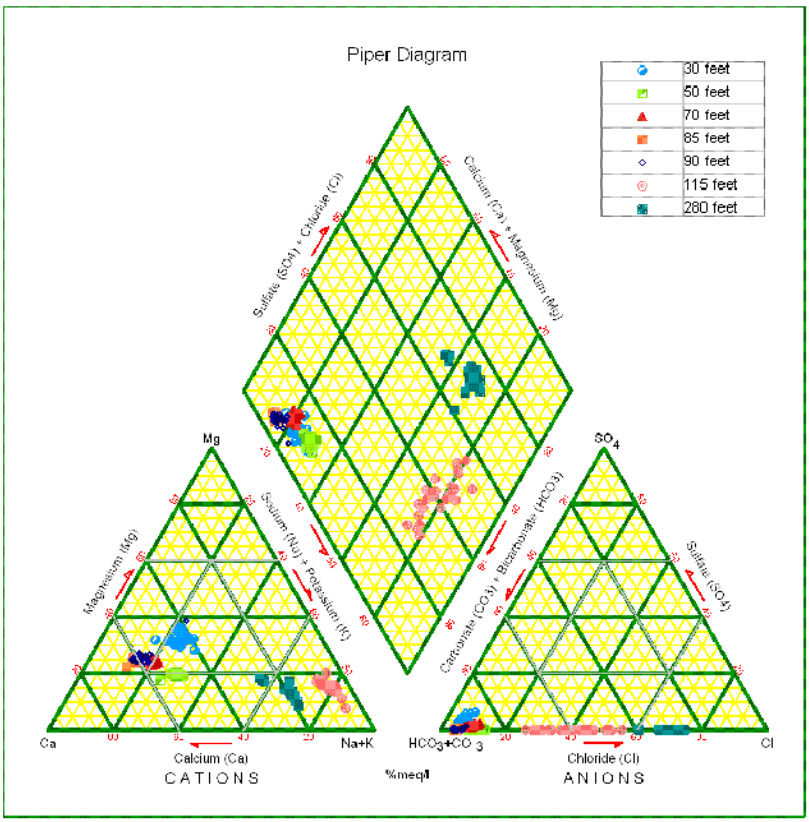

Figure 33 *Trilinear Piper diagram showing the percentages of the major cations (HCO_3^-+CO_3^{-2}, SO_4^-, Cl^-) and anions (Na^++K^+, Ca^{2+}, Mg^{2+}) [%meq/L] in the samples taken over time at the test site wells. The sum parameter [HCO_3^-+CO_3^{-2}] represents the measured alkalinity (HCO_3^-) values. The amount of CO_3^{-2} can be assumed to be zero, because all waters in the study featured pH below 8.2). The displayed data include complete data sets only.*

Ahmed et al. (2004) reports Ca-HCO_3 and Ca-Mg-HCO_3 groundwaters as common groundwater type in Holocene arsenic enriched aquifers, but locally also the Ca-Na-HCO_3 and Na-Cl type is not untypical. Groundwaters, containing much Na and Cl (280 ft, 115 ft) probably are influenced by entrapped ancient sea waters. (Zahid et al., 2008).

4.2.2.2 Results of all measured groundwater parameters vs. depth

4.2.2.2.1 Arsenic

Regarding the average dissolved total Arsenic concentrations shown in Figure 34 vs. depth it has to be mentioned that all wells exceeded the 10 µg As(tot)/L WHO-limit. Only the 30 ft well had As(tot) below the Bangladesh 50 µg As(tot)/L limit. The results for the sum of arsenic species are widely comparable, but show slightly more expanded RSD intervals. The maximum As concentration exhibits the sand lense (115 ft) with 248 ± 32 µg As(tot)/L. The 85 ft well shows highest As(tot) within the shallow aquifer (220 ± 16 µg As(tot)/L). In contrast, in the deep aquifer Arsenic concentrations were distinctly lower (65 ± 18 µg As(tot)/L.

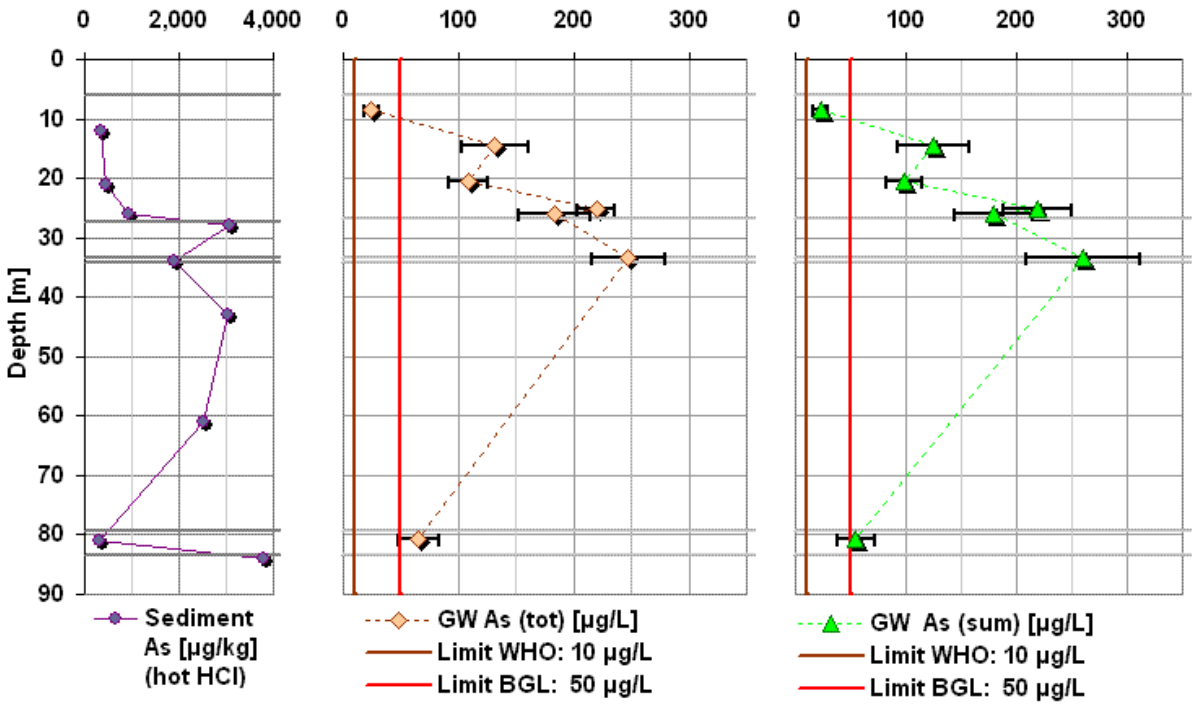

Figure 34 *Moderately bound Arsenic(hot HCl) in sediments and average values ± RSD found for As(tot) [determined with ICP-MS] and As(sum) [determined with AEC-ICP-MS] in groundwaters.*

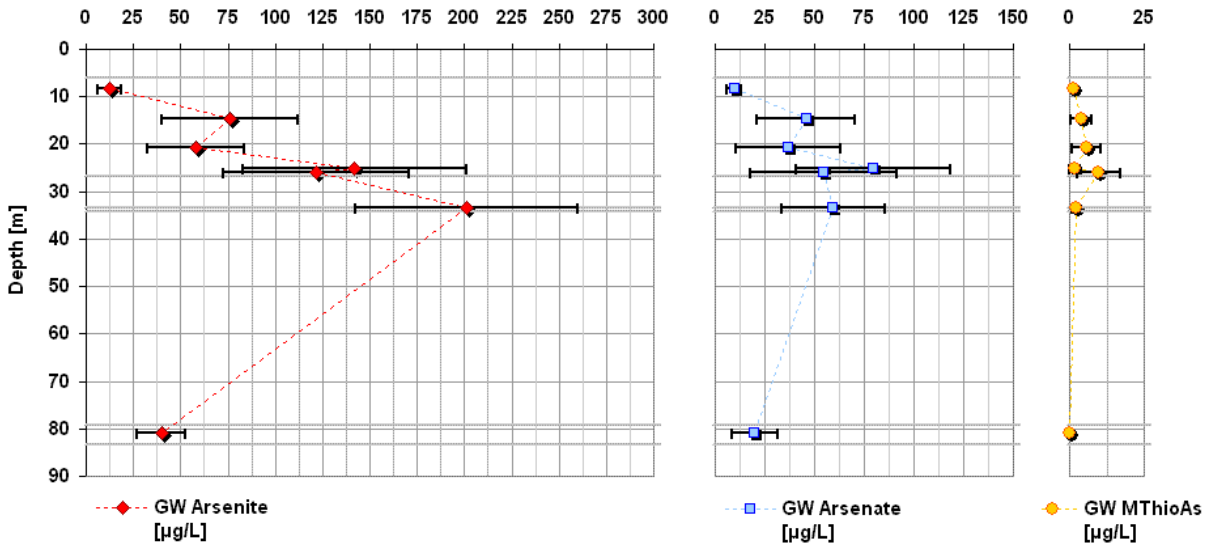

Figure 35 *Speciation of Arsenic [determined with AEC-ICP-MS] – Arsenite, Arsenate and Monothioarsenate (abbreviated: MThioAs) vs. depth*

The toxicity of Arsenic is highly species-dependent. Thus, total As-concentrations can not reflect the true level of hazard of the element (Burgess and Ahmed, 2006). Against this background, the determination of the arsenic species was of great importance during this survey. Average values and their standard deviation over depth are shown in Figure 35, whereas Figure 36 shows average percentages of each species found per well in 2007.

The most toxic and more mobile species Arsenite is predominant in all wells (50 – 77 %), followed by Arsenate (21 – 44 %). The least toxic Monothioarsenate ($[AsSO_3]^{-3}$) is the minor species. In the 280 ft well Monothioarsenate values generally ranged below detection limit (<0.5 µg/L). Also Smedley and Kinniburgh (2001) reported Arsenite as dominant species. From Eh-pH-diagrams (Figure 4), and the redox and pH conditions measured in the field (Figure 38) it can be concluded that Arsenite occurs fully protonated $H_3AsO_3^0$, while Arsenate is deprotonated and predominates as $HAsO_4^{2-}$ and $H_2AsO_4^-$.

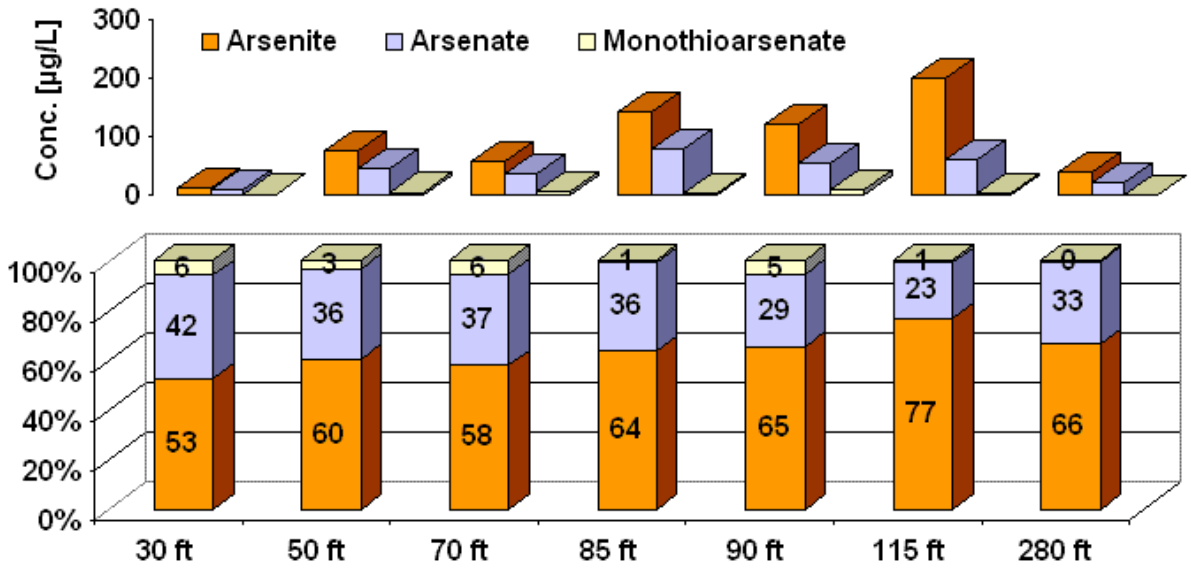

Figure 36 *Average percentages and concentrations of the As-species in each sampled test site well in 2007*

Lissner (2008) reports that no weakly bound As could be released by artificial groundwater (AGW[2]) from the sediments. It can be assumed that this As portion already was dissolved and released into groundwater. The depth distribution of moderately bound As (hot HCl[3]) vs. depth only partly corresponds to As concentrations found in the wells (see Figure 34). It can be assumed that not only the absolute amount of As found in sediment controls absolute dissolved As quantities in groundwater. Of great influence will be the underlying Arsenic release mechanism(s). Likely are depth-dependent or temporal varying magnitudes of the release mechanisms, which might be due to changing conditions in the groundwater chemistry. Such indications will be pursued and evaluated in the following chapters.

4.2.2.2.2 Major Cations and major anions

As already pointed out during classification of groundwater types (Table 22, Figure 33), Calcium forms the major cation in the shallow aquifer. In contrast, in the sand lens and deep aquifer Sodium predominates. Bicarbonate is the major anion in the sand lens and the shallow aquifer wells, characterizing them as "fresh groundwaters" (Langmuir, 1997). In the deep aquifer, Chloride predominates. Here also Bromide features highest values (3.7 ± 0.9 mg Br-/L). Chloride and the geo-

[2] **AGW leach** means leaching sediments with a water adapted to test site conditions - "artificial groundwater". Leaching with AGW targets As, P, Fe and Mn that is weakly bound (Lissner, 2008)

[3] **Hot HCl leach** targets As, P, Fe and Mn that is moderately bound and associated with poorly crystallized and amorphous Fe-hydroxides, Mn-hydroxides, acid volatile Sulfides and Carbonates (Lissner, 2008).

chemical connatural Bromide, are very mobile and were found to be enriched in sea waters (Matthess, 1994). Zahid et al. (2008) points out that elevated Na and Cl values indicate relict sea-water, entrapped during the Holocene sea water transgression. Thus, an influence of ancient brackish sea water in 115 ft and particularly in 280 ft depth can be assumed.

A conspicuous difference exists between the measured Alkalinity and the calculated Bicarbonate contents in Figure 37. Alkalinity is usually assumed to correspond to the Bicarbonate concentrations, because the most abundant weak acid is carbonic acid, which builds a buffer-system with Bicarbonate. Usually other weak acids like organic (e.g. fulvic, humic), silicic, phosphoric, boric acids and hydroxides (e.g. $Al(OH)_4^-$) are seldom in groundwater (Matthess, 1994). Due to the obvious deviations, at Titas's wells it is assumable that other weak acids contribute to the measured alkalinities.

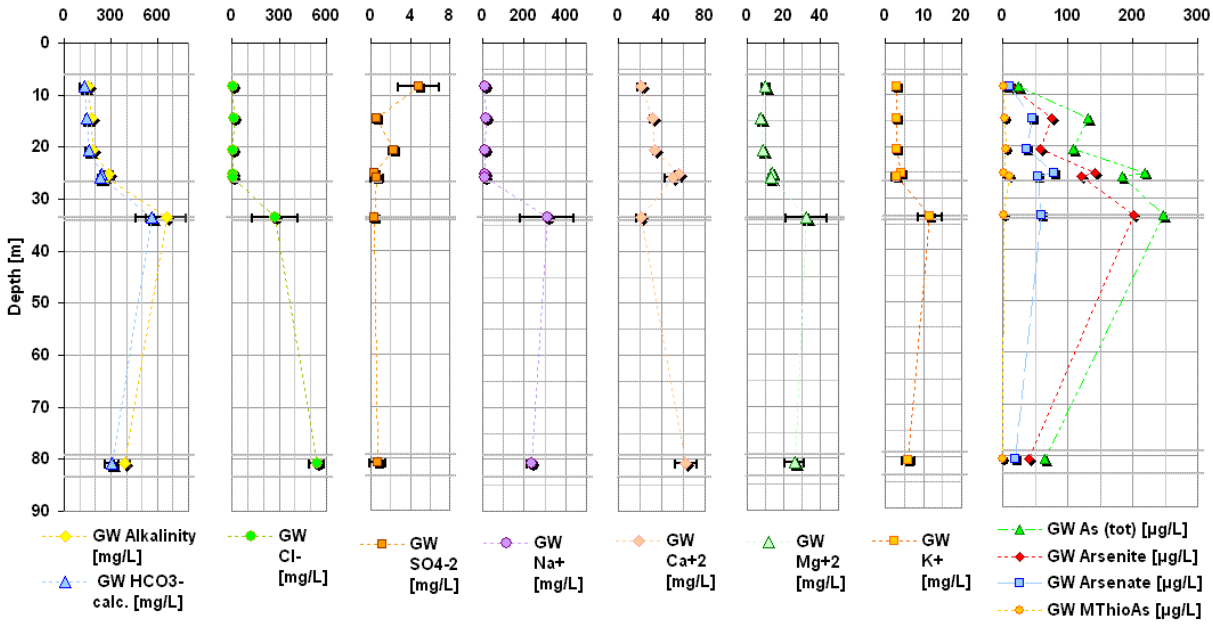

Figure 37 *Average values and standard deviations of the major cat- and anions in groundwater (GW) vs. depth at the test site, confronted with average Arsenic concentrations.*

4.2.2.2.3 Electrochemical Parameters

The parameters O_2, E_H and T in Figure 38 did not show very distinct differences depending on depth. Measured E_H-values of approx. 100 – 300 mV lie within the transition area (0 – 400 mV) between fully reducing and fully oxidizing conditions. The groundwaters were under-saturated with oxygen, with a measured average of 4 mg O_2/L (approx. 50 % saturation) in all wells. The pH measurements showed near neutral average values of pH 7.1 to 7.2 in the wells of the shallow aquifer and the sand lens. Only the deeper aquifer exhibits a lower, slightly acidic average pH of 6.4 ± 0.1.

EC (Figure 38) reflects the increasing mineralisation with depth, which mainly results from the quantities of the major cat-/anions, shown in Figure 37. MATTHESS (1994) defines waters with an EC between 30 – 2,000 µS/cm as fresh groundwaters. This classification fully meets conditions of the shallow aquifer wells, but not in the deep aquifer and only temporarily those in the sand lens (Figure F, Appendix A1). The parameter TDS (TDS = 0.65* EC) was calculated to estimate the potability of a groundwater regarding its taste (Figure G, Appendix A1). A health based TDS limit is not proposed by the WHO. Waters with a TDS below 600 mg/L, like in general valid for the shallow aquifer, are considered to be potable. It becomes unpalatable when TDS exceeds 1,000 mg/L, which is in general the case in the deep aquifer, but temporarily also occurred in the sand lens in the beginning of 2007, as Figure G in Appendix A1 shows (WHO, 2006).

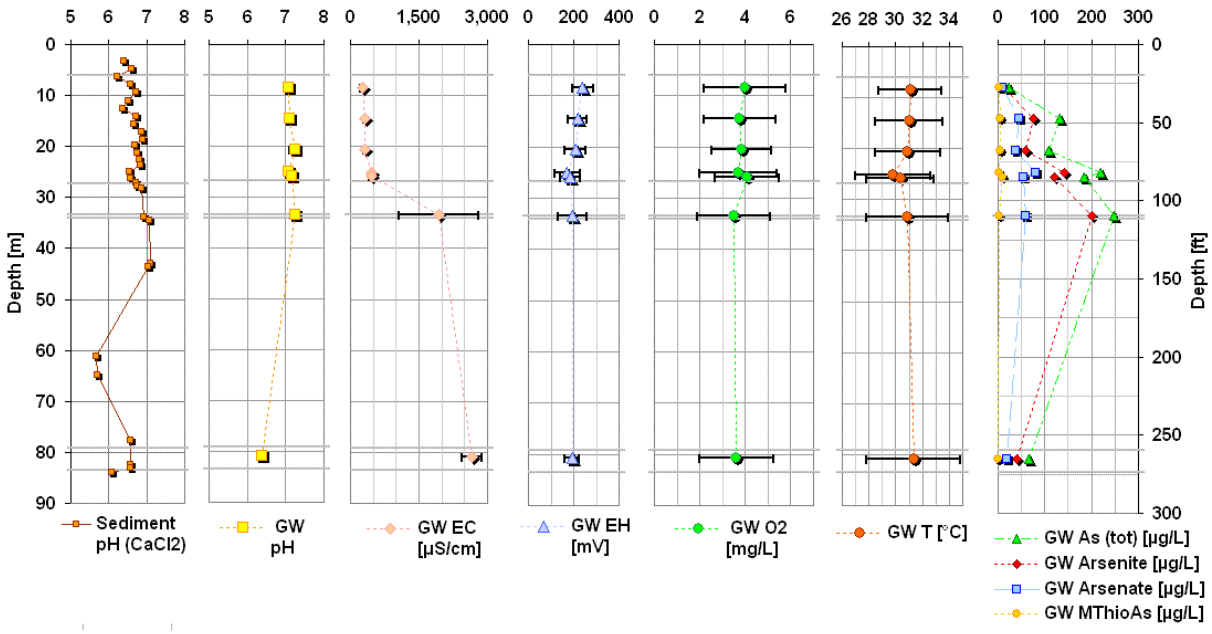

Figure 38 *Sediment pH determined by Lissner (2008) as well as mean values and standard deviations of the electrochemical parameters pH, EC, E_H, O_2 and T in groundwater (GW) vs. depth at the test site, confronted with average Arsenic results.*

4.2.2.2.4 Organic and inorganic Carbon

In Figure 39, both, TIC and DOC show increasing values with depth, with lowest values in 30 ft depth (31 ± 6 mg TIC/L, 0.8 ± 0.3 mg DOC/L) and highest in the sand lens (126 ± 22 mg TIC/L, 14.3 ± 6.8 mg DOC/L) and the deep aquifer (108 ±17 mg TIC/L, 13.0 ± 2.3 mg DOC/L). The curve characteristic does not fit directly to Carbonate and TOC concentrations found by Lissner (2008) in the sediments, especially regarding the 280 ft well. The depth-location of known peat deposits (= DOC-source) at the test site is shown in the litholog in Figure 39. DOC concentrations may indicate the presence of dissolved organic acids in water, causing the aforementioned difference between measured Alkalinity and calculated HCO_3^-.

In the deep aquifer, comparatively lower bicarbonate concentrations come along with correspondingly higher H_2CO_3-contents. This should be due to the slightly acidic pH (6.4 ± 0.1) in 280 ft depth, because pH strongly controls the carbonate speciation (Matthess, 1994).

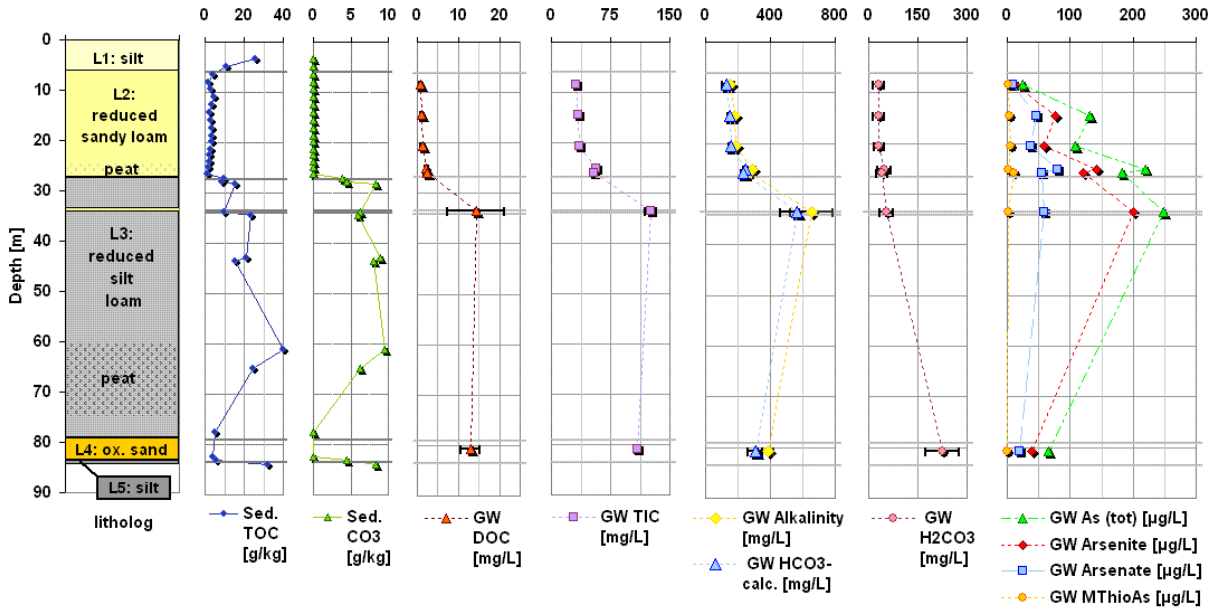

Figure 39 *Total organic (TOC) and inorganic (CO_3) carbon in the sediments (Sed.) determined by Lissner (2008)) and average DOC, TIC, Alkalinity, HCO_3^-calc and Acidity (H_2CO_3) values in groundwater (GW) vs. depth and confronted with average Arsenic concentrations at the test site. TIC was determined as C(+IV). Acidity (H_2CO_3) and Alkalinity (HCO_3^-measured) were determined via titration. HCO_3^-calc. was calculated from the TIC-values with PhreeqC.*

4.2.2.2.5 Phosphorus

Results for Phosphorus totals and its speciation are shown in Figure 40. Lowest values are found in 30 ft depth (0.34 ± 0.12 mg P(tot)/L), whereas highest concentrations are encountered in the 115 ft well (4.44 ± 0.55 mg P(tot)/L). Without exception, Phosphate represents the predominant P-species in all wells. Thus, it shows a similar distribution over depth like P(tot) or the sum of P-

species (P(sum)). The other P-species P(unid) remained unidentified. P(unid)-values slightly increased with depth from approximately 0.1 up to 0.4 mg P(unid)/L. The curve progressions of P(tot), P(sum) and Phosphate are similar to the As(tot), As(sum), Arsenite and Arsenate curves vs. depth, suggesting a similar release mechanism for As and P (Kinniburgh and Smedley, 2001), (Acharyya et al., 2000). Lissner (2008) reports that no weakly bound P (AGW) was leachable, but moderately bound P (hot HCl) (Figure 40).

P in the lithosphere mainly occurs as and is released from the mineral apatite (variations: [$Ca_5(PO_4)_3F$], [$Ca_5(PO_4)_3Cl$], [$Ca_5(PO_4)_3(OH)$]). Subsequently, P gets strongly adsorbed by clay minerals and metal hydroxides, especially Iron hydroxides. Further it plays an essential role in the biological circle. On one hand, in the subsurface it can be released in high amounts by microbial degradation of organic matter. On the other hand, it will be consumed by bacteria, because of its importance for the energy transport in the cell (Adenosine Triphosphate (ATP)). Due to this, it usually occurs in low concentrations below 0.1, or even below 0.01 mg P/L in groundwaters (Matthess, 1994). In contrast, Ahmed et al. (2004) reports that values up to 8.75 mg PO_4^{-3}/L can occure in Bangladesh's groundwaters, whereas similar high values of up to 6 mg P(tot)/L) were found at Titas. This gives rise to the assumption that high quantities of organic matter must be available and are degraded in these sediments. Concurrently, P is released in relatively high quantities to the groundwater. It appears, clay and solid Iron hydroxide sorption sites are not available in such corresponding high amounts that all P could be adsorbed on their surfaces.

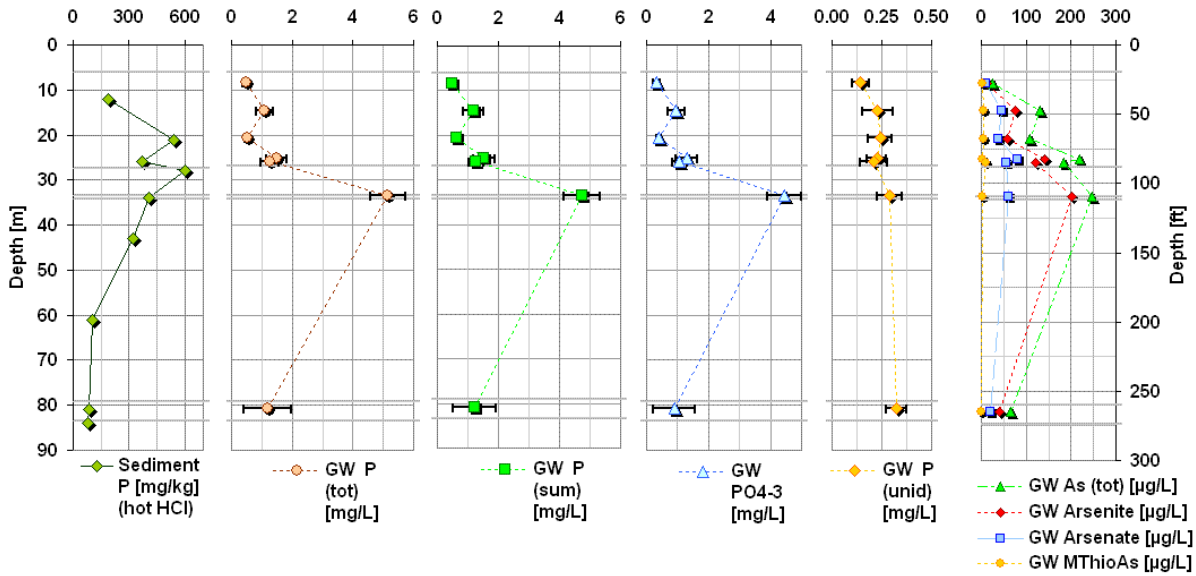

Figure 40 *Moderately bound P in sediment samples (Lissner, 2008) and average values and standard deviation of total P and its species in groundwater samples collected at Titas during February – December 2007, confronted with average Arsenic concentrations.*

4.2.2.2.6 Iron

Total Iron concentrations and its speciation vs. depth are shown in Figure 41. Iron concentrations varied distinctly with depth, with lowest values in 30 ft depth (0.5 ± 0.3 mg Fe(tot)/L) and extremely high values in the deep aquifer (84 ± 52 mg Fe(tot)/L). Additionally, the waters in 280 ft depth had a reddish-brown colour and high turbidity.

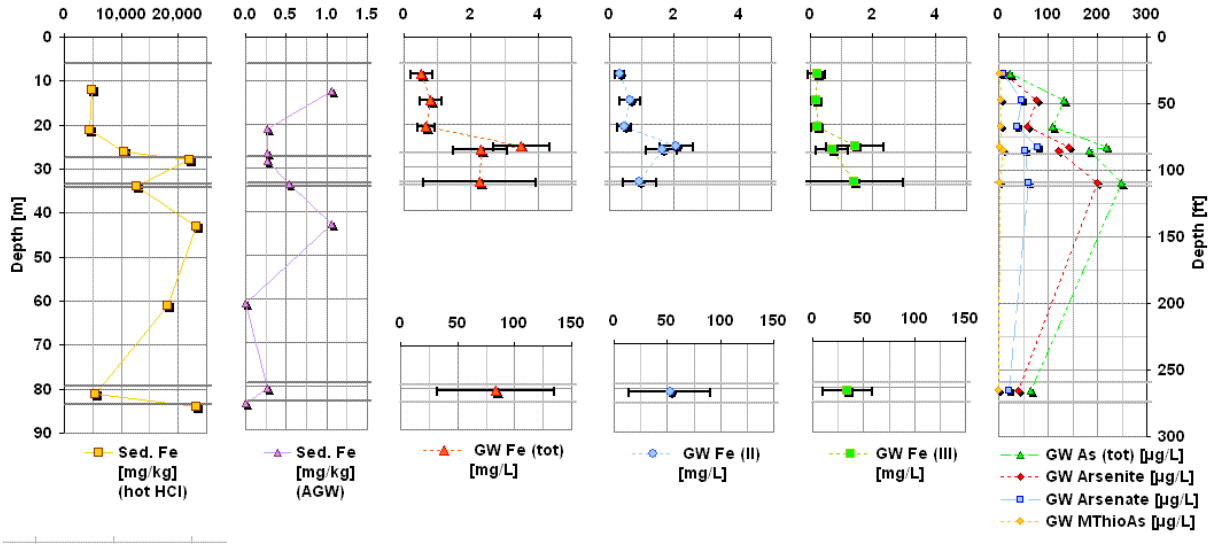

Figure 41 *Moderately (hot HCl) and weakly (AGW) bound Iron in sediment samples determined by Lissner (2008) and average values with their standard deviation of total, ferrous and ferric Iron in groundwater samples collected and analysed on-site at Titas during February – December 2007, confronted with average Arsenic concentrations.*

With exception of the 115 ft well, ferrous Iron (Fe(II)) in average is the dominant species in the wells. Calculated average percentages of ferrous Iron were 61 % (30 ft), 80 % (50 ft), 69 % (70 ft), 59 % (85 ft), 71 % (90 ft), 41 % (115 ft) and 63 % (280 ft).

Elevated iron concentrations are not of health concern, but result in colour development, turbidity, and negatively affect the taste of waters at values > 0.3 mg Fe(tot)/L (WHO, 2006). The existence of high dissolved total iron amounts (i.e. > 0.2 mg Fe(tot)/L (Smedley and Kinniburgh, 2001), 0.4 – 15.7 mg Fe(tot)/L (Ahmed et al., 2004)), accompanied by a high percentage of ferrous iron, indicates that the reduction of solid iron oxides takes place in variable magnitudes depending upon depth. It is assumable that weakly bound iron (AGW), which was determined by Lissner (2008) only in negligible amounts, was consumed first by microorganisms during the reduction process. Moderately bound iron (hot HCl) still is available in the sediments.

4.2.2.2.7 Manganese

Results for Mn(tot) and Mn(II) are represented in Figure 42. Mn(II) in average was in a similar concentration range around 0.2 mg Mn(II)/L in all wells. Mn(tot) showed more distinct variations, with minimum values in the sand lens (0.2 ± 0.2 mg Mn(tot)/L) and maximum values in the deep aquifer (0.9 ± 0.5 mg Mn(tot)/L).

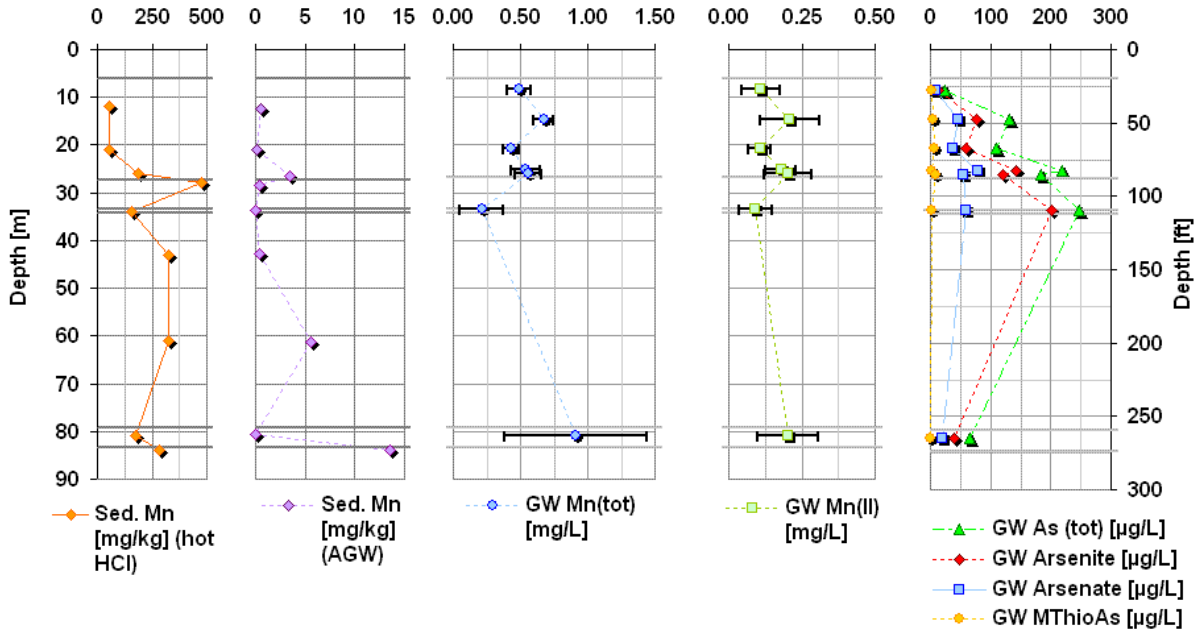

Figure 42 *Moderately (hot HCl-leach) and weakly (AGW-leach) bound Manganese in sediment samples determined by Lissner (2008) and average values with their standard deviation of total and divalent Manganese in groundwater samples collected and analysed on-site at Titas during February – December 2007, confronted with average Arsenic concentrations.*

The high detected dissolved Mn(tot) concentrations lie in the typical concentration range for Bangladesh's arsenic rich groundwaters. Ahmed et al. (2004) reports 0.02 – 1.86 mg Mn(tot)/L. With exception of the 115 ft well, Mn(tot) exceeds the health-based WHO guideline value (neurological effects) of 0.4 mg Mn(tot)/L in groundwaters (WHO, 2006). The occurrence of divalent manganese in all depths indicates reduction of solid manganese oxides. Calculated average percentages of the divalent Manganese species were 23 % (30 ft), 31 % (50 ft), 24 % (70 ft), 33 % (85 ft), 36 % (90 ft), 44 % (115 ft) and 22 % (280 ft). Lissner (2008) found only negligible amounts of weakly bound Mn within sediments, suggesting they were already dissolved due to reductive processes. A moderately bound manganese fraction (hot HCl) still is available in the sediments.

4.2.2.2.8 Nitrogen-Species

Figure 43 shows the average concentrations of Ammonium, Nitrate and Nitrite vs. depth. Ammonium concentrations in the sand lens (29 ± 20 mg NH_4^+/L), but particularly in the deep aquifer (101 ± 50 mg NH_4^+/L) were distinctly higher than in the shallow aquifer wells (below 2 mg NH_4^+/L). A taste threshold of 35 mg NH_4^+ /L is proposed, but there is no immediate health relevance. Natural levels in groundwaters are usually below 0.2 mg/L, but anaerobic groundwaters may contain up to 3 mg/L (WHO, 2006). Higher Ammonium concentrations in groundwaters derive from microbial degradation of organic matter (McArthur et al., 2001). Also widespread fertilizer application in south-eastern Bangladesh or latrines in villages may cause Ammonium in groundwater (Zahid et al., 2008), but then it would be expected to be highest in shallow wells, which is not the case here. Thus, higher Ammonium concentrations probably must derive from organic matter degradation within the sediments. Peat deposits found below 27 and below 61 m depth (see litholog in Figure 39) support this hypothesis.

Nitrate values oscillated in a wide range around approx. 0.8 mg NO_3^-/L in all investigation wells, showing no distinct depth-dependent characteristic. The same is valid for Nitrite (approx. average 0.05 mg NO_2^-/L). Nitrate concentrations below 1 mg/L are typical for Bangladesh groundwaters (Smedley and Kinniburgh, 2001) The concurrent occurrence of Nitrite may indicate that reduction of Nitrate is taking place (Matthess, 1994), caused by organic matter degradation. Both parameters did not exceed health-related WHO guideline values (i.e. < 50 mg NO_3^-/L short term exposure, < 0.2 mg NO_2^-/L long term exposure (WHO, 2006)).

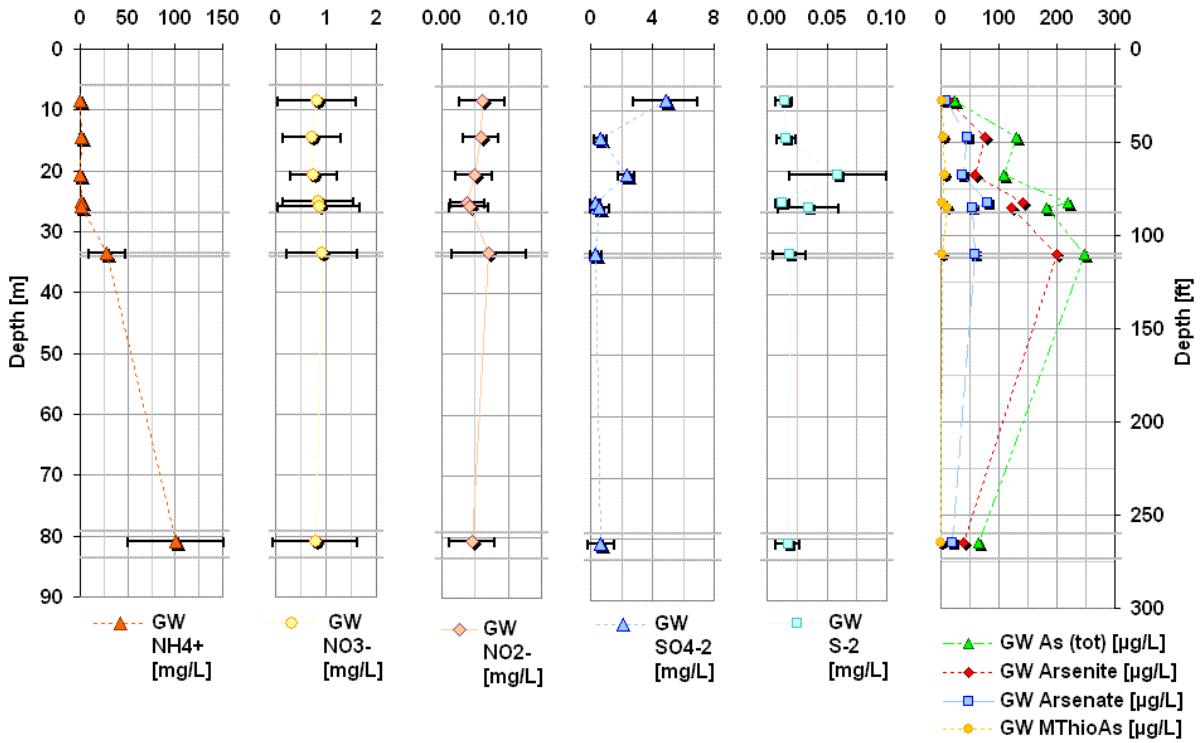

Figure 43 *Average values and standard deviation of Ammonium, Nitrate and Nitrite, as well as Sulphate and Sulphide vs. sampling depth in groundwater collected at Titas during February – December 2007, confronted with average Arsenic concentrations.*

4.2.2.2.9 Sulphur-Species

Average Sulphate and Sulphide concentrations, found in different depths, are shown in Figure 43. Sulphate concentrations were low (< 3 mg/L), which is typical for arsenic rich Bangladesh groundwaters (Ahmed et al., 2004). Only in the 30 ft well slightly higher Sulphate values occur (5 ± 2 mg/L), possibly due to atmospheric entry (acid rain). Sulphide was detected in all wells (> 0.01 mg/L), by reaching highest values in the 70 ft well (0.06 ± 0.04 mg/L). Under reducing conditions Sulphate can be reduced to Sulphide during microbial degradation of organic matter (Matthess, 1994). However, the very low Sulphide concentrations alone can not explain why such low Sulphate concentrations occur in the waters.

4.2.2.2.10 Lithium and Fluoride

Lithium in all wells was below detection limit, i.e. < 0.05 mg Li^+/L. Average Flouride values lay between maximum 0.3 ± 0.2 mg F^-/L (30 ft depth) and minimum 0.1 ± 0.0 mg F^-/L (280 ft). In general, the concentrations did not exceed the health-based WHO-guideline value of 1.5 mg F^-/L, regarding fluorosis (WHO, 2006).

4.2.2.3 Conclusions regarding Arsenic

4.2.2.3.1 Shallow Aquifer (30, 50, 70, 85 and 90 ft wells)

The predominantly grey reduced shallow aquifer sediments are characteristic for young, poorly flushed sediments that were deposited under reducing conditions during marine transgressions. Formerly, in general low flow conditions must have existed within these Holocene aquifers. Only nowadays (for 20 – 40 years), irrigation may trigger more intense water exchange and flushing processes (Kinniburgh and Smedley, 2001). The groundwaters in the grey-reduced shallow aquifer sediments had the Ca-HCO_3-type in common. Average redox conditions were partially reducing, due to an under-saturation of the waters with oxygen. DOC was available in all depths, indeed in differing amounts. The occurrence of Nitrite, Sulphide, besides high amounts of dissolved Iron(II) and Mn(II) indicated that the microbial reduction of dissolved Nitrate (Denitrification), and Sulphate as well as solid Iron-, and Manganese-oxides takes place. Alone these findings indicate that the release of Arsenic due to reductive dissolution of Iron, Manganese and other metal (hydr)oxides during degradation of organic matter, as already described in section 2.1.2 and as suggested by Kinniburgh and Smedley (2001), McArthur et al. (2004), Zheng et al. (2004), Ravenscroft et al. (2001, 2005), and Nickson (2000), is a possible and the most probable scenario. Kinniburgh and Smedley (2001) further suggested, achieving anaerobic conditions in Holocene aquifers up to the Sulphate reduction may additionally trigger the transformation of adsorbed Arsenate to the more mobile Arsenite, or simply dissolve Arsenic bearing Iron and Manganese hydroxides. The latter process might be the more important one, considering that sorption experiments of Arsenate and Arsenite on FeOOH by Dixit and Hering (2003) showed comparable sorption of Arsenite and Arsenate at near-neutral pH. Arsenite hereby probably forms an innersphere binuclear surface complex with the FeOOH-surface. Reduction of Arsenate to Arsenite alone would, thus not release significant amounts of arsenic into solution, while dissolution of the Iron hydroxide sorbent would ((Dixit and Hering, 2003)). Another secondary process may be the diagenetic aging of iron (hydr)oxides, leading to the reduction of their surface area or changes in surface structures that formerly were available for adsorption of Arsenic. Figure 44 illustrates the aforementioned scenario.

Earlier studies suggested, distinct water withdrawals expose surficial aquifer layers to atmospheric oxygen and release Arsenic bearing pyrite. Redox conditions of grey reduced shallow aquifer sediments and groundwaters in all wells were not oxidizing. The occurrence of Sulphide (tempo-

rary highest in 70 and 90 ft depth, see Appendix A1) pointed out that Sulphate reduction must take place. A significant inverse correlation between As (As(sum), As(tot), Arsenite, Arsenate) and $SO4^{2-}$ was found within the shallow aquifer wells over depth (Appendix A4). Arsenic concentrations were lowest in the 30 ft well, nearest to the surface, and increased with depth. All these arguments speak against concurrent release of Sulphate and Arsenic by oxidative dissolution of pyrite. Harvey et al. (2002) additionally suggested that the low dissolved sulphur levels appear to limit precipitation as As-pyrite.

The hypothesis that fertilizer-phosphate mobilizes As can not be followed either. P-and As-concentrations were found to be lowest in the 30 ft well, nearest to the surface, where the entries of fertilizer phosphate are expected to be highest. In contrast, highest P-concentrations were found in deeper strata, coming along with highest Arsenic concentrations. In contrast, the positive significant correlations between As and P in the shallow aquifer wells vs. depth rather speak for a common release mechanism of both. A competitive exchange of P against As would imply an inverse correlation between both anions.

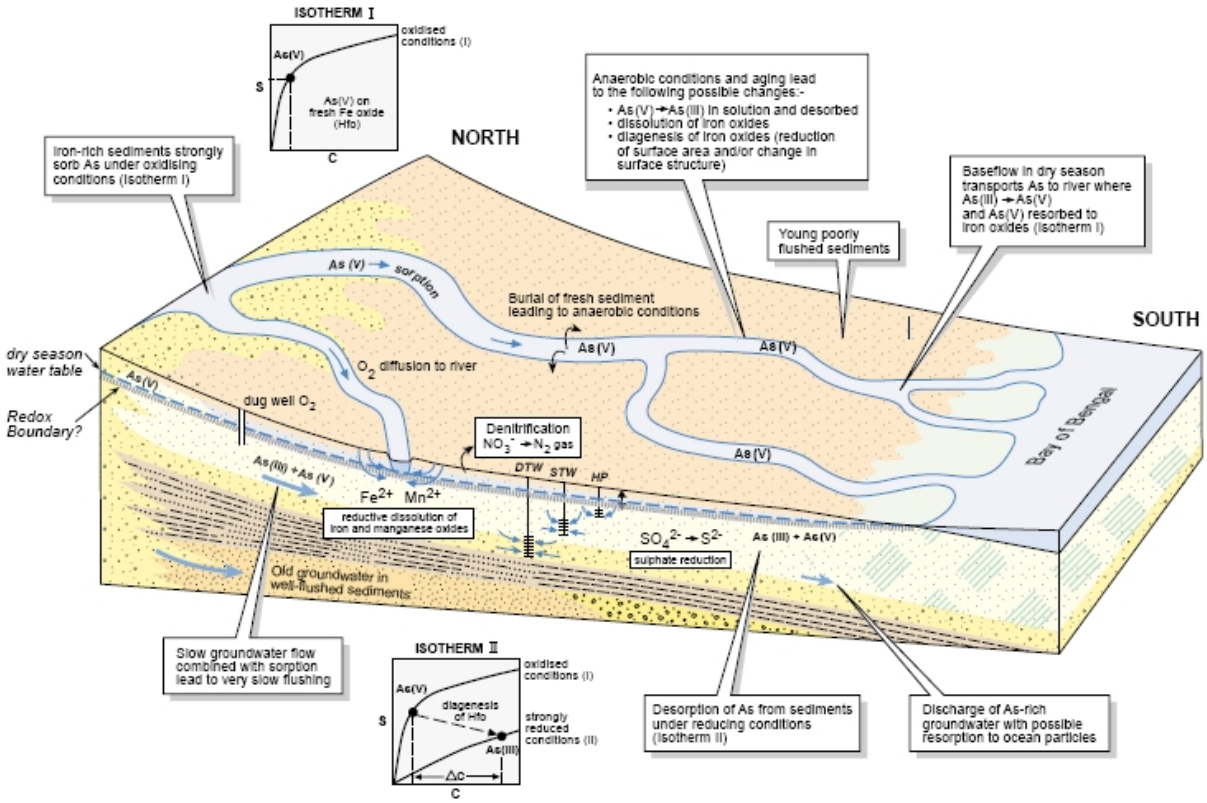

Figure 44 *Schematic diagram showing the processes leading to the generation of high arsenic groundwaters in the Bengal Basin, taken from Kinniburgh and Smedley (2001). (abbreviations: As(III) = Arsenite, As(V) = Arsenate)*

Obviously, in the shallow aquifer wells the total As-concentrations, as well as Arsenite and Arsenate tend to increase concurrently with the concentrations of Phosphorus, Iron, Manganese, DOC, TIC, Bicarbonate and Ammonium with depth (Table 23, Figure 38 - Figure 43). Further, total Arsenic and Arsenite concentrations seem to be the higher, the lower (i.e. the more reducing) the average measured redox potential is (see Figure 38). This impression is affirmed by the correspondingly significant results of the Spearman rank correlation test. The rank correlation results for the shallow aquifer wells are listed in Appendix A4.

The HCl-leachable amounts of Fe, Mn, As, and P in the shallow aquifer sediments increased with depth. Peat, and suddenly higher TOC-concentrations within sediments, were found below 27 m depth. They form a possible source for high DOC in groundwater. It seems, degradation of organic matter (DOC) takes place with increasing magnitude with depth, releasing carbon dioxide as by-product, which thereafter largely transforms into Bicarbonate under the near neutral pH-conditions existent at the test site. The detected Oxygen deficit conditions (especially regarding the more reliable early year data (see Appendix A1) and pump test data (see Appendix A2) and slightly increasing redox potential, indicate reducing conditions. They come along with correspondingly higher release rates of the by-products Iron, Manganese, inorganic Carbon (TIC, HCO_3^-, H_2CO_3), Ammonium and Phosphorus with depth. Suggesting that Arsenic and Phosphorus form connatural anions that adsorbed preferential on Iron hydroxides (Acharyya et al., 2000), (Kinniburgh and Smedley, 2001), their release also elevates with depth. Organic matter degradation is the common initial redox driver for all these processes that show increasing magnitude with depth. This and the As-/P-/Mn-/Fe-pool that increases with depth (HCl-leach) finally may result in generally significant correlations between total As, Arsenite and Phosphorus, Iron, Manganese, DOC, TIC, Bicarbonate and Ammonium by testing the results of connatural groundwaters from different depths together (Appendix A4).

Table 23 *Average concentrations ± standard deviations of all measured values for As(tot), P(tot), Fe(tot), DOC, TIC and Bicarbonate in the shallow aquifer wells in 2007*

	As(tot) [µg/L]	P(tot) [µg/L]	Fe(tot) [mg/L]	DOC [mg/L]	TIC [mg/L]	HCO_3^- [mg/L]	NH_4^+ [mg/L]
30 ft	**24 ± 6**	**491 ± 119**	**0.5 ± 0.3**	**0.8 ± 0.3**	**31 ± 6**	**155 ± 24**	**0.2 ± 0.1**
50 ft	131 ± 29	1,098 ± 287	0.8 ± 0.3	1.1 ± 0.4	34 ± 2	178 ± 13	0.7 ± 0.2
70 ft	108 ± 17	522 ± 77	0.7 ± 0.3	1.3 ± 0.4	35 ± 3	183 ± 19	0.6 ± 0.2
85 ft	**220 ± 16**	**1,475 ± 335**	**3.5 ± 0.8**	**2.2 ± 0.4**	**57 ± 3**	**287 ± 25**	**1.6 ± 0.5**
90 ft	184 ± 31	1,271 ± 309	2.3 ± 0.8	2.4 ± 0.9	54 ± 3	271 ± 26	1.4 ± 0.5

The concurrent occurrence of higher Arsenic concentrations with high organic Carbon contents in sediment and groundwater may also indicate their former co-deposition. Meharg (2006) realized that highest Arsenic-affected groundwaters are found in vegetated wetland sediments. In Bangladesh this includes first of all the coastal mangrove swamps (Sundarbans) and the seasonally inundated south-central areas of Bangladesh, related to the floodplains of Ganges, Brahmaputra and Meghna. Nowadays, these areas feature no (Sundarbans) or less intense (south-central region) irrigation activities than the lower Arsenic affected north-western part of Bangladesh. Young forest-floor sediments in the low populated Sundarbans showed distinctly higher As and organic Carbon than non-vegetated overbank sediments (Meharg et al., 2006). In wetlands it is well known that plant roots release oxygen into a generally anaerobic and Fe(II)-rich environment (Chen et al., 2005; Hansel et al., 2002; Kirby et al., 2002; Meharg et al., 2006). An oxygen-gradient develops from the rhizosphere outward, transforming dissolved Fe(II) to Iron(III)hydroxide, which deposits in the rhizosphere-environment. In the Sundarbans red Fe(III)oxide enriched sediments are visible around plant and tree roots, encased in a matrix of grey-green reduced sediments. Dissolved As, percolating with waters from rivers into the soil, concentrates on the iron surfaces under oxidation of Arsenite to Arsenate. This may indicate that As and organic Carbon probably were co-deposited in (seasonal) terrestrial wetland habitats. Iron-oxide associated As also is reported to accumulate in living invertebrate burrows in wetland soils (Doyle and Otte, 1997; Meharg et al., 2006). Later, after burial, As, Fe and organic matter may be liberated again by the aforementioned re-release processes (see Figure 44).

The fact that highest DOC and concurrently higher Arsenic concentrations were found in deeper strata seems to indicate that buried organic matter (peat-deposits below 27 m depth) actually must play a more important role as redox driver for arsenic release than young organic carbon, as suggested by Harvey et al. (2002). Otherwise, the highest DOC and As-concentrations would be expected in more surficial aquifer strata, which should be more influenced by young organic carbon than deeper strata. Nevertheless, young organic carbon as another potential redox driver can not be completely excluded. If to some extent young organic carbon should be available, it will be metabolised more easily than peat (higher percentage of recalcitrant, higher molecular fulvic and humic acids) by microorganisms. High potential hydraulical permeabilities (17 m/d = 119 m/week, see section 4.1.2.1) were calculated for the shallow aquifer. Due to extensive irrigation activities, young organic carbon surely is drawn down much faster and in higher quantities to deeper strata, than it is possible without irrigation in a low-flow system with low natural gradients. Neverthe-

less, the TOC-measurements indicate relative enrichment of younger organic Carbon only in very shallow depths above 5 m depth (11.0 – 25.6 g/kg).

It astonishes that DOC consistently increased with depth in shallow aquifer groundwaters (from 0.8 to 2.4 mg/L), whereas TOC showed relatively low, less variable concentrations between 5-27 m depth (between 1.09 – 3.42 g/kg), but suddenly increased at the barrier to more clay rich and peat-bearing sediments below 27 m depth (9.86 g/kg). On this background and with Meharg's (2006) co-deposition theory in mind, it is assumable that groundwaters, featuring high DOC and Arsenic concentrations, also may be shifted from their common source below 27 m depth to shallower depths by irrigation pumping. Such a relocation-process may explain, why former studies (Harvey et al., 2002) found high Arsenic concentrations in groundwater, but concurrently did not find any peat.

More definite conclusions regarding the role of organic Carbon in Arsenic mobilization are not possible from the shallow aquifer data. ^{14}C Age dating could give additional information, which type of organic matter predominates in what depth. Further investigations, if TOC in sediments and DOC in groundwater represent easily degradable or predominantly recalcitrant organic carbon species would give more meaningful information about the origin of DOC and the role of irrigation activities for Arsenic mobilization.

Both, Monothioarsenate and Sulphide seemed to show highest values in 70 and 90 ft depth. It is just a suggestion, but probably Monothioarsenate only forms under stronger reducing conditions, when concurrently Sulphide is available.

4.2.2.3.2 Sand lens (115 ft well)

The maximum total As-concentrations (248 ± 32 µg/L) of the Na-HCO_3-Cl-type groundwaters in the grey reduced sand lens sediments come along with the highest total Phosphorus (5,158 ± 587 µg/L), Phosphate (4,445 ± 553 µg/L), DOC (14.3 ± 6.8 mg/L), TIC (126 ± 22 mg/L), and Bicarbonate (657 ± 131 mg/L) concentrations observed at the test site wells. Measured TOC-sediment concentrations are 9.9 g/kg within the sand lens, but even reach 15.6 to 23.5 mg/kg in the neighbouring clay-rich layers. The 115 ft litholog (Appendix C2) shows a peat layer below 30 m depth, close to the well screen (33.5 ± 1.5 m). Ammonium (29 ± 20 mg/L) is distinctly elevated here. Again, these results indicate that organic carbon acts as main redox driver. Iron concentrations (2.3 ± 1.7 mg

Fe(tot)/L) are in the concentration range of the 90 ft well, which showed relatively high Arsenic-values, too.

Even though Arsenite shows highest ratios (77 %), suggesting stronger reducing conditions than in the other wells, the ferrous iron percentage is with 41 % lowest, compared to the other wells (up to 80 %). Although Mn(tot) concentrations are the lowest recognized at the test site (0.2 ± 0.2 mg Mn(tot)/L), yet it featured the highest percentage of its reduced divalent Mn species (44 %). HCl-leachable Iron and Arsenic were a bit higher (12,700 mg Fe/kg, 1,900 µg As/kg), whereas Manganese was slightly lower (156 mg/kg) than the maximum shallow aquifer sediment concentrations. Considering that both, a higher iron and arsenic pool than in the shallow aquifer is available, it astonishes that As(tot) and its reduced species Arsenite reach their maximum concentrations, whereas the results for Fe (tot) and Fe(II) indeed show high, but no congruently elevated higher values. In the sand lens the As-release coupled to Fe-hydroxide reduction obviously seems to be overlain by more complex processes that must not necessarily result in the congruent dissolution of As and Fe. A study by Hornemann et al. (2004) gives a possible explanation for the not-congruent release of As and Fe. It confirms that the release of As is linked to the transformation of predominantly Fe(III) oxyhydroxide coatings on sand particles. Reflectance spectra showed that Fe(III)-oxyhydroxides at least partially transform into Fe(II) or mixed Fe(II/III) solid phases, such as siderite ($FeCO_3$), vivianite (Fe_3PO_4) or even magnetite (Fe_3O_4) (Horneman et al., 2004). Related incubation experiments showed that As and Fe mobilization processes are decoupled. Liberated As remains in solution, whereas Fe seems to re-precipitate, following the reduction of Fe(III) hydroxides (van Geen et al., 2004).

The fact that the highest Arsenic concentrations at the test site wells are socialized with highest measured DOC and a peat layer, may indicate the co-deposition of both. It is not likely that young organic Carbon plays a significant role for As-mobilization in the sand lens.

4.2.2.3.3 Deep Aquifer (280 ft well)

In contrast to the shallow aquifer and the sand lens, brown sediments around 81 m depth (280 ft) appeared to be thoroughly oxidized. The sediments must have had longer contact with atmospheric oxygen. It is a fact that several sea level changes occurred during Pleistocene (1.8 Ma – 10 Ka BP) with lowest levels during the last glacial maxima 18,000 years BP (see Figure 45). They induced large hydraulic gradients that facilitated subaerial erosion and an extensive oxidative

flushing of Pleistocene and late Tertiary sediment strata (Acharyya et al., 2000). Considered on this background, the oxidized sediments already may form the margin to Pleistocene sediments.

Nevertheless, regarding the litholog in Figure 6 (section 2.2.1) it is obvious that the oxidized sediment found during this survey has a very limited thickness (approx. 4 m) and again is underlain by grey reduced sands, down to minimum 286 m, which are interrupted by two clay lenses. These did not undergo intensive flushing. Breit et al. (2001) found a thin layer (5 cm) of similar appearance within Holocene strata, and suggests it must be a product of capillary fringe or water table fluctuations (Breit et al., 2001). Due to the aforementioned, it appears possible that the sediments are of Holocene age, but, were not buried as fast as other sediments during Holocene. Potentially fluctuating sea waters (relict Na-Cl-type groundwater) may have oxidized and flushed this segment of the deeper aquifer, before it was buried by the younger clay-sediments.

Acharyya et al. (2000) reports rapid sea level rises between 7,000 to 5,500 years BP that reached higher than present day levels (see Figure 45). During the mid-Holocene sea-level rise an extensive development of marine and fresh water peat in the Bay of Bengal (mangrove forests) is reported. Further, Arsenic became entrapped in fine-grained, organic-matter rich sediments that preferentially deposited under these low energy conditions in the Ganges delta, Meghna floodplains and Sylhet Basin. Then (5,500 years BP), sea level began to decline to present day conditions (Acharyya et al., 2000). Seen on this background, the extensive clay layer that concurrently featured remarkable peat deposits and comparatively high Arsenic concentrations (up to 3,050 µg As/kg) may be linked to the mid-Holocene sea-level rise (7,000 – 5,500 years BP). The relict seawater character of waters found in 280 ft depth (screen: 84.4 ± 4.6 m, below clay layer) and 115 ft depth (screen: 33.5 ± 1.5 m, sand lens within upper part of clay layer) supports this hypothesis. On this background, the brown oxidized, and underlying grey reduced, predominantly coarser sediment may represent strata older than 7,000 years BP. The absolute thickness of late Pleistocene (18,000 years BP) to Holocene (10,000 years BP) alluvial and deltaic floodplain sediments is more than 330 m. But, only the upper part of this sequence includes the Holocene aquifers that reach a maximum thickness of about 100 m (Burgess and Ahmed, 2006; Ravenscroft et al., 2005). Considering the latter, it simply appears unlikely that the grey-reduced sediments reaching down to 286 m depth still represent Holocene strata. Altogether, it is more probable that the brown-oxidized sediment below 76 m depth already forms the margin to Pleistocene sediments. However, only age determination (i.e. ^{14}C dating) may give evidence for this hypothesis.

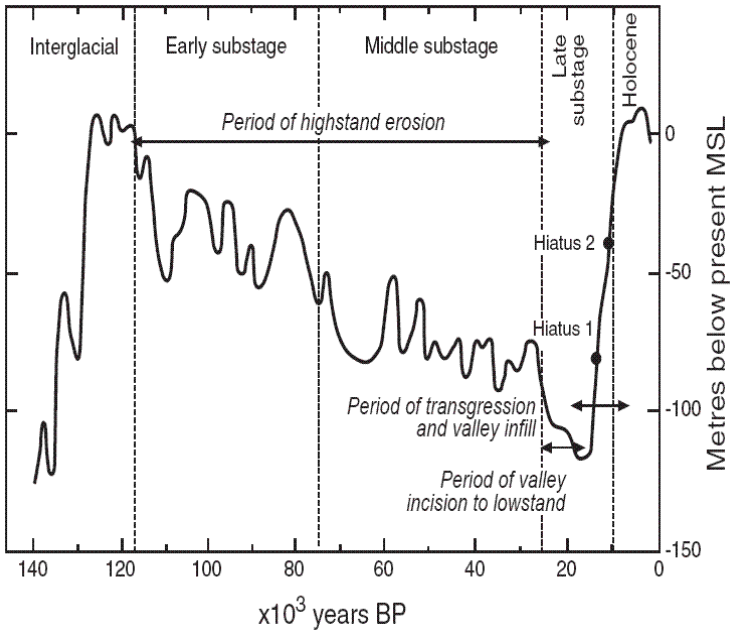

Figure 45 *Sea-level changes during the last interglacial-glacial transition, after Pirazzoli (1991), in (Kinniburgh and Smedley, 2001)*

Although the sediments show oxidative appearance, nowadays the average redox potential of the groundwaters is partially reducing (193 ± 31 mV) like in the other test site wells. The most characteristic feature of the Na-Cl-type-groundwaters are the extremely high, but temporarily variable Iron (84 ± 52 mg/L) and Ammonium (100 ± 50 mg/L) values. These distinctly exceed maximum values of 15.7 mg Fe/L (Ahmed et al., 2004) and 23 mg NH_4^+/L (McArthur et al., 2001) reported for Bangladesh groundwaters. In contrast, comparatively low concentrations of 65 ± 18 µg As(tot)/L and 1,202 ± 791 µg P(tot)/L were detected. Nevertheless, TIC (108 ± 16 mg/L) and DOC (13.0 ± 2.3 mg/L) are almost as high as in the sand lens. Total Manganese reached maximum values in this depth, in average 0.9 ± 0.5 mg Mn(tot)/L. Distinctly elevated DOC, TIC and NH_4^+ values suggest a near organic Carbon source, although TOC was low in the 280 ft-sediments. Assuming that the aquifer section was already flushed in the past, it is unlikely that the oxidized sediments served as source for As afterwards. Behind this background it is reasonable that the concentrations found for Fe, Mn, TIC, DOC, NH4, P and As probably originate from the degradation of the huge peat deposits within the aquitard layer above. From the water table measurements (section 4.1.1) it can be assumed that water in general slowly would move downward from the shallow aquifer through the aquitard to the leaky-confined deep aquifer. A triggering effect from irrigation is not likely, most of the irrigation well screens sit in the shallow aquifer between 20 – 60 ft (6 – 18 m) depth (Steinborn, 2008). Only deeper drinking water wells may have some effect on deep aquifer groundwaters.

The clay layer features distinctly higher leachable Fe and As (approx. 20,000 mg Fe/kg; 3,000 µg As/kg HCl-leach), compared to aquifer sediments (deep aquifer: approx. 5,000 mg Fe/kg; 300 µg As/kg, shallow aquifer: approx. 5,000 – 10,000 mg Fe/kg; 330 – 940 µg As/kg). The relatively high Fe concentration in groundwater might be due to the higher Fe-supply from the clay layer, dissolved by organic matter degradation. Transformation of Fe(II) to Fe(III) and its re-precipitation might be prohibited by the lower pH found in the peat-enriched sediments (pH 5.7, see Figure 38). Sediment pH of approximately 6.5 in 280 ft equals that of the shallow aquifer. In contrast, the groundwater pH (6.4, deep aquifer) was comparatively lower (approx. pH 7.1, shallow aquifer). This slight acidification may indicate that the waters are enriched with organic acids and originate from the peat layer. In contrast to other metals, the mobility of Arsenic distinctly increases with pH, especially above pH 7 Arsenic is released (causes: increasing negative charge of Arsenite and Arsenate, increasing negative charge of competitive organic anions, de-protonation of sorbents (Litz et al., 2004)) On the other hand, the relatively lower pH-values found within peat, may result in stronger retention of Arsenic on clay, released by the reduction process. Due to broken edge sites, Arsenic shows similar pH-dependent sorption/desorption behaviour to that of Fe/Al hydroxides on Kaolinite, Halloysite, Illite, Montmorillonite, and Chlorite (Gräfe and Sparks, 2006). As-sorption on Kaolinite is suggestible in the Titas aquitards (see Table 2). Although clay sorbs 40 to 60 times less Arsenic compared to Fe/Al hydroxides (Goldberg, 2002; Gräfe and Sparks, 2006; Lin and Puls, 2000), the great abundance of clay in the aquitard layer may play an important role (see Table 2). A strong retention of As in the aquitard sediments, probably dominated by clay and mica, was detected from batch experiments (Lissner, 2008). But, Arsenic released within the clay layer also might be re-adsorbed by the formerly flushed deep aquifer sediments, because the brownish oxidized iron (hydr)oxides nowadays even may constitute a sink for As. Lissner (2008) found that Arsenic sorption rates were higher in the oxidized deep aquifer material, than in the grey-reduced shallow aquifer sediments. Concurrently, As was retarded more in the oxidized aquifer sediments, then in reduced grey sediments (Lissner, 2008).

This scenario may serve as one possible explanation for extremely high iron concentrations, coming along with comparatively low, but yet elevated As-concentrations above threshold values in a brown oxidized, potentially Pleistocene age sequence. Nevertheless, it may further indicate that high concentrations of As or other water quality parameters found in the groundwaters of a sediment strata must not necessarily derive directly from the same sediment strata. In reverse, this

means for the shallow aquifer that high water withdrawals in this strata may trigger even more distinct relocation of waters.

4.2.3 Seasonal changes of the groundwater chemistry

The temporal variations of all measured parameters are graphically visualized in Appendix A1. In general (exemplary in Figure 46) average results of QC-triplicate samples are highlighted in these representations and error indicators were attached, which represent the absolute standard deviation (ASD) determined from these triplicate samples. (If no error indicators are visible, then this reflects the very low measured deviations of triplicate samples. It does not mean that indicators were not attached.)

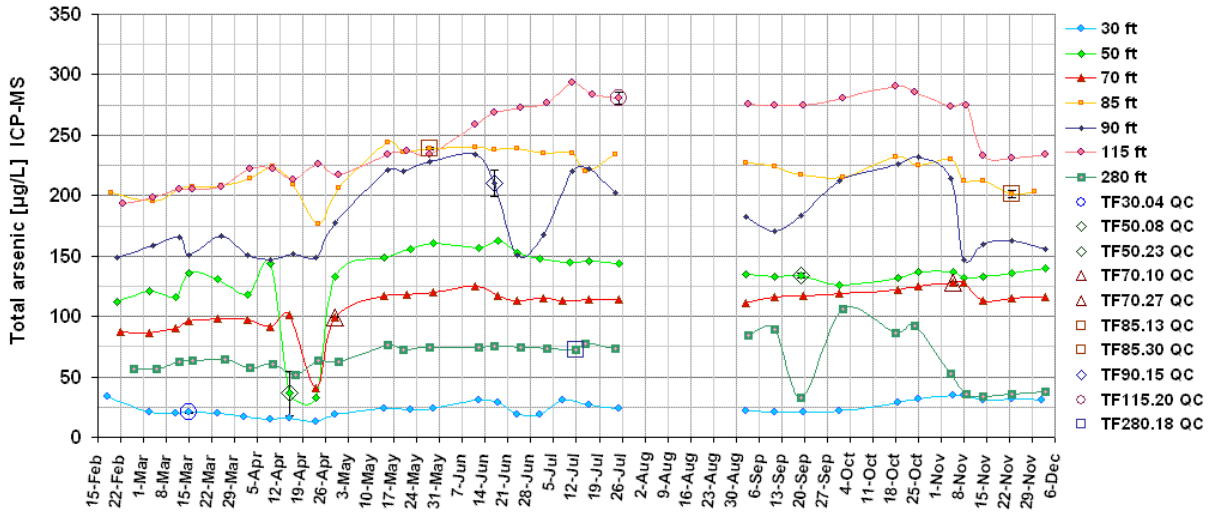

Figure 46 *Temporal variations of As(tot) [ICP-MS] at Titas in 2007. Variations detected since 8th of November may reflect influences of the pumping tests carried out at TF280 (07-11-06), TF115 (07-11-07), and TF85 (07-11-08).*

First of all, there are variations visible in the quantities of several measured parameters since monitoring No. 28 (8th of November 2007, see Figure 46). These are probably related to the aquifer tests at the 280, 115 and 85 ft wells (6th/7th/8th of November 2007) and will be discussed in chapter 4.3.

4.2.3.1.1 Single dips

Remarkable temporary limited dips were detected concurrently for As-totals (As(tot), As(sum)), Arsenite, and Arsenate in the 50 ft, 70 ft and 85 ft well between April, 12th, and May, 3rd , 2007 (Figures HH-KK). The total Arsenic concentrations suddenly decreased by approximately 125 (50

ft), 60 (70 ft), and 30 (85 ft) µg As(tot)/L. During this event the 50 and 70 ft concentrations reached As-levels, comparable with average concentrations in the 30 ft well (24 ± 6 µg/L). P-total (P(tot), P(sum)), Phosphate and especially P(unid) data exhibit a concurrent lowering within the same time-frame as As (Figures DD-GG, Appendix A1).

The reason for these dips is not clear. Steinborn (2008) reports some single heavy rainfalls in April (see Figure 10), suggesting there might be a relation between infiltrating rainwater and the observed decrease in arsenic concentration. But, it should be considered that most of the rainwater during the hot pre-monsoon season will be consumed by evapo(transpi)ration (see Figure 12). And, if percolating rainwaters had caused the flushing, then distinct changes in 30 ft depth should have occurred, but they did not.

Nevertheless, considering potential hydraulical permeabilities of 17 m/d (119 m/week) in the shallow aquifer, it still appears possible to draw sufficient amounts of water from shallower depths down to 85 ft (27 m) depth within a short time interval. Eventually the flushing waters derive from shallower groundwater strata, e.g. from 30 ft depth, where an average load of 24 ± 6 µg As(tot)/L was detected. If this was the case, it should also cause changes of other parameters than As and P. The fact that no distinct variations of TIC, DOC, anion and cation concentrations could be detected within the same time interval, might be due to comparatively similar concentrations of these parameters in 30, 50, 70 and 85 ft depth. Also regarding concentrations of Fe, Mn and NH_4^+ , these are relatively similar in 30, 50 and 70 ft depth, whereas the temporal oscillations in the 85 ft well are generally to high, to observe distinct variations linked to this event. The Fluoride values in 30 and 50 ft depth increased distinctly from approx. 0.25 mg/L up to approx. 1 mg/L with some time shift, between 19th April -17th of May. This may indicate that contaminated surface waters were drawn down to deeper strata, because Fluoride can be accumulated in the soil due to application of Phosphate fertilizers (Flourapatite: $Ca_5(PO_4)_3F$) and F^--bearing pesticides. However, due to the uncertain data situation, the As/P-dip can not sufficiently implicate an influence from irrigation activities. If the event really should be linked to water withdrawals, yet it astonishes that such effects did not appear more often during the dry season.

A single dip of As(tot), As(sum), occurring during rainy monsoon in the 280 ft well (19th of September 2007), definitely can not be due to irrigation activities. The As-decrease in 280 ft depth seems to come along with a sudden high decrease of total dissolved Manganese. But, regarding the general curve progression of both parameters, there appears no continual dependency between As

and Mn. Nevertheless, the sudden decrease in Mn (tot) may indicate the formation of solid Mn-hydroxides, serving as a sorbent for Arsenic. The initial cause for such a transformation yet is unclear. Besides natural causes, the effect of inadequate purging of the well still must be taken into account as another reason.

In any case the seasonal change detection points out that one single sampling does not necessarily describe the actual state of the Arsenic contamination at a well with sufficient certainty, as it was done during the BGS/DPHE- survey all over Bangladesh (see Figure 1). Without any knowledge about temporal variations, one runs the risk to underestimate (or overestimate) the magnitude of the Arsenic contamination in groundwater.

4.2.3.1.2 Seasonal Changes

The sand lens shows the comparatively highest increase of As-totals in the first half of the year. Remarkable is the great variance of EC over time in 115 ft depth. Until May 2007 EC intensely oscillated around 3,000 µS/cm, then suddenly declined. Since end of June it lies below 1,500 µS/cm and with slight oscillations remains on this level. Similar variations are visible for TDS, the major cations and anions, as well as TIC, and DOC, (Figures F, G, Q, S, T, U, V, W, BB, CC in Appendix A1). It appears, less mineralised waters intruded the sand lens in the first half of the year. It is unlikely that low natural hydraulic gradients would allow such a fast exchange of waters. Irrigation activities were most intense in the hot dry season. One suggestion is that irrigation lead to an exchange of groundwaters in the depth. Eventually the waters originate from the shallow aquifer, which has a hydraulical connection to the lens, or may derive from another connected lens within the transition area between shallow aquifer and aquitard layer.

In contrast to EC, TIC, DOC and major cat-/anions, Arsenic values (totals and Arsenite) distinctly increased in the first half of the year, from approx. 200 µg/kg As(tot) in February up to nearly 300 µg As(tot)/kg in beginning of July. Thereafter, the As(tot) values remained on this level. It might be that the intruding waters already featured a higher initial Arsenic load and this lead to an increase of As(tot). An additional competition between As and P for surface sorption sites seems possible, too. Phosphate competes stronger for exchangeable sites on solids than Arsenite, i.e. Arsenite can be easily exchanged by Phosphate (Lissner, 2008; Manning and Goldberg, 1997; Radu et al., 2005; Violante and Pigna, 2002). In contrast, the sorption of Arsenate to the soil surface appears to be stronger than that of Phosphate (Manning and Goldberg, 1996). The increasing total As-values come along with an distinct increase of Arsenite, whereas Arsenate concentrations do

not change significantly in the first half of the year. However, P(tot) and P(sum) do not show comparable results in 115 ft depth in the first half of the year. Probably P(tot) results are more reliable, as explained in section 4.2.1.4. Yet it is unclear, if the lowering of the P(tot)-values over time partially results from these exchange processes, or if the intruding waters featured generally lower P-values, accompanied by higher As-concentrations. One possible explanation for the visible decrease of Arsenite and increase of Arsenate in 115 ft depth since September might be the later acidification during this survey (see Appendix A1, Figures HH, JJ). But also due to the interaction of the seemingly ingressed groundwaters with the local sediments, it seems possible that Arsenite partly transformed into Arsenate over time.

The shallow aquifer wells which are situated closest to a peat layer (90, 85 ft) showed a trend of increasing arsenic values during the first half of the year, too. A slight, similar trend can be detected in the 50 ft and 70 ft well. Concentrations in 30 ft depth remain almost on the same level throughout the year. During the second half-year with exception of the 90 ft piezometer, As concentrations widely seem to remain on these levels. Within the shallow aquifer the 90 ft (screen: 10 ft, screen depth 25.9 ± 1.5 m) groundwaters showed most intense fluctuations of its As values during the whole year. The 85 ft (screen: 5 ft, screen depth: 25.1 ± 0.8 m) well did not show such frequent fluctuations. Both well screens overlap, but the 90 ft screen is longer, representing more mixed waters of a wider vertical aquifer section. This may be the cause for higher detected oscillation in the 90 ft well. Both well screens are close to a peat layer recognized below 27.4 m during the 90 ft well construction, which was detected first below 26.2 m in the litholog, too.

Results of continuous two-weekly monitorings by the BGS/DPHE-survey of piezometers at different depths at Lakhshmipur, Faridpur, and Chapai Nawabganj between April 1999 until April 2000 are represented in Figure 47 (Kinniburgh and Smedley, 2001). The greatest variations over time seem to occure in shallow depths between 10 to 50 m that are concurrently affected by higher absolute Arsenic concentrations. In these depths highest water movement due to irrigation is expected and may be the cause. Fluctuating Arsenic concentrations, apparent at the beginning of monitorings, even may be related to disturbances from drillings. Considering the short time-scale (1 year), the authors concluded, yet there is no convincing evidence for seasonal changes deducible.

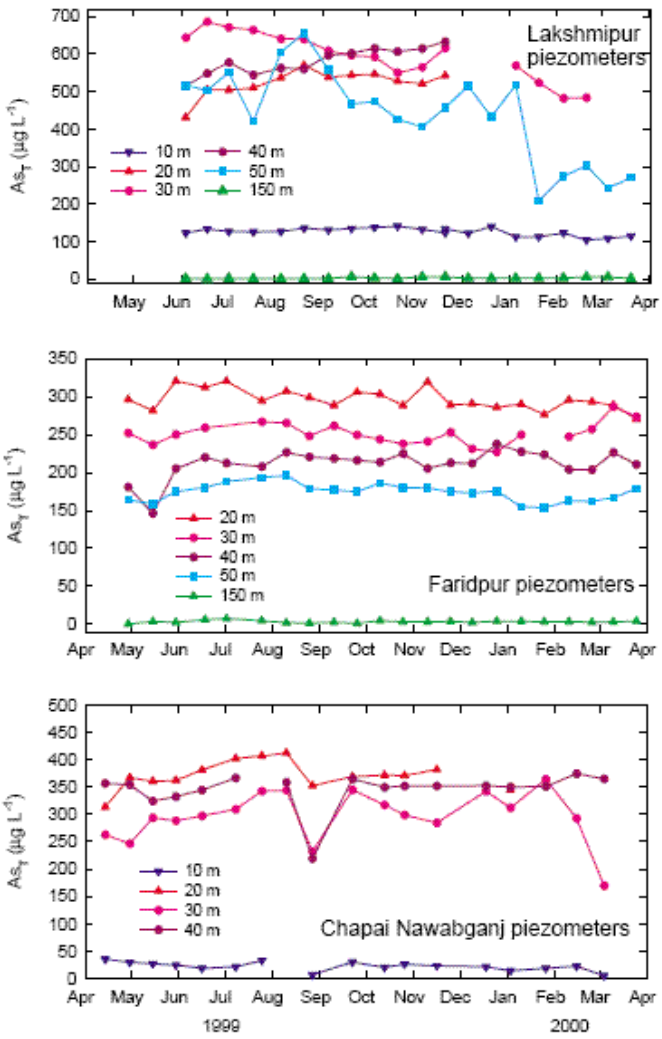

Figure 47 *Temporal variations of arsenic concentrations found during the DPHE/BGS-study (Kinniburgh and Smedley, 2001)*

To detect factors triggering mobilization of Arsenic over time, the seasonal results per well for As were compared with the results for P, TIC, DOC, HCO_3^-, H_2CO_3 and redox sensitive parameters with the Spearman rank correlation test. The results are listed in Appendix A4. Monothioarsenate and Sulphide were excluded from correlation tests, because values often were close to or below detection limit. Several significant correlations were found between As and the other test parameters, but none of the interrelationships occurs concurrently in all wells. Just for example, Arsenic totals (As(tot), As(sum)) and P(tot) positively correlate in the 30, 50, 70 and 90 ft well, show no significant correlation in 85 and 280 ft depth, but even correlate negatively in 115 ft depth. As another example may serve the correlation between Arsenic totals and DOC. Both correlate positively in 30 and 280 ft depth, negatively in 115 ft depth and no significant correlation is found in 50, 70, 85 and 90 ft depth. On this background it was questionable, how to handle the further

evaluation of the correlation results. First of all, it must be considered that other processes (degradation, dissolution, complexation, competitive sorption and desorption) may overlay arsenic mobilisation processes. Especially in 115 ft depth it is obvious that the overall water chemistry changed distinctly over the year due to intruding, less mineralised waters, probably superimposing any dissolution/sorption/desorption processes regarding Arsenic. Also in the 50, 70 and 85 ft wells evident flushing processes temporary changed the water chemistry. Variations of Arsenic measured in 30 ft depth were very low, potentially too low to reflect significant variations? Another fact is that errors of the measurement may influence the correlation results, too. The 280 ft well is the most critical candidate in this case. Due to comparatively lower pumping rates in the field (reduced purging effect), high sample colour and turbidity, as well as the high iron contents, oxidation and (co)-precipitation of water constituents after contact with atmospheric oxygen may have falsified the measurements more than in other wells, resulting in nearly no significant correlations.

Most frequently significant positive correlations were detected between As-totals (As(tot), As(sum)) on one side and P(tot), P(sum), PO_4^{3-}, and P(unid) on the other side in single wells. Further, positive correlations between As-totals/Arsenite and Fe(tot), Fe(II), Fe(III), Mn(tot), Mn(II) NH_4^+, H_2CO_3 that also occurred during correlation of all shallow aquifer wells together, were detected for some of the single well results again (see Appendix A4). Possible causes for these interrelationships were already discussed in section 4.2.2.3. In contrast, TIC (30, 70, 115 ft), HCO_3^- (30, 115 ft), and H_2CO_3 (30 ft) showed also inverse correlations with As-totals. If this is caused by competition for sorption sites between HCO_3^- and As, or just a relict from overlay processes and/or measurement errors yet is unclear. The results of Lissner's (2008) As desorption experiments with 0.04 M $NaHCO_3$ speak for the latter, because only very small amounts of As were released then.

In several wells the increase of As-values in the first half of the year was observed. By comparing the absolute variations with the BGS/DPHE-monitoring, it seems that only long-term monitorings can establish whether significant seasonal variations were detected and/or long-term trends in water chemistry. The inconsistent rank correlation results per well, as well as the relatively small variations of As concentrations found in some of the wells during this survey (30 ft) and the BGS/DPHE-survey pointed out that very careful sampling , followed by high-precision analysis is a prerequisite for meaningful conclusions. Otherwise, seasonal or long-term trends as well as complex interactions between As and other water quality parameters can not be detected reliably.

4.3 Influence of pumping tests on water chemistry

4.3.1 On-site parameters during water withdrawal

In Appendix A2 a summary of the results for electrochemistry measurements, found within 1-hour time-steps are listed for comparison with results from Monitoring No. 27 (04./05.11.2007, before pumping tests) and the average values plus standard deviation in 2007. Figure 48 and Figure 49 represent the variations of electrochemical parameters in 10-minute steps in the pumping wells. The first electrochemical measurement was started 10 minutes after pump start.

Measured temperatures quickly reach stable values in all wells. Temperatures found during pump tests are distinctly lower than those measured during Monitoring 27. This is valid also for average T in 2007 during monitorings (Appendix A2). It points out that waters heat up during low-flow sampling. The values for pH remain stable during all pumping tests and are similar to the low-flow sampling results.

Even though there is a short contrary curve progression for E_H in the beginning in the 280 and 85 ft well, a trend to more reducing conditions continues in all wells until the last reading. Oxygen values reached in the 115 ft (3.3 mg O_2/L), and especially in 280 ft (3.8 mg/L) depth distinctly lower values than those found during monitoring 27 with low-flow sampling (115 ft: 4.4 mg O_2/L, 280 ft: 5.9 mg O_2/L). Results for 85 ft depth were comparable, indeed it was pumped for only two hours. This points to insufficient purging times during low-flow sampling, at least regarding the deeper wells. EC increases over time in 115 ft and 85 ft depth, but continues to decrease in 280 ft depth. Thus, the mineralisation of the 280 ft waters declines, but rises in the shallower wells during pumping.

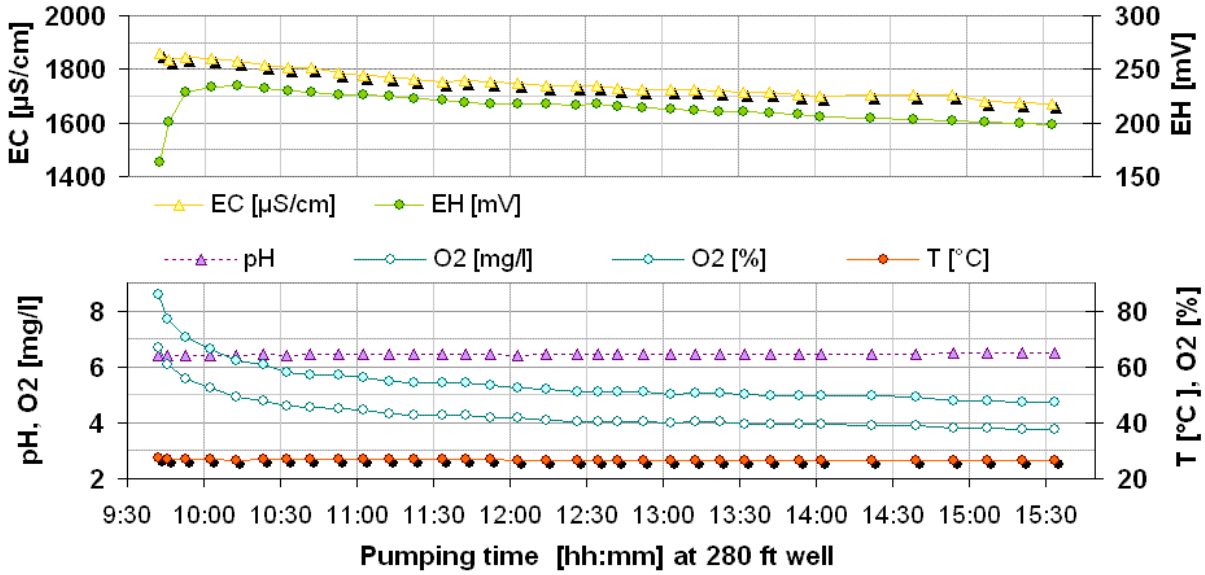

Figure 48 *Variations of pH, O_2, EC and E_H during the pumping test at the **280 ft** well (pump start time: 09:30 AM, 6 hours pumping, Q = 0.0024 m^3/s necessary time for removing 3 well casing volume's: 15 min)*

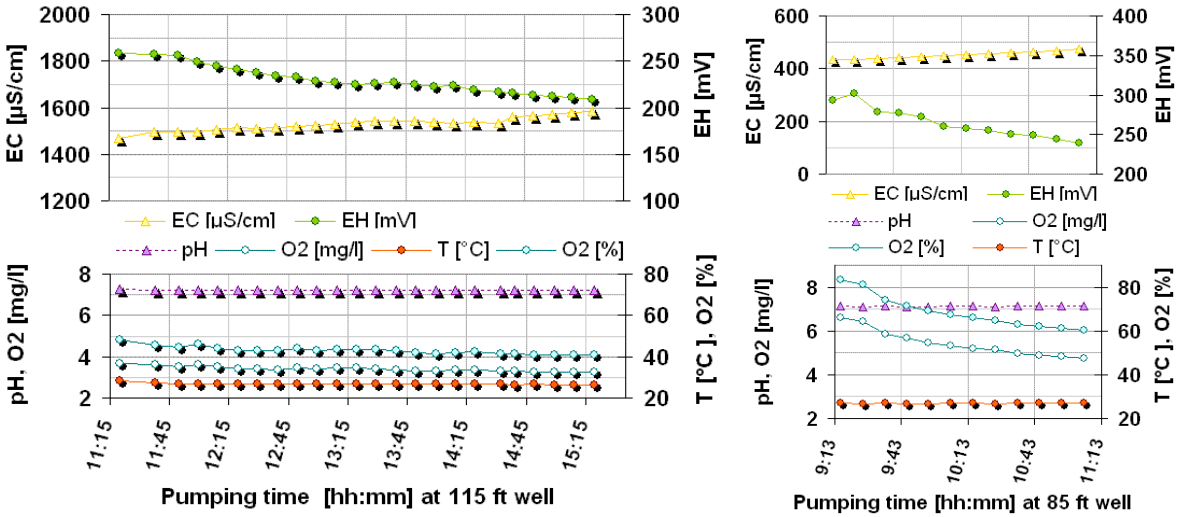

Figure 49 *Variations of pH, O_2, EC and E_H and T during pump tests at the **115 ft** and **85 ft** well (115 ft pump start: 11:15 AM, 4 hours pumping, Q = 0.0005 m^3/s, time for removing 3 well casing volumes: 8 min; 85 ft pump start: 09:13 AM, 2 hours pumping (generator broke down), Q = 0.0006 m^3/s, time for removing 3 well casing volumes: 4 min)*

4.3.2 Effects of water withdrawals on Arsenic and other water quality parameters

The results found for total Arsenic (As(tot), As(sum)) before pump start, before pump stop and after recovery are represented in Figure 50 in comparison to the variations during regular monitorings. Samples taken during pump tests are marked by a coloured frame, i. e. green = PT280, pink = PT115 and yellow = PT 85. The 85 ft aquifer test had small, but observable influence on the water tables of the 90, 70 and 50 ft well. Unfortunately the pump broke down after approximately 2 hours of pumping. Thus, no samples could be taken before pump stop in the piezometric wells, except at the 85 ft well a sample was still available. During the 280 ft pump test and the115 ft pump test no drawdown occurred in the other 6 piezometric wells. There's no direct hydraulical connection between groundwaters in 280 ft depth and the other six piezometers (see section 4.1). Thus, the variations of As(tot) in 85, 115, and especially in 90 and 70 ft depth during PT280 must have a natural cause or are due to methodological errors, but can not be linked to PT280. Variations in other wells during PT115 did not show significant higher variations, thus can not be linked to this with certainty. As totals in 280 ft depth seem to lower due to pumping (PT280) and remain on this level afterwards. As(tot) and As(sum) don't show comparable, meaningful results in 115 ft depth during PT115, but deplete afterwards. Significant changes between sample PT85-1 and PT85-2 in 85 ft depth are not visible, again As(sum) values show higher general fluctuations than As(tot).

Sudden changes for other water quality parameters since monitoring No. 28 (8th of November 2007) may result from pumping tests (see Appendix A1). In 280 ft depth occurred a short increase in EC, Ca^{2+} and Mg^{2+} and decrease in Na^{+}, Cl^{-}, DOC, and NH_4^{+}. Depletion of Na^{+}, Ca^{2+}, Mg^{2+}, K^{+}, Cl^{-}, and TIC is detected in 115 ft depth since monitoring No. 29, changes during monitoring No. 28 don't show significance. Regarding the 85 ft shallow aquifer test, in the 85 ft and 90 ft well small dips for Fe(tot), P(sum), PO_4^{-3}, and TIC during monitoring No. 28 are visible. Also Ca^{2+} and Mg^{2+} slightly decrease in 90 ft depth. The relocation of waters causes differing intense variations of the measured chemical composition. This also may induce the variations visible for As(tot) and As(sum). However, the results can not deliver reliable conclusions regarding Arsenic mobilization.

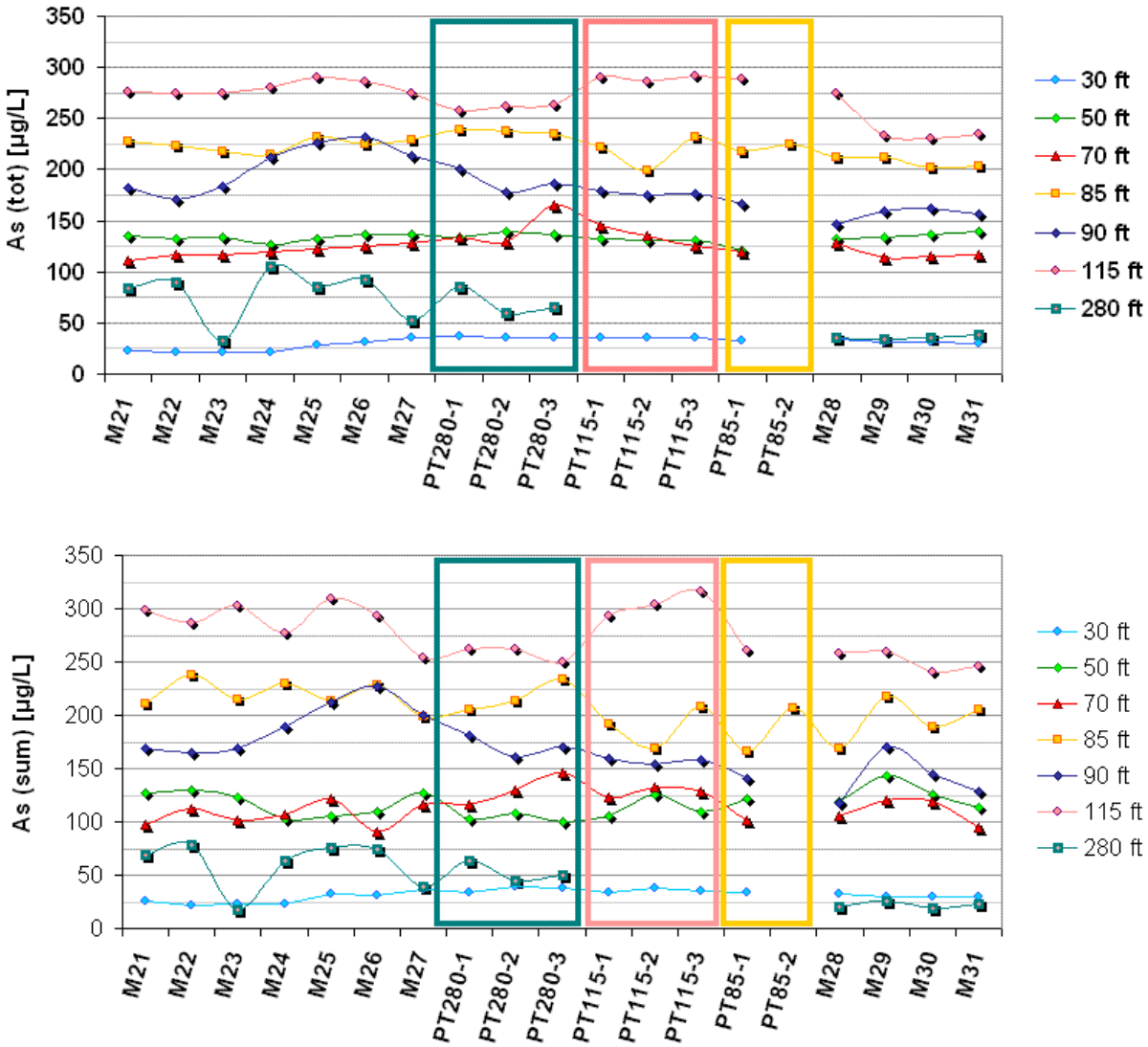

Figure 50 *Results for As(tot) and As(sum) in samples taken during pump tests in comparison with the results of the Monitorings 21 – 31 from September until December 2008 (cyan frame: PT280, pink frame: PT115, yellow frame: PT85)*

4.4 Injection spike

4.4.1 Spike Solution

Theoretical concentrations of K, H, and P inserted by the KH_2PO_4 spike solution are126 mg K/L, 6.5 mg H/L, and100 mg/L P. The spike solution was analysed only for the P(tot) and As(tot) concentrations with ICP-MS. For total Phosphorus 93 mg P/L were found, which roughly equals to the purposed 100 mg P/L. The error might base on an imprecise scale. Also impurities in the KH_2PO_4-salt might lead to the lower values. In example, the As impurity of 44 µg As (tot)/L, detected in the spike solution is unlikely to derive from the distilled water.

4.4.2 Results of the Injection Spike Test

Before looking at the chemical results, the following should be minded: The exact initial composition of the stagnant 85 ft water that was pressed into the aquifer is unknown, because samples were not taken. Since the water stood in the well tube for a long time, by having more intense contact to atmospheric Oxygen than the groundwater, stronger oxidizing redox-conditions are expectable. It is reasonable that redox-sensitive constituents like Iron and Manganese already precipitated to some extent. Phosphate and Arsenate co-precipitated on their surfaces. Arsenite transformed into Arsenate over time. Thus, a thinning effect by the stagnant water must be expected.

The volume of hand tube well water (HTW) used for flushing (50 l) slightly exceeded the amount of stagnant water in the 85 ft well (49 l) at the 30th of November 2007. The 5 ft (1.5 m) filter sits in 25.1 ± 0.8 m depth, whereas the well casing expands down to 27.5 m. So it is likely that besides the stagnant 85 ft water also some of the HTW-water that was used for flushing and partly mixed up with the stagnant one, was pressed into the aquifer. So besides the changes induced by the P-spike and the stagnant 85 ft well water also this influence must be taken into account.

The graph in Figure 51 represents the variable amounts found for P and As species, sum of species and totals before and during the injection test in comparison to the measured on-site parameters. It is questionable if the values found for As and P totals are as reliable as the As/P(sum)-values, because these data lack the drift correction with the internal standard (see Appendix B2). Especially in the HTW the discrepancy between the As/P-totals and As/P-sum is apparent. But also the measurements for totals and sum of species show distinct differences for As after 52 hours and for P after 28 and 52 hours.

Monothioarsenate in HTW and the 85 ft samples only occurs in negligible amounts below or near the detection limit, thus it will not be considered further. As Figure 51 shows P(tot), P(sum), PO_4^{-3}, Arsenite, Arsenate, As(sum), As(tot), Fe (tot), Fe(II), Mn(tot), Mn(II), NO_3^-, NO_2^-, NH_4^+, EC in the HTW are lower than in the initial 85 ft groundwater, hence in these cases the mix with HTW water will have a thinning effect. On the other hand, the reduced species S^{-2} is found in higher quantities, besides the fact that slightly lower E_H was detected in the HTW (182 mV) compared to initial 85 ft (203 mV), although the hand-pumped HTW-water was Oxygen over-saturated (102 %). The unidentified P-species is a bit higher in the HTW. The consequences of the mix of HTW with the 85 ft stagnant water and the spiked groundwater in particular reflects the sample taken after 2 hours: As(sum), As(tot), Arsenate and Arsenite are lowered due to dilution effects, whereas

P(sum), P(tot) and PO_4^{-3} still considerably increased due to spiking. Slightly higher P(unid) in part may arise from the higher HTW values. Yet it is questionable, if the stagnant 85 ft water didn't bring in higher P(unid), too.

All the measured P values after injection by far exceed the initial 85 ft concentrations of 897µg P(sum)/L and 628 µg PO_4^{3-} /L, respectively. Values for P(sum) and PO_4^{3-} distinctly increase with time, become highest after 52 hours with 3,213 µg P(sum)/L and 2,942 µg (PO_4^{3-})/L, respectively, and then decrease. The P-concentration after 52 hours minus the initial P-concentration gives the maximum added spike concentration recognized in groundwaters:

3,212 µg P(sum)/L – 897 µg P(sum)/L = 2,315 µg P(sum)/L = ***2.3 mg P(sum)/L***

2,942 µg PO_4^{3-}/L – 628 µg PO_4^{3-}/L = 2,314 µg PO_4^{3-}/L = ***2.3 mg PO_4^{3-}/L***

2.3 mg/L P(sum) and PO_4^{3-}/L (both determined as PO_4^{3-}) equal **0.8 mg/L pure Phosphorus**. Thus, at least parts of the spike-influenced aquifer section had to face a final spike concentration that reached an eightfold excess concentration regarding P-concentrations (0.1 mg P/L) that are equimolar to natural As-concentrations (0.2 mg As/L). A tenfold excess concentration of 1 mg P/L (see section 3.1.6) was assumed in advance.

In the beginning, due to thinning effects As (sum) values are lower than the original values, but after 28 hours reach values that nearly equal the initial 85 ft values and remain in this range even when maximum P-concentrations are achieved. No significant mobilisation effect for Arsenic totals is visible, even though P-concentrations distinctly increased due to the P- spike solution. Indeed, column experiments carried out by Lissner (2008) with Titas's shallow and deep aquifer sediments, showed that the continuous addition of a 1 mg P/L-solution mobilised both, Arsenate and Arsenite. But, the sediment-columns were equilibrated with 200 µg/L Arsenite or Arsenate solutions, before P was added, respectively. In contrast, As desorption experiments with an artificial groundwater solution released no weakly bound As from the sediment, suggesting equilibrium conditions between natural groundwater and aquifer sediments. Only moderately bound As could be released by hot HCl-leach in shallow aquifer sediments (940 µg As/kg in 24 m depth, see Figure 34). Considering the fact that a weakly bound As-fraction is not available, it is not astonishing that the P spike solution did not dissolve significant As-amounts.

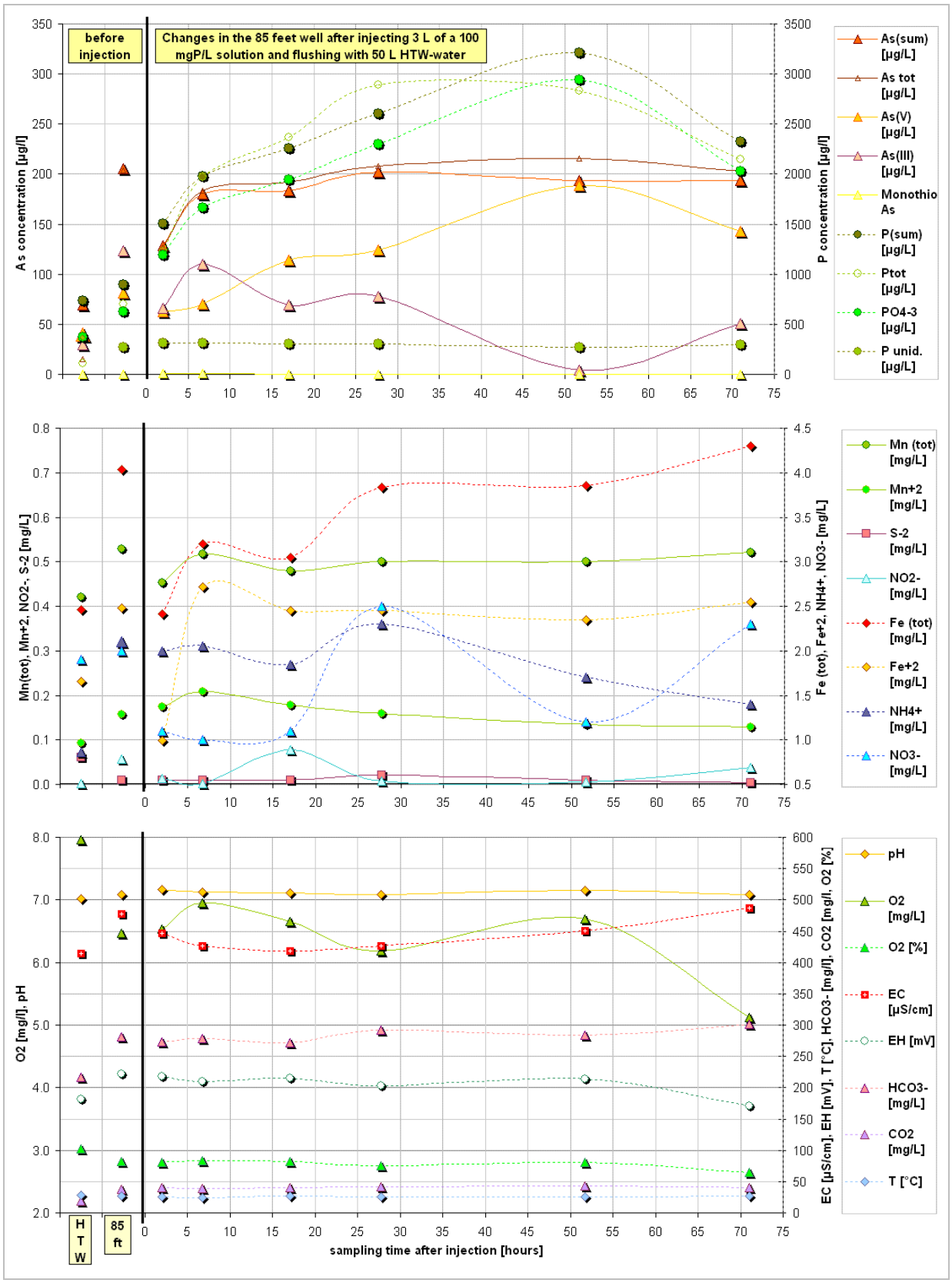

Figure 51 *Results of the As/P and on-site chemistry measurements in samples collected from the HTW (hand tube well water used for flushing) and the 85 ft well before and after spiking*

Nevertheless, there were distinct changes in the As speciation detectable. With the rise of P, Arsenate increases and Arsenite decreases. In the original 85 ft groundwater 60 % Arsenite and 40 % Arsenate made up whole As. In contrast, when P is highest, the portion of the species is 2 % Arsenite and 98 % Arsenate. The measured Oxygen concentrations are quite variable, with two peaks, the first after 7 hours and the second after 52 hours, when Arsenate and P is highest. The distilled water used for the spike solution was not de-aerated, thus probably was to 100 % saturated with Oxygen and probably causes the second O_2 peak after 52 hours. Further it can be assumed that the 85 ft stagnation water and the turbulent flushing with HTW water brought in Oxygen too and results in the first O_2-peak. It is more probable that the oxidation of Arsenite to Arsenate either results from O_2-insertion during turbulent flushing and/or is due to uneven sample acidification times. Moreover, the sorption of arsenate to the soil surface is reported to be stronger than that of Phosphate and the access of phosphate to certain exchangeable sites is said to be inhibited. In contrast, Arsenite can be easily displaced by Phosphate (Lissner, 2008; Manning and Goldberg, 1996; Manning and Goldberg, 1997; Radu et al., 2005; Violante and Pigna, 2002; Zhao and Stanforth, 2001). That means, if there had been any mobilization effect by Phosphate, it would have predominantly resulted in the release of Arsenite. Altogether it can be concluded, there was no competitive desorption effect induced by P at all.

5 RECOMMENDATIONS

There is need for very careful sampling and high-precision analysis, if seasonal long-term trends shall be detected reliably, to get reliable statistical results. Of highest importance are the sampling conditions. Purging of the well during low-flow sampling until stable conditions for the on-site parameters E_H, O_2, pH and EC are achieved, is inevitable. The sampling for on-site measurements and laboratory analyses should not be started earlier. An adequate energy supply is a prerequisite. A smaller, if possible airproof, flow cell during low-flow sampling will give more secure results. One of the main methodological mistakes during this survey was that As/P samples were not acidified immediately after filtration. Doing it immediately, will give more reliable data anyway and will facilitate data interpretation.

As-pollution of groundwaters is a known problem occurring in several river deltas of south-east Asia. This points on a predominantly natural context behind As-poisoning. Investigations at a highly irrigation affected district like Titas/Daudkandi can not solve the question, if a natural hydraulical control stood behind As-mobilization in the Bengal delta under pre-disturbance conditions. Polizzotto et al. (2008) found indications for this in an irrigation-unaffected area in the Mekong-Delta/Cambodia. As appeared to enter the aquifer system predominantly after release from surficial, river-derived wetland sediments. Then, it seemed to be transported on a centennial timescale through the aquifer back to the river. Influx in and efflux from the aquifer were in approximate balance (Polizzotto et al., 2008). Investigations in the outskirts of the low-populated Sundarbans mangrove forests, might give information about pre-disturbance As-mobilization conditions in the Bengal Delta.

If further investigations shall be performed at Titas's test site wells, the analysis should include age determination (e.g. ^{14}C radio carbon dating of peat, DOC, TIC) to get understanding, which sedimentary processes are coupled with high Arsenic concentrations in sediment and/or groundwater. It may solve the question, to which sedimentary age (Holocene or Pleistocene) the uncommon oxidized layer (280 ft depth) and other strata actually belong. It also may give information, if the high DOC and TIC concentrations in groundwater mainly originate from aged or young (organic) carbon sources. The species-composition of DOC may be of interest (e.g. which types of humic or fulvic acids) to see if these include easily biodegradable or more persistent forms. Adequate quantities of biodegradable organic carbon will play the more important role for Arsenic mobilization

regarding the Iron hydroxide mobilization hypothesis. The structure of the organic carbon species also may enlighten, from which sources (peat or young OC) they originate.

The unknown Phosphorus species should be identified (P(unid)). First of all, it may play a role for Arsenic mobilisation. Without knowledge about its exact chemical nature, interrelationships to Arsenic can not be enlightened. Further its occurrence may be of health concern.

The P-spike did not mobilize As from sediment surfaces. A repetition of the P-spike under more precise laboratory conditions with Titas sediments may show, if there is any small release effect visible that can't be detected under less precise field conditions. Prerequisite must be that sediments remain in their natural state, i.e. are not equilibrated in advance with Arsenic.

Field injection experiments with molasses (by-product of sugar refining, rich in easily biodegradable carbohydrates, including Sulphate) and Nitrate (an oxidant) were carried out at wells in Munshiganj (Ganges floodplains), Bangladesh (Harvey et al., 2002). The latter caused adsorption of As at sediment surfaces, potentially on iron oxyhydroxides. Molasses induced initial As-increase, then decrease, accompanied by distinct drop of redox potential and pH (pH 6.7 to 5.6, 100 mV to -230 mV) in groundwaters. The scenario shows that organic carbon induced microbial reduction of iron solids and liberation of As, followed by precipitation of As with sulphides. Repeating such a spike experiment at Titas may give information if remarkable As-concentrations potentially can be released by young organic carbon. In particular the role of shallower sediment strata for As-mobilization, which featured lower background concentrations of As and TOC, may be enlightened.

The role of fine-grained material as As-source material and for its mobilization should be illuminated further. During this survey, the fine-grained Aquitard sediments (partially co-deposited with peat) showed distinctly higher arsenic background concentrations than the coarse-grained aquifer sediments. It is of interest, if concurrently highest dissolved Arsenic concentrations in pore-waters generally are linked to fine-grained (peat-bearing) sediments. Low-flow sampling is applicable within aquitard layers, if adequate little flow rates are used (Puls and Barcelona, 1996). It may give evidence, whether the water chemistry in 280 ft depth really is influenced by waters percolating from the clay-peat-deposit above, or if this hypothesis has to be rejected.

BIBLIOGRAHY

Acharyya, S.K., Lahiri, S., Raymahashay, B.C. and Bhowmik, A., 2000. Arsenic toxicity of groundwater in parts of the Bengal basin in India and Bangladesh: the role of Quaternary stratigraphy and Holocene sea-level fluctuation. Environmental Geology, 39(10): 1127-1137.

Ahmed, K.M. et al., 2004. Arsenic enrichment in groundwater of the alluvial aquifers in Bangladesh: an overview. Applied Geochemistry, 19(2): 181-200.

Blüthgen, J. and Weischet, W., 1980. Allgemeine Klimageographie, 3. Walter de Gruyter, Berlin, 887 pp.

Breit, G.N. et al., 2001. Preliminary Evaluation of Arsenic Cycling in the Sediments of Bangladesh. USGS Report: 4.

Bühl, A., 2006. SPSS 14. Einführung in die moderne Datenanalyse. Pearson Studium München.

Burgess, W. and Ahmed, K.M., 2006. Arsenic in aquifers of the Bengal Basin. In: R. Naidu, E. Smith, G. Owens, P. Bhattacharya and P. Nadebaum (Editors), Managing arsenic in the environment. CSIRO Publishing, Collingwood Victoria, pp. 31 - 56.

Center for Environmental and Geographic Information Services (CEGIS). Bangladesh - Flood Affected Areas 3rd August 2007. CEGIS is setup under the aegis of the Ministry of Water Resources (MoWR), Government of Bangladesh (GoB), http://www.cegisbd.com/flood2007/index.htm, access date: June 2008

Chen, Z., Zhu, Y.-G., Liu, W.-J. and Meharg, A.A., 2005. Direct evidence showing the effect of root surface iron plaque on arsenite and arsenate uptake into rice (Oryza sativa) roots. New Phytology 165: 91 - 97.

Coury, L., 1999. Conductance measurements, Part 1: Theory. Current Separations.com, http://www.currentseparations.com/issues/18-3/cs18-3c.pdf, date accessed: July 2008, pp. 91 - 96.

Dixit, S. and Hering, J.G., 2003. Comparison of Arsenic(V) and Arsenic(III) Sorption onto Iron Oxides: Implications for Arsenic Mobility. Environmental Science & Technology, 37: 4182 - 4189.

Doyle, M.O. and Otte, M.L., 1997. Organism-induced accumulation of Iron, Zinc and Arsenic in wetland soils. Environmental Pollution(96): 1-11.

Goldberg, S., 2002. Competitive adsorption of arsenate and arsenite on oxides and clay minerals. Soil Science Society of America Journal, 66(2): 413-421.

Gräfe, M. and Sparks, D.L., 2006. Solid phase speciation of Arsenic. In: R. Naidu, E. Smith, G. Owens, P. Bhattacharya and P. Nadebaum (Editors), Managing Arsenic in the environment. From soil to human health. CSIRO Publishing, Collingwood VIC.

Hansel, C.M., La Force, M.J., Fendorf, S. and Sutton, S., 2002. Spatial an temporal association of As and Fe species on aquatic plant roots. Environmental Science & Technology, 36: pp. 1988 - 1994.

Harvey, C. et al., 2002. Arsenic Mobility and Groundwater Extraction in Bangladesh. Science, 298(5598): 1602.

Horneman, A. et al., 2004. Decoupling of As and Fe release to Bangladesh groundwater under reducing conditions. Part 1: Evidence from sediment profiles. Geochimica Et Cosmochimica Acta, 68(17): 3459-3473.

Hötzl, H. and Witthüser, K., 1999. Methoden für die Beschreibung der Grundwasserbeschaffenheit. DVWK Schriften 125. Wirtschafts- und Verlagsgesellschaft Gas und Wasser, Bonn.

Islam, S., 2003. Banglapedia: National Encyclopedia of Bangladesh. Banlapedia Trust, Asiatic Society of Bangladesh, Dhaka. Available online: www.banglapedia.search.com.bd, access date: July 2008

Kinniburgh, D.G. and Smedley, P.L., 2001. Arsenic contamination of groundwater in Bangladesh, Volume 1: Summary, British Geological Survey & Department of Public Health Engineering.

Kirby, J., Maher, W., Chariton, A. and Krikowa, F., 2002. Arsenic concentrations and speciation in a temperate mangrove ecosystem. Applied Organometallic Chemistry, 16: 192 - 201.

Kruseman, G.P. and de Ridder, N.A., 2000. Analysis and evalutation of pumping test data. Wageningen International Institute for Land Reclamation and Improvement.

Langmuir, D., 1997. Aqueous environmental geochemistry. Prentice Hall, New Jersey.

Lin, Z. and Puls, R.W., 2000. Adsorption, desorption and oxidation of arsenic affected by clay minerals and aging process. Environmental Geology, 39(7): 753-759.

Lissner, H., 2008. Column experiments simulating various scenarios for arsenic mobilization in Bangladesh. Master Thesis, Freiberg University of Mining and Technology, Freiberg, Freiberg Online Geology, FOG Vol. 18 2008, http://www.geo.tu-freiberg.de/fog/FOG_Vol18.pdf, date accessed: October 2008, pp. 112.

Litz, N., Wilcke, W. and Wilke, B.-M., 2004. Bodengefährdende Stoffe. Wiley-VCH, Weinheim.

Manning, B.A. and Goldberg, S., 1996. Modeling competitive adsorption of arsenate with phosphate and molybdate on oxide minerals. Soil Science Society of America Journal, 60(1): 121-131.

Manning, B.A. and Goldberg, S., 1997. Arsenic(III) and arsenic(V) absorption on three California soils. Soil Science, 162(12): 886-895.

Matthess, G., 1994. Lehrbuch der Hydrogeologie. Bd. 2. Die Beschaffenheit des Grundwassers. Gebrüder Borntraeger, Berlin-Stuttgart.

McArthur, J.M. et al., 2004. Natural organic matter in sedimentary basins and its relation to arsenic in anoxic ground water: the example of West Bengal and its worldwide implications. Applied Geochemistry, 19(8): 1255-1293.

McArthur, J.M., Ravenscroft, P., Safiulla, S. and Thirlwall, M.F., 2001. Arsenic in groundwater: Testing pollution mechanisms for sedimentary aquifers in Bangladesh. Water Resources Research, 37(1): 109-117.

Meharg, A.A. et al., 2006. Codeposition of organic carbon and arsenic in bengal delta aquifers. Environmental Science and Technology, 40(16): 4928 - 4935.

Merkel, B. and Planer-Friedrich, B., 2002. Integrierte Datenauswertung Hydrogeologie, Freiberg Online Geology, FOG Vol. 7 2002, ISSN 1434-7512, http://www.geo.tu-freiberg.de/fog/FOG_Vol_7.pdf, date accessed: June 2008, pp. 64.

Mirza, M.M.Q., Warrick, R.A. and Ericksen, N.J., 2003. The implications of climate change on floods of the Ganges, Brahmaputra and Meghna rivers in Bangladesh. Climatic Change, 57(3): 287-318.

Nickson, R.T., McArthur, J.M., Ravenscroft, P., Burgess, W.G. and Ahmed, K.M., 2000. Mechanism of arsenic release to groundwater, Bangladesh and West Bengal. Applied Geochemistry, 15(4): 403-413.

Pike, J.G., 1964. Estimation of Annual Runoff from Meteorological Data in a Tropical Climate. Journal of Hydrology, 2: 116-123.

Planer-Friedrich, B., London, J., McClesky, Nordstrom, D.K., Wallschläger, D., 2007. Thioarsenates in geothermal waters of Yellowstone National Park: Determination, Preservation, and Geochemical importance. Environmental Science and Technology, 41(15), 5245-5251

Polizzotto, M.L., Kocar, B.D., Benner, S.G., Sampson, M. and Fendorf, S., 2008. Near-surface wetland sediments as a source of arsenic release to ground water in Asia. Nature, 454: 505-508.

Puls, R.W. and Barcelona, M.J., 1996. EPA. Ground Water Issue. Low-flow (minimal drawdown) groundwater sampling procedures. United States Environmental Protection Agency (EPA), http://www.epa.gov/tio/tsp/download/lwflw2a.pdf, date accessed: July 2008.

Radu, T., Subacz, J.L., Phillippi, J.M. and Barnett, M.O., 2005. Effects of dissolved carbonate on arsenic adsorption and mobility. Environmental Science & Technology, 39(20): 7875-7882.

Ravenscroft, P., Burgess, W.G., Ahmed, K.M., Burren, M. and Perrin, J., 2005. Arsenic in groundwater of the Bengal Basin, Bangladesh: Distribution, field relations, and hydrogeological setting. Hydrogeology Journal, 13(5-6): 727-751.

Ravenscroft, P., McArthur, J. and Hoque, B., 2001. Geochemical and palaeohydrological Controls on Pollution of Groundwater by Arsenic. In: W.R. Chappell, C.O. Abernathy and R.L. Calderon (Editors), Arsenic exposure and health effects. Elsevier Science Ltd., Oxford, pp. 53-78.

Rossum, J.R., 1975. Checking the accuracy of water analysis through the use of conductivity. Journal of the American Water Works Association, 67: 204 - 205.

Smedley, P.L. and Kinniburgh, D.G., 2001. A review of the source, behaviour and distribution of arsenic in natural waters. Applied Geochemistry, 17: 517-568.

Steinborn, J., 2008. Seasonal changes in the arsenic distribution of newly drilled wells tapping different aquifers in the Bangladesh delta. Master Thesis. Technical University Bergakademie Freiberg, pp. 98.

van Geen, A. et al., 2004. Decoupling of As and Fe release to Bangladesh groundwater under reducing conditions. Part II: Evidence from sediment incubations. Geochimica et Cosmochimica Acta, 68(17): 3475-3486.

Violante, A. and Pigna, M., 2002. Competitive Sorption of Arsenate and Phosphate on Different Clay Minerals and Soils. Soil Sci Soc Am J, 66(6): 1788-1796.

Wallschläger, D. and Stadey, C.J., 2007. Determination of (Oxy)thioarsenates in Sulfidic waters. Analytical Chemistry, 79(10), 3873-3880.

WHO, 2006. World Health Organization. Guidelines for drinking-water quality (electronic resource): Vol. 1, Recommendations. – 3rd ed. Electronic version for the Web. www.who.int/entity/water_sanitation_health/dwq/gdwq0506begin.pdf, access date: July 2008.

Zahid, A., Hassan, M.Q., Balke, K.-D., Flegr, M. and Clark, D.W., 2008. Groundwater chemistry and occurence of arsenic in the Meghna floodplain aquifer, southeastern Bangladesh. Environmental Geology, 54: 1247-1260.

Zhao, H.S. and Stanforth, R., 2001. Competitive adsorption of phosphate and arsenate on goethite. Environmental Science & Technology, 35(24): 4753-4757.

APPENDIXES

APPENDIX A1: GRAPHICAL REPRESENTATION OF TEMPORAL VARIATIONS OF THE MEASURED PARAMETERS AT THE TEST SITE AT TITAS IN 2007[4]

a. Electrochemical parameters pH, E_H [mV], $O2_{conc}$[mg/L], $O2_{sat}$[%], T [°C], EC [µS/cm] and derived TDS (0.65*EC) [mg/L]

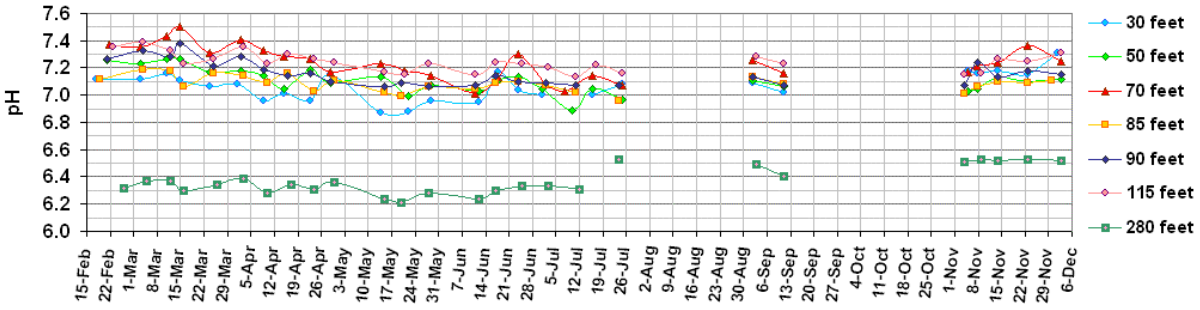

Appendix A1, Figure A *pH-values – temporal variations in 2007 (only pH-values measured with the HACH-probes are represented, measurements with the pHep from Hanna-Instruments (Sep/Oct 2007) were not reliable)*

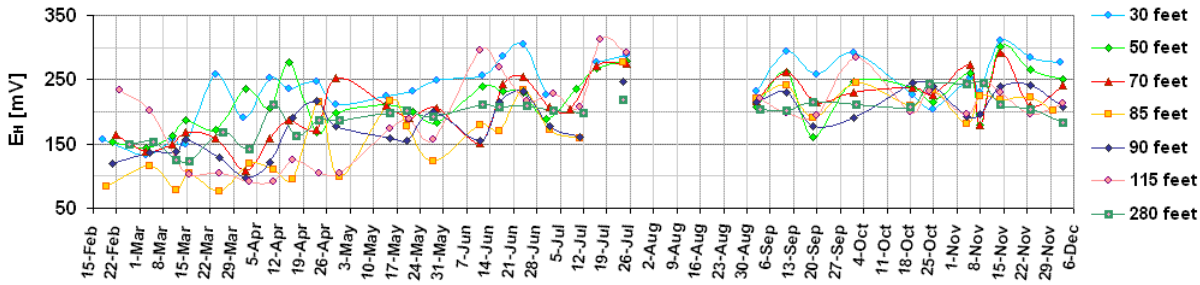

Appendix A1, Figure B *Redox potential [mV] – temporal variations in 2007*

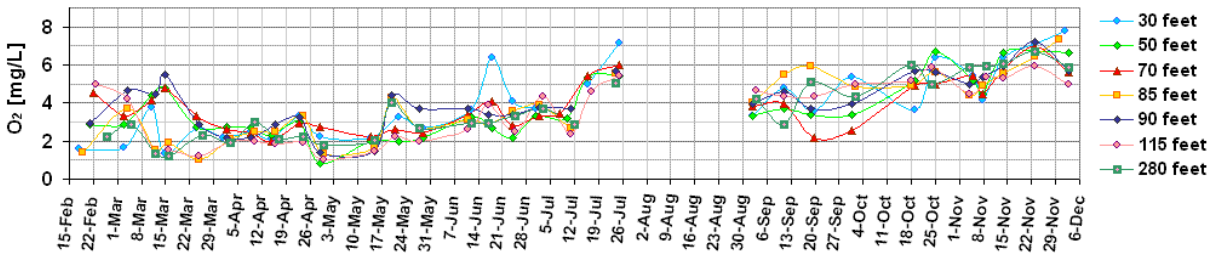

Appendix A1, Figure C *Oxygen concentration [mg/l] – temporal variations in 2007*

[4] Results shown here for samples taken during February throughout July 2007 were collected by Steinborn (2008), whereas samples since September 2007 were taken by the author.

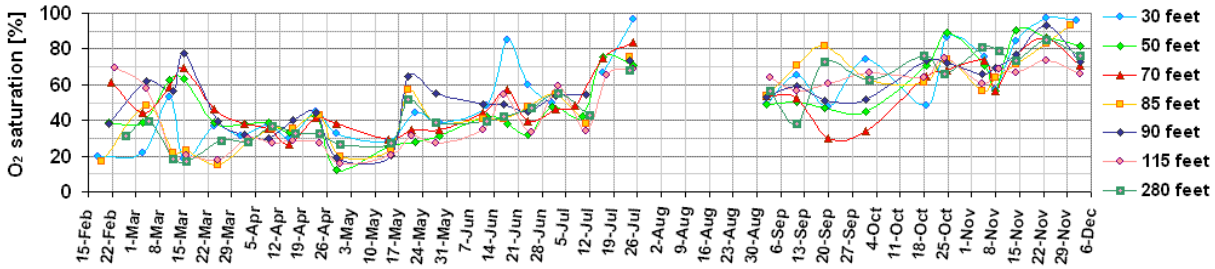

Appendix A1, Figure D *Oxygen saturation [%] – temporal variations in 2007*

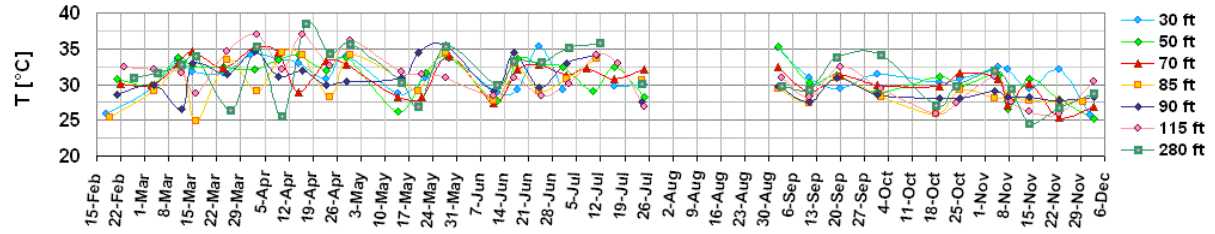

Appendix A1, Figure E *Temperature [°C] – temporal variations in 2007*

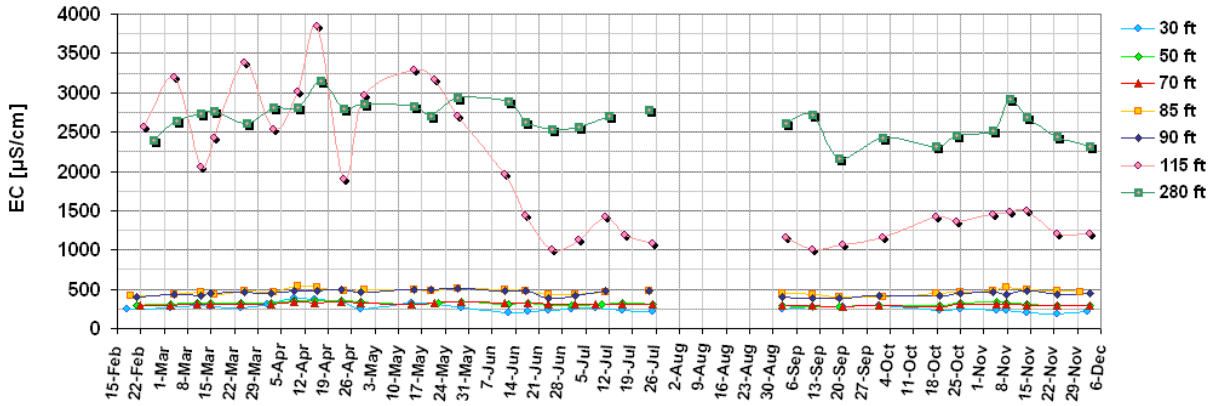

Appendix A1, Figure F *Electrical conductivity [µS/cm] – temporal variations in 2007*

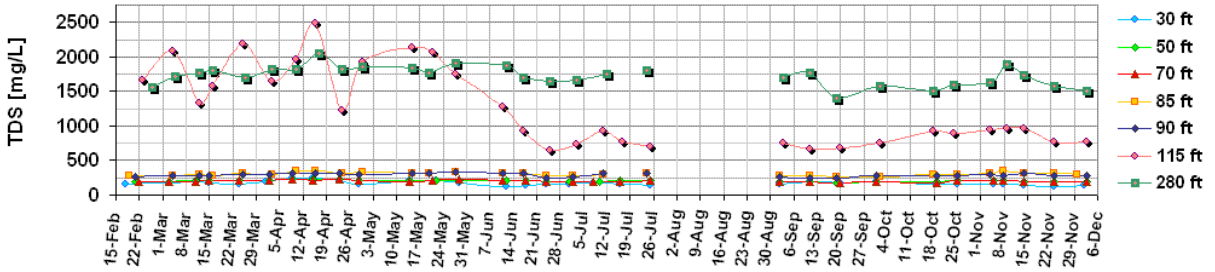

Appendix A1, Figure G *Total dissolved solids (TDS) [mg/l] – temporal variations in 2007*

b. Photometrical determined parameters Fe(II), Fe(III) Fe(tot), Mn^{2+}, Mn(tot), S^{2-}, NO_3^-, NO_2^-, NH_4^+ in [mg/L]

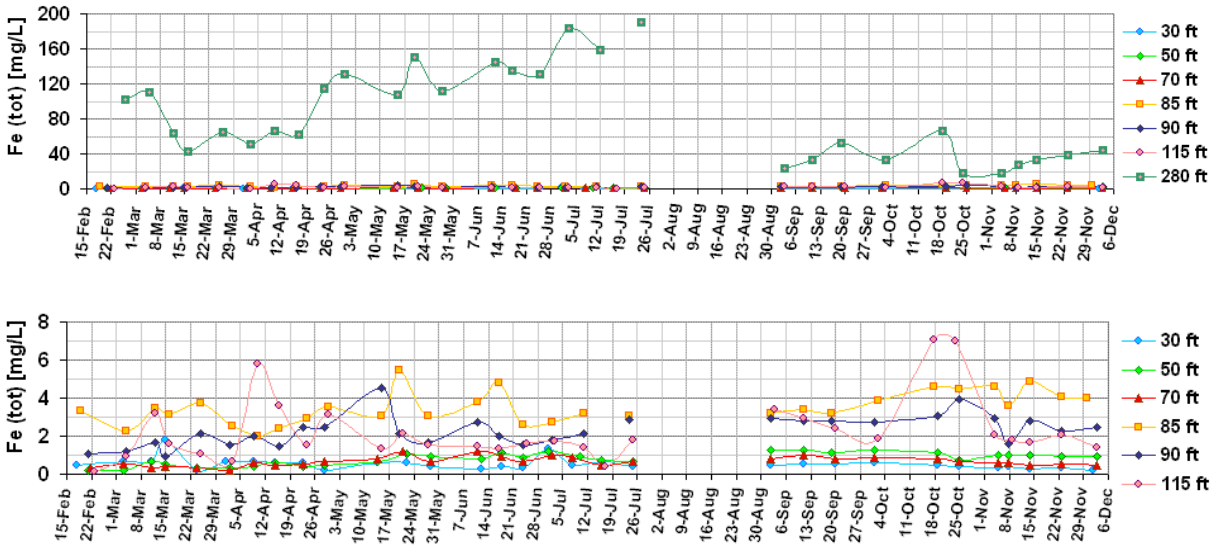

Appendix A1, Figure H *Total iron [mg/l] – temporal variations in 2007*

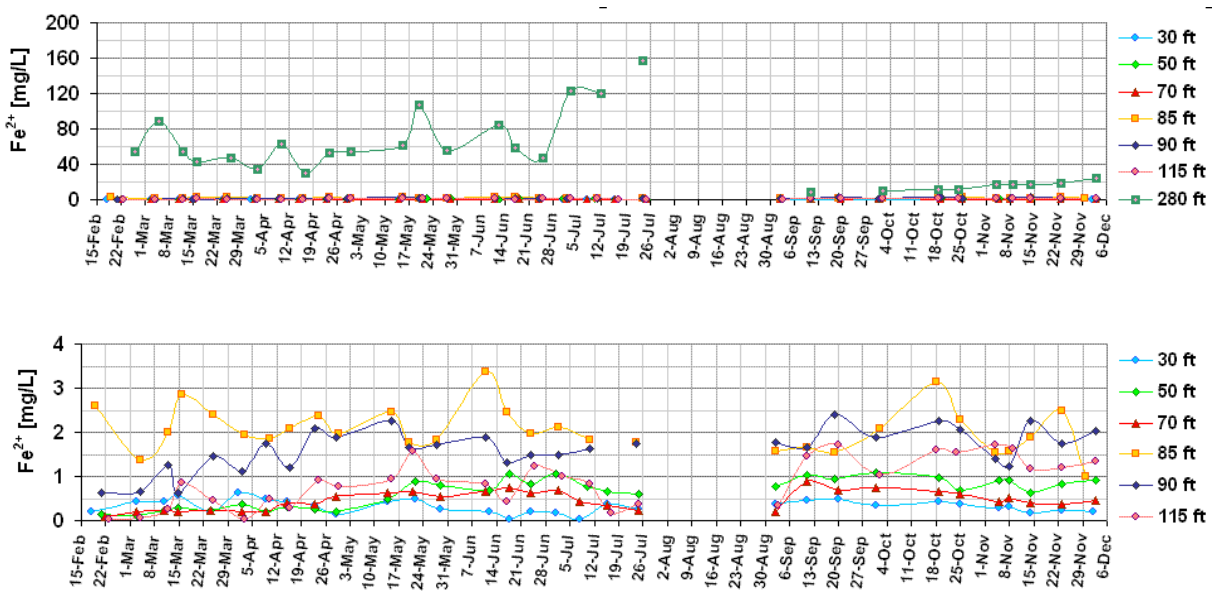

Appendix A1, Figure I *Ferrous iron [mg/l] – temporal variations in 2007 (Missing iron(II)-values during monitoring TF280.21 and TF280.23 were not reliable, Fe(II) was not determined immediately, due to bad weather conditions)*

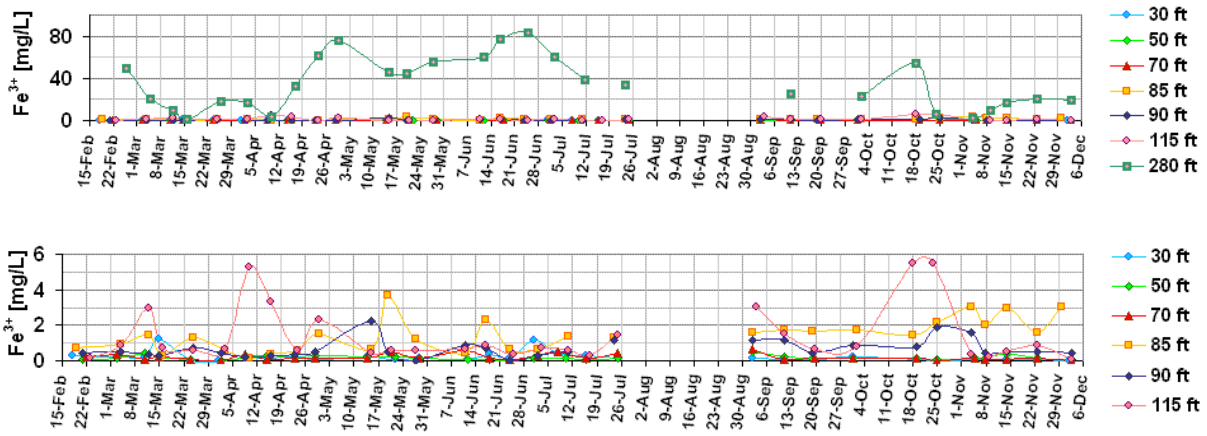

Appendix A1, Figure J *Ferric iron [mg/l] – temporal variations in 2007 (calculated from difference Fe(tot)-Fe(II))*

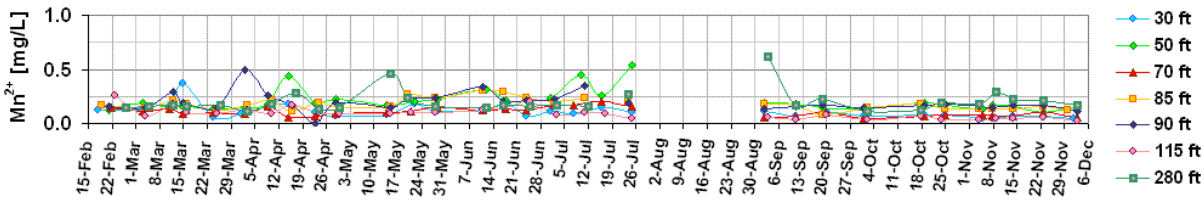

Appendix A1, Figure K *Two-valued manganese [mg/l] – temporal variations in 2007*

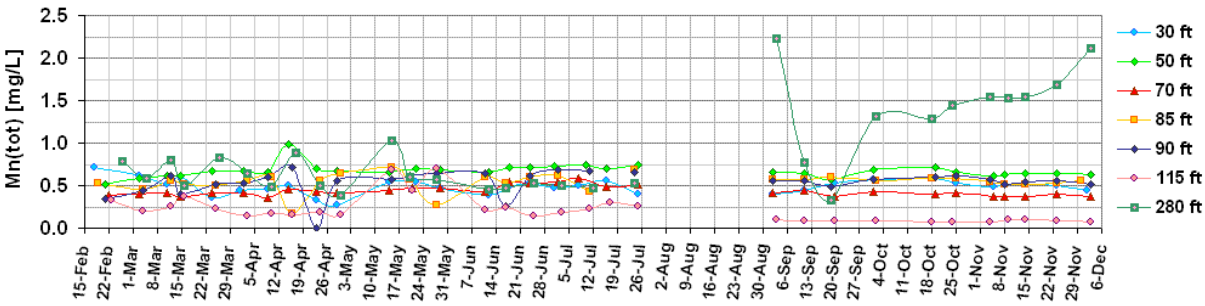

Appendix A1, Figure L *Total manganese [mg/l] – temporal variations in 2007*

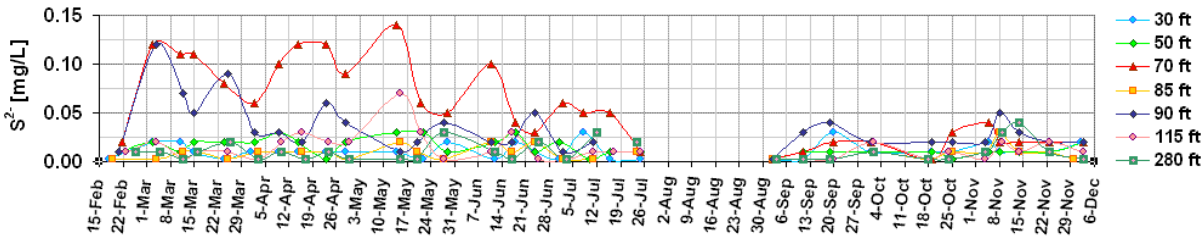

Appendix A1, Figure M *Sulphide [mg/l] – temporal variations in 2007*

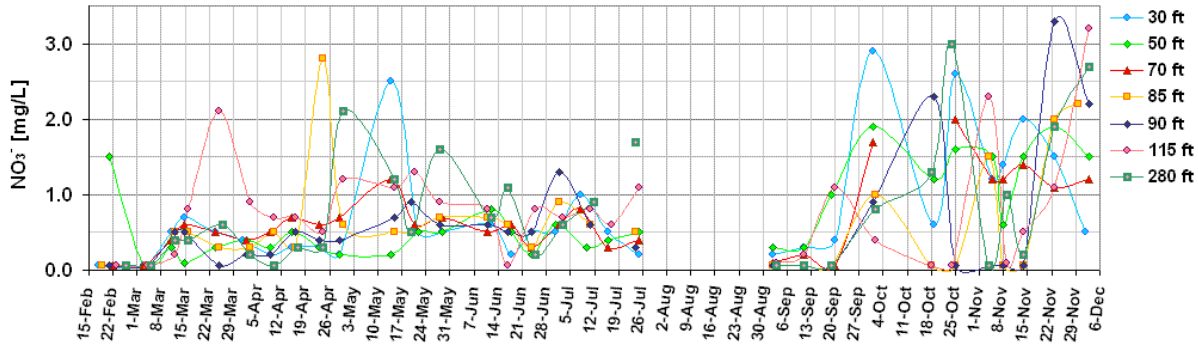

Appendix A1, Figure N *Nitrate [mg/l] – temporal variations in 2007*

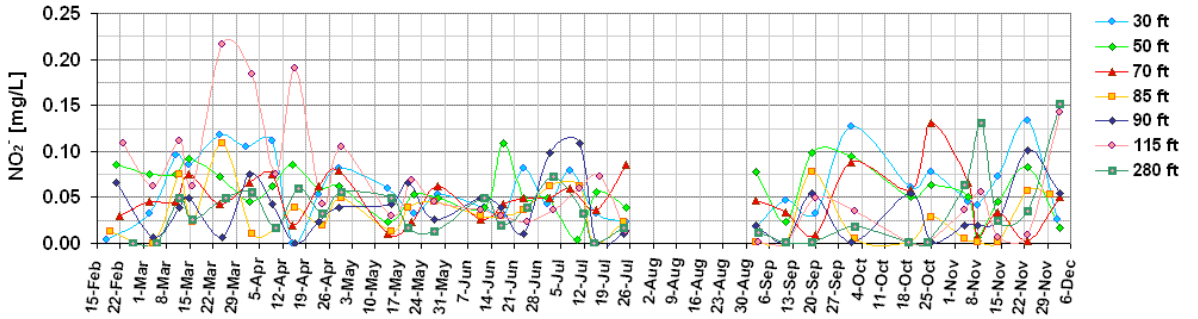

Appendix A1, Figure O *Nitrite [mg/l] – temporal variations in 2007*

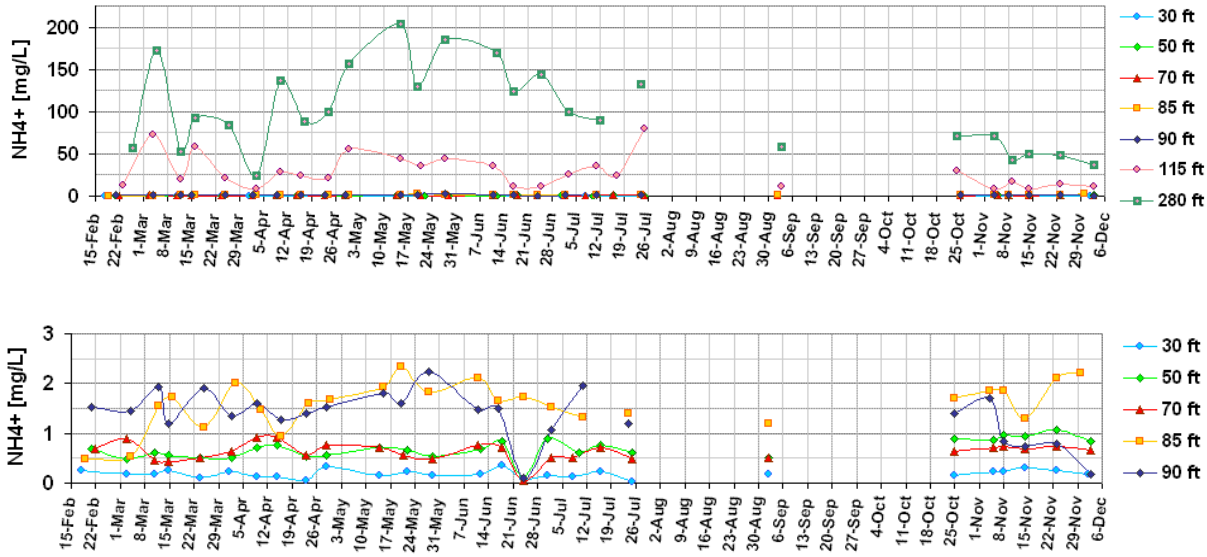

Appendix A1, Figure P *Ammonium [mg/l] – temporal variations in 2007 (Missing values in Sep/Oct 2007 are due to the wet, not utilizable cyanurate reagent. Single low NH4-values in 50, 70 and 90 ft depth at 26th of June 2007 might also be an measuring artefact – possibly due to a wet cyanurate reagent?)*

c. Titration of alkalinity and acidity, as well as HCO_3^- modelling based on TIC-values with PhreeqC [mg/L]

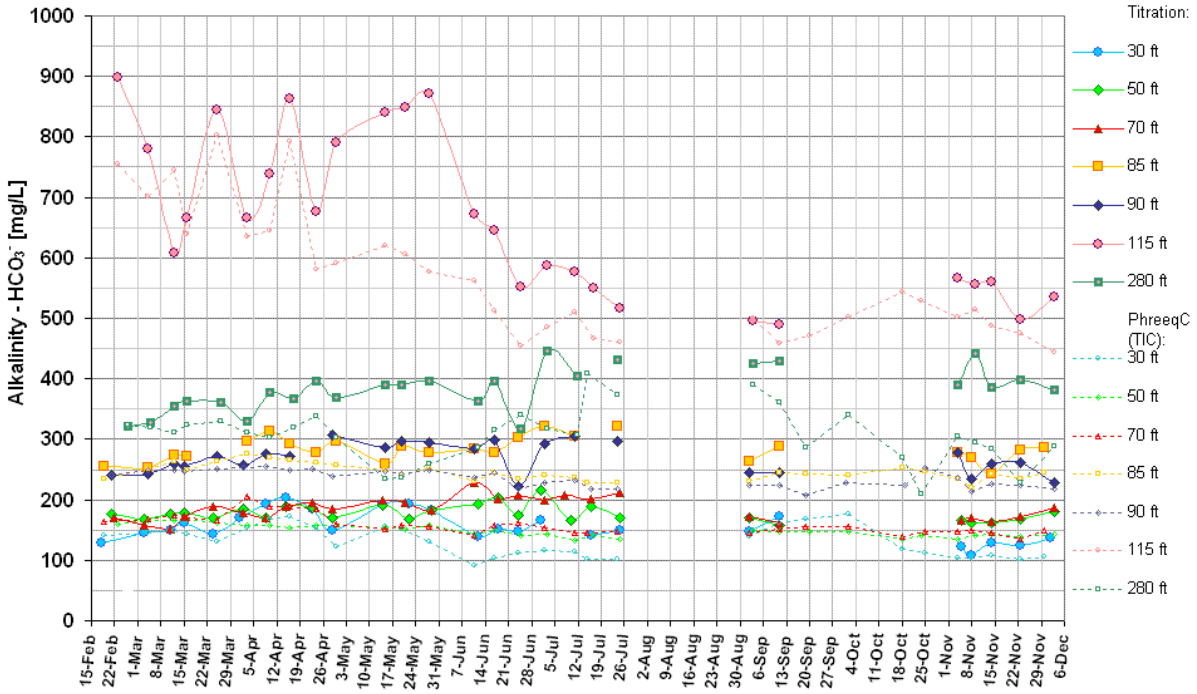

Appendix A1, Figure Q *Alkalinity resp. bicarbonate, determined by titration (only values determined with the HACH-probes are represented) and calulated with PhreeqC, based on the TIC values [mg/l] – temporal variations in 2007*

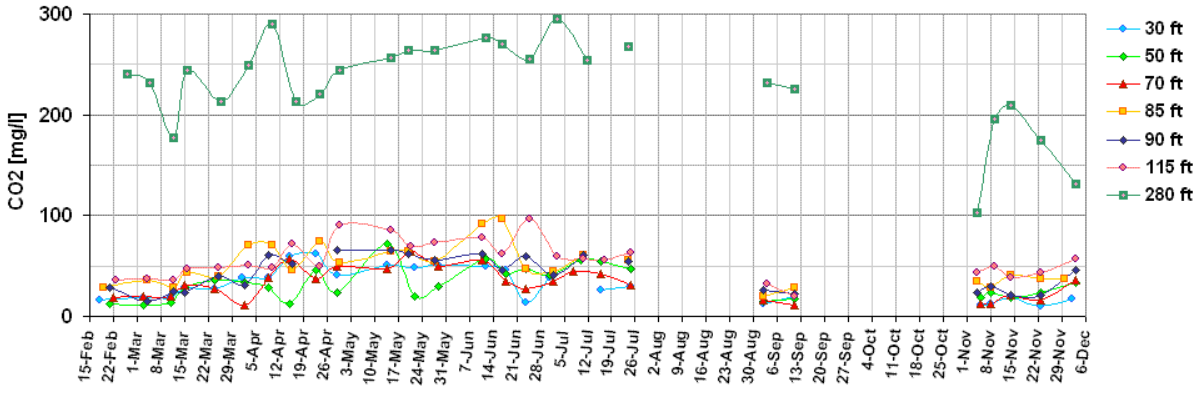

Appendix A1, Figure R *Acidity resp. dissolved carbon dioxide [mg/l] (only values determined with the HACH-probes are represented) – temporal variations in 2007*

d. Ionchromatographical measurement of Na^+, Ca^{2+}, Mg^{2+}, K^+, Cl^-, SO_4^{2-}, Br^- and F^- [mg/L]

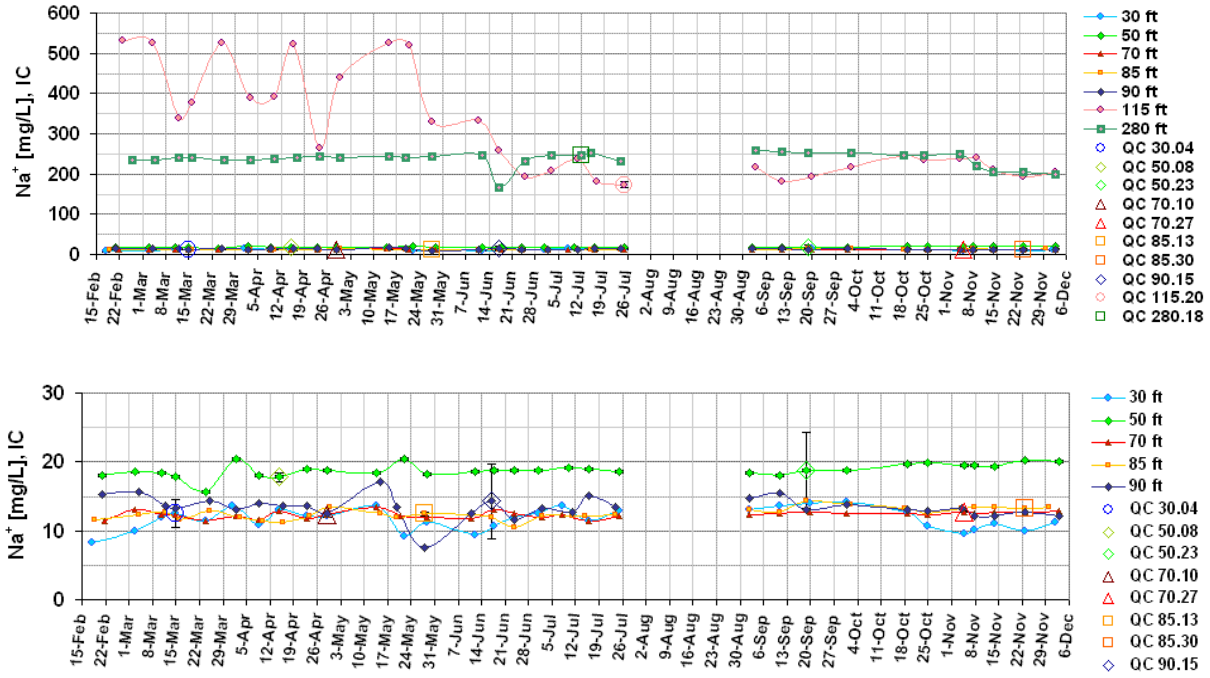

Appendix A1, Figure S *Sodium [mg/l] – temporal variations in 2007 and results of the quality control (QC)*

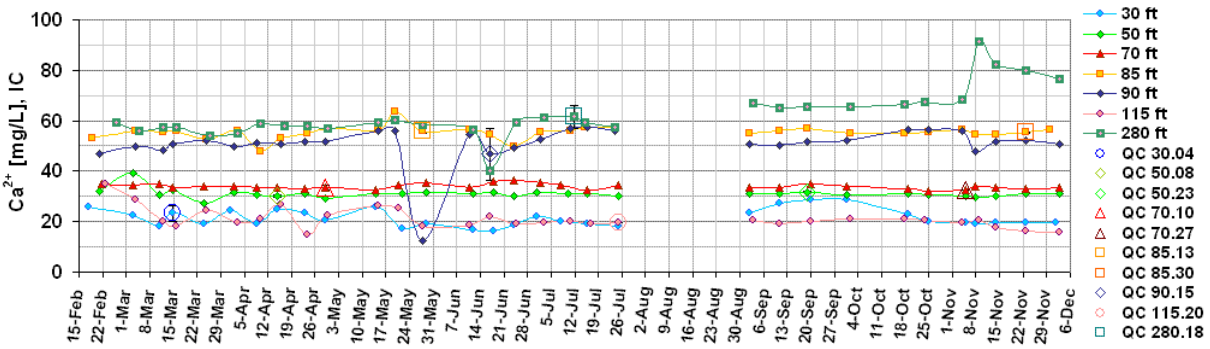

Appendix A1, Figure T *Calcium [mg/l] – temporal variations in 2007 and results of the quality control (QC)*

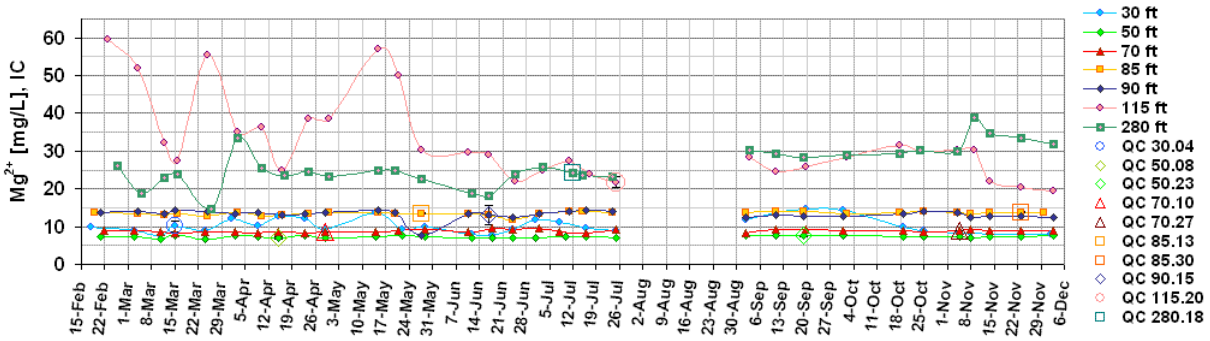

Appendix A1, Figure U *Magnesium [mg/l] – temporal variations in 2007 and results of the quality control (QC)*

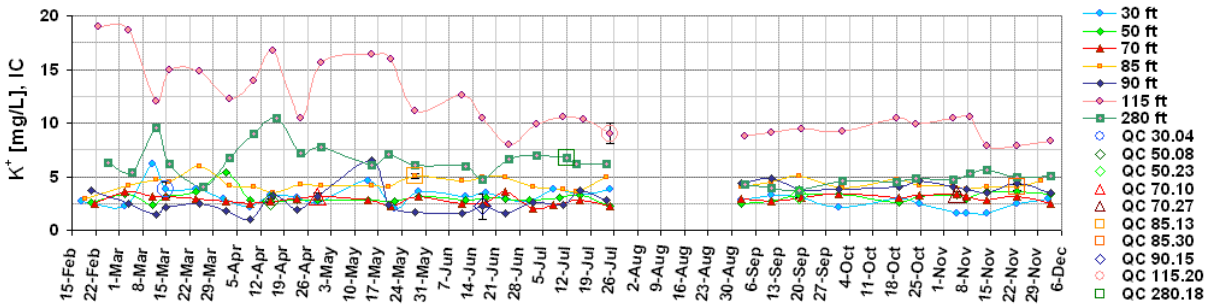

Appendix A1, Figure V *Potassium [mg/l] – temporal variations in 2007and results of the quality control (QC)*

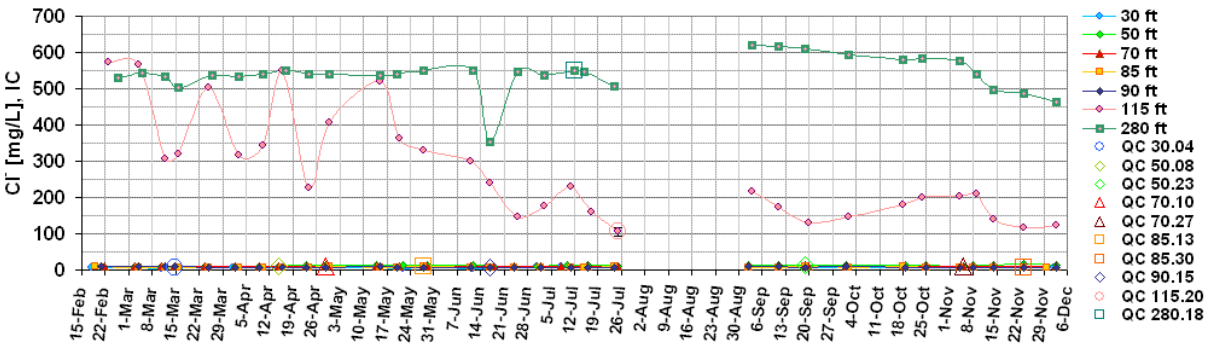

Appendix A1, Figure W *Chloride [mg/l] – temporal variations in 2007 and results of the quality control (QC)*

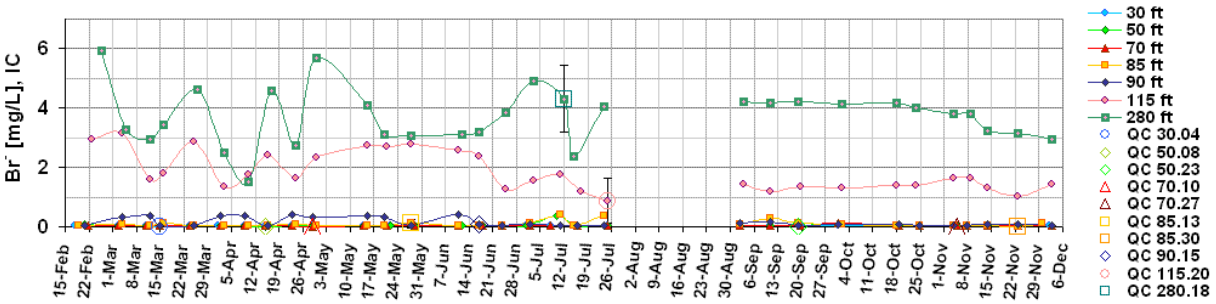

Appendix A1, Figure X *Bromide [mg/l] – temporal variations in 2007 and results of the quality control (QC)*

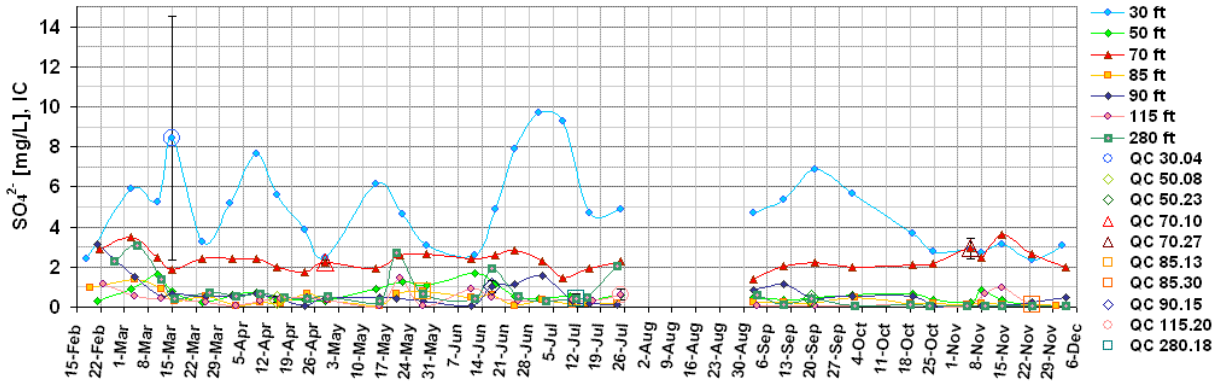

Appendix A1, Figure Y *Sulphate [mg/l] – temporal variations in 2007 and results of the quality control (QC)*

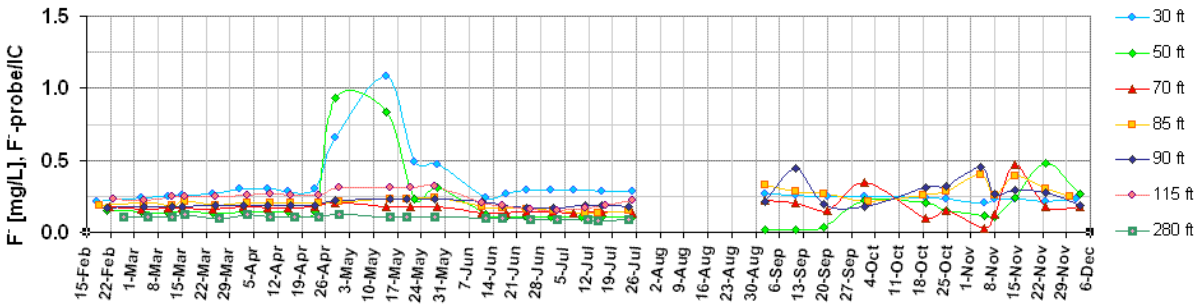

Appendix A1, Figure Z *Fluoride [mg/l] – temporal variations in 2007 (measurements with sensitive probe from Feb.-Jul., and 30 ft Sep.-Dec., other F-values during Sep.-Dec. determined with IC, no values available for 115ft and 280 ft due to peak overlay)*

e. Determination of total inorganic (TIC), dissolved organic (DOC), and total carbon (TC) [mg/L]

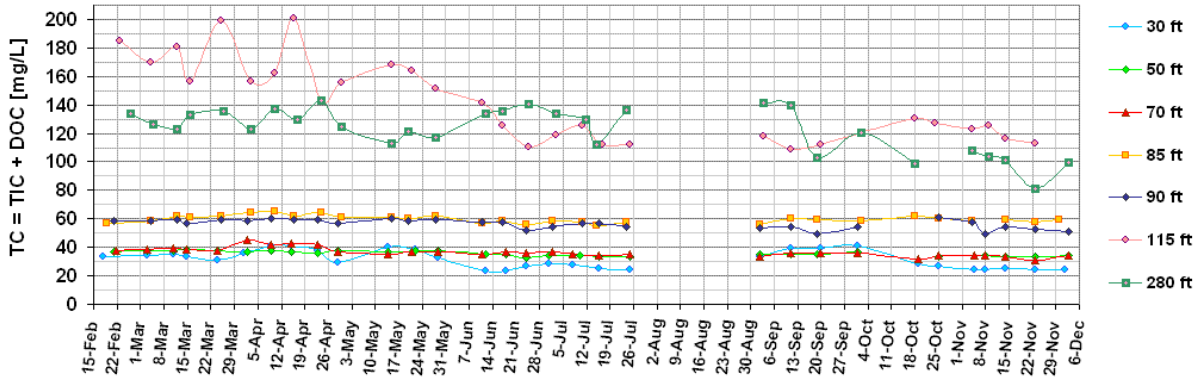

Appendix A1, Figure AA *Total carbon [mg/l] – temporal variations in 2007*

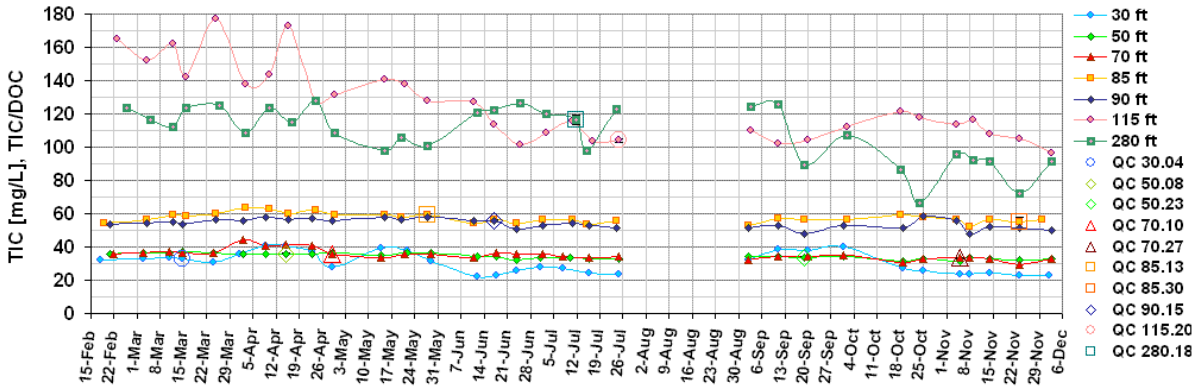

Appendix A1, Figure BB *Total inorganic carbon [mg/l] – temporal variations in 2007 and results of the quality control (QC)*

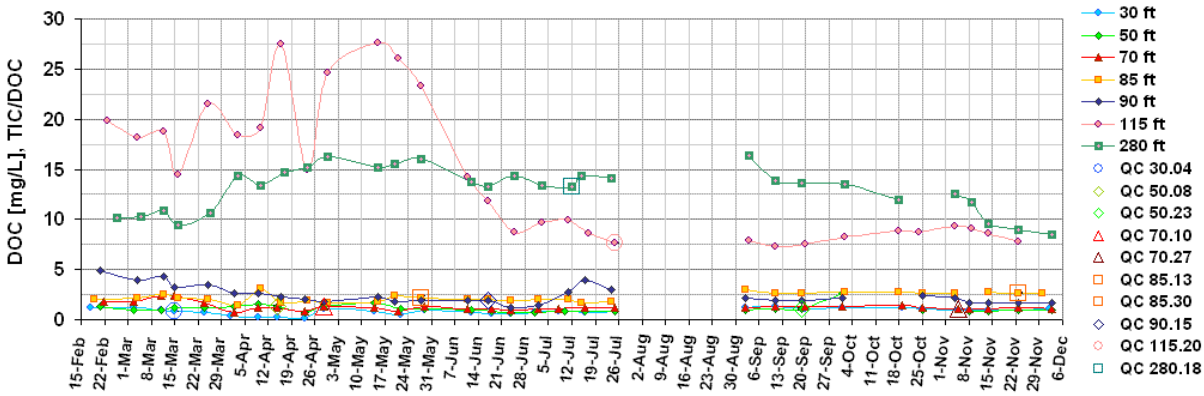

Appendix A1, Figure CC *Dissolved organic carbon [mg/l] – temporal variations in 2007 and results of the quality control (QC) (Lacking DOC values are due to broken glass bottles during transport, TIC-values for these samples were determined in the plastic bottles, which were collected primarily for IC)*

f. ICP-MS and AEC-ICP-MS determination of Phosphorus totals and species [mg/L]

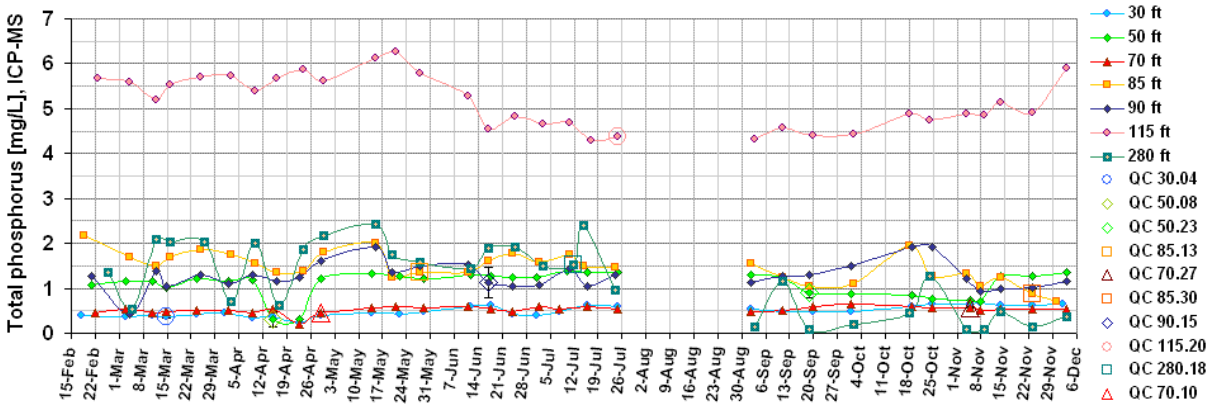

Appendix A1, Figure DD *Total phosphorus [mg/l] – temporal variations in 2007and results of the quality control (QC) (Attention: later acidification of the samples during Sep.-Dec. 2007)*

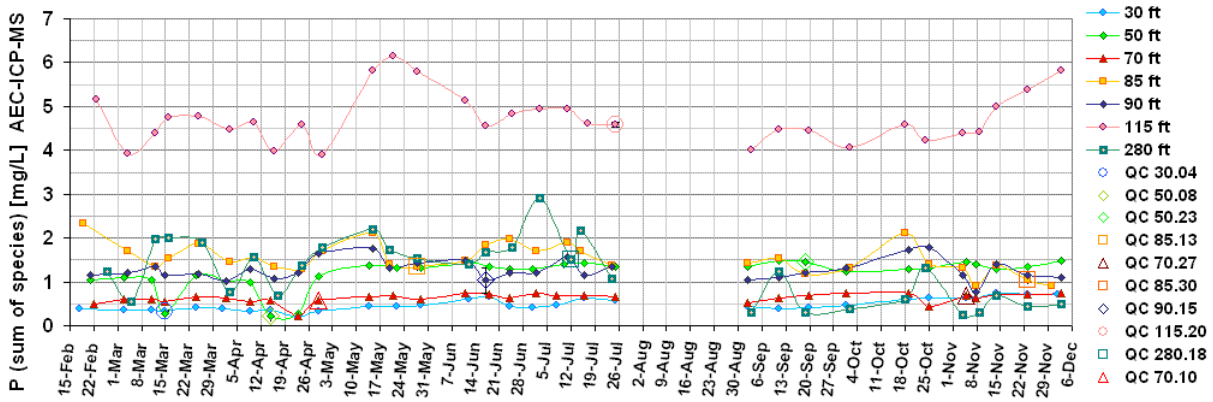

Appendix A1, Figure EE *Sum of phosphorus species [mg/l] – temporal variations in 2007 and results of the quality control (QC) (Attention: later acidification of the samples during Sep.-Dec. 2007)*

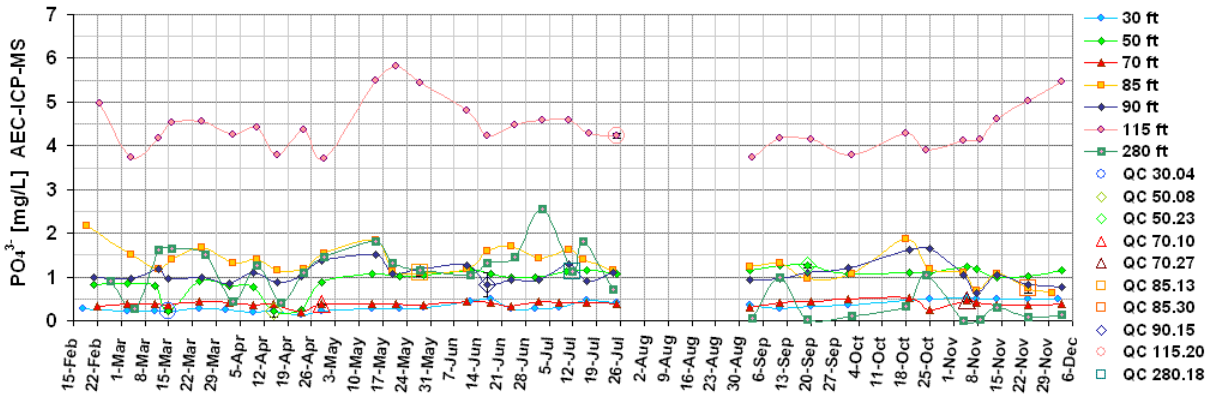

Appendix A1, Figure FF *Phosphate [mg/l] – temporal variations in 2007 and results of the quality control (QC) (Attention: later acidification of the samples during Sep.-Dec. 2007)*

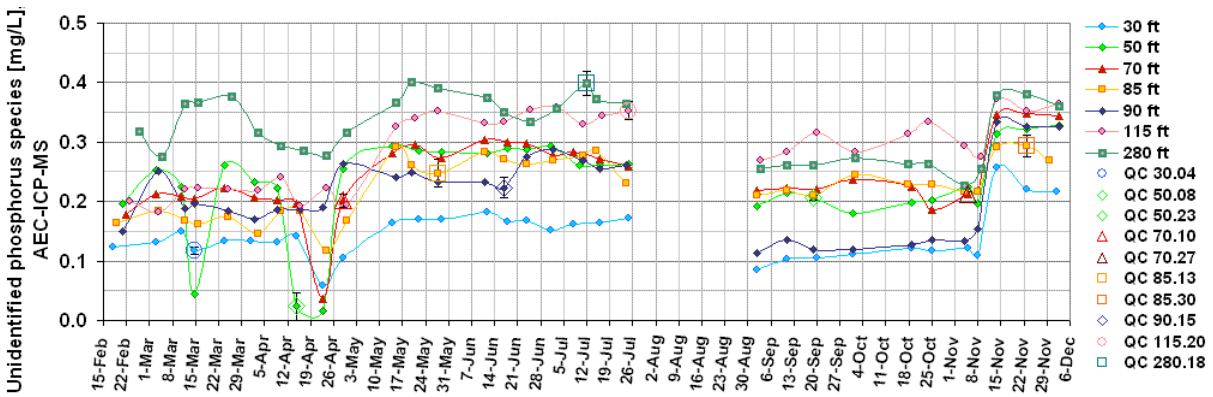

Appendix A1, Figure GG *Unidentified phosphorus species [mg/l] – temporal variations in 2007 and results of the quality control (QC) (Attention: later acidification of the samples during Sep.-Dec. 2007, ➔ sudden changes of the concentrations might be due to varying sensitivities during AEC-ICP-MS analysis, because the lowering after August and sudden increase after 8th November - in all wells - concurrently mark single analysis runs where new calibration solutions were utilized)*

g. ICP-MS and AEC-ICP-MS determination of Arsenic totals and species [µg/L]

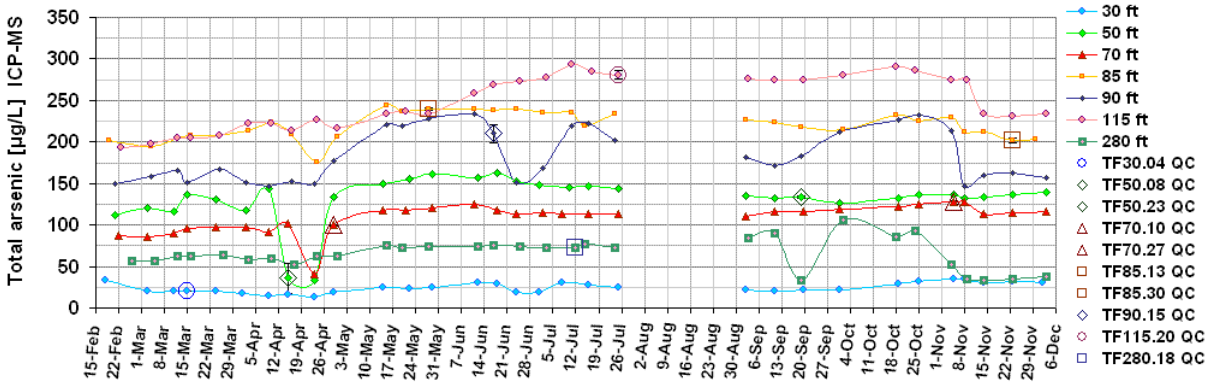

Appendix A1, Figure HH *Total arsenic [mg/l] – temporal variations in 2007 and results of the quality control (QC)*

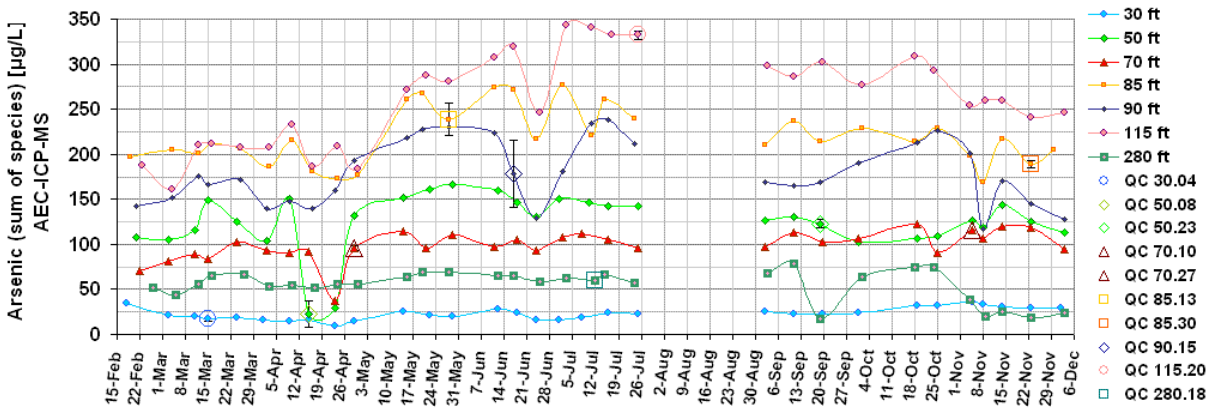

Appendix A1, Figure II *Sum of arsenic species [mg/l] – temporal variations in 2007 and results of the quality control (QC)*

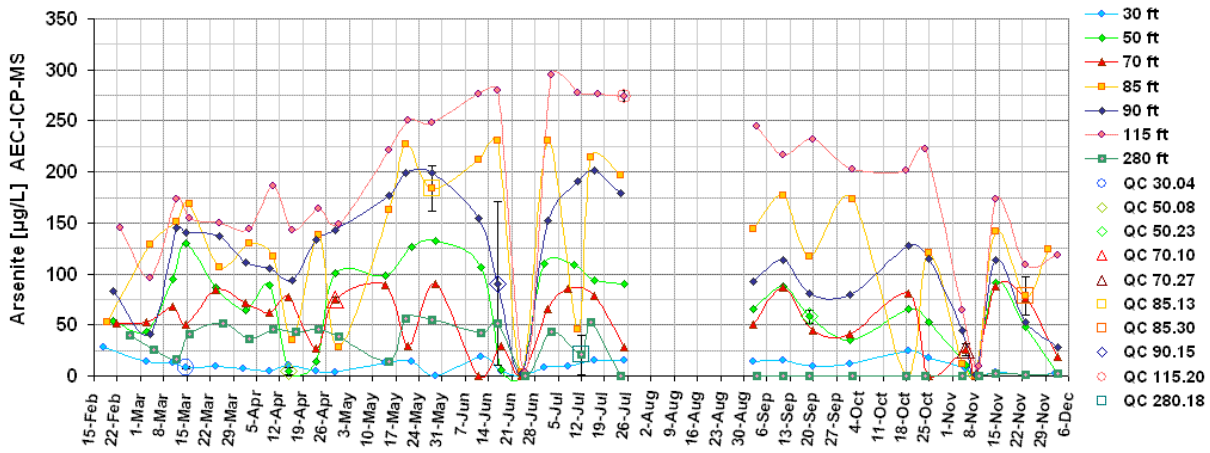

Appendix A1, Figure JJ *Arsenite [mg/l] – temporal variations in 2007 and results of the quality control (QC) (Attention: later acidification of species samples during Sep.-Dec. 2007)*

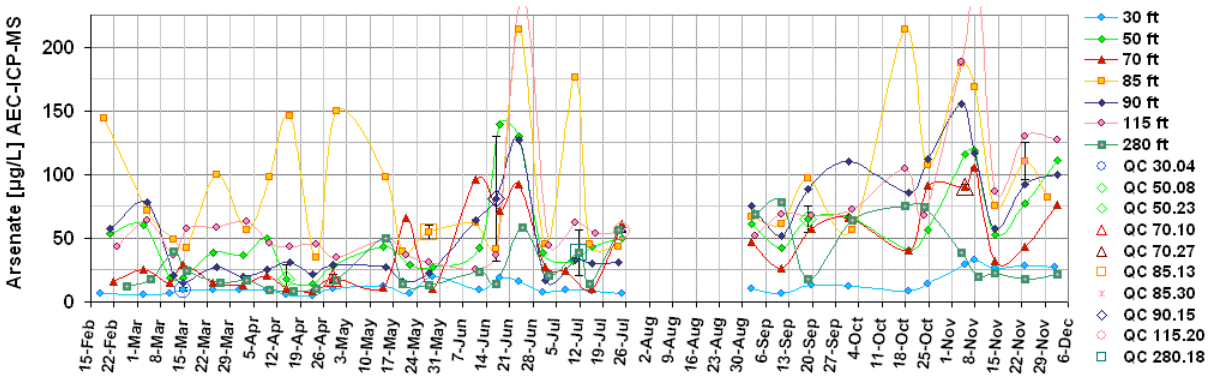

Appendix A1, Figure KK *Arsenate [mg/l] – temporal variations in 2007 and results of the quality control (QC) (Attention: later acidification of species samples during Sep.-Dec. 2007)*

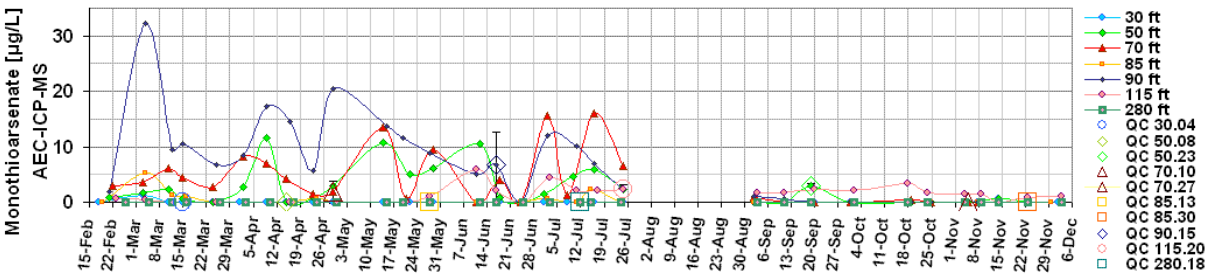

Appendix A1, Figure LL *Monothioarsenate [mg/l] – temporal variations in 2007 and results of the quality control (QC) (Attention: later acidification of species samples during Sep.-Dec. 2007)*

APPENDIX A2: ON-SITE PARAMETERS DURING WATER WITHDRAWAL

Pumping Time		approx. 10 min	1 hour	2 hours	3 hours	4 hours	5 hours	6 hours	M27	'07 average monitoring
EC [µS/cm]	**85**	436	450	**474**	-	-	-	-	**478**	**448** ± 36
	115	1,467	1,515	1,536	1,536	**1,583**	-	-	**1,457**	**1,943** ± 874*
	280	1,862	1,808	1,755	1,740	1,715	1,704	**1,671**	**2,510**	**2,655** ± 217
E_H [mV]	**85**	293	260	**239**	-	-	-	-	**181**	**185** ± 43
	115	258	241	225	219	**208**	-	-	**196**	**195** ± 64
	280	164	230	221	217	210	204	**199**	**243**	**194** ± 31
pH	**85**	7.2	7.1	**7.1**	-	-	-	-	**7.0**	**7.2** ± 0.1
	115	7.3	7.2	7.2	7.2	**7.2**	-	-	**7.2**	**7.2** ± 0.1
	280	6.4	6.4	6.4	6.4	6.5	6.5	**6.5**	**6.5**	**6.4** ± 0.1
O_2 [mg/L]	**85**	6.6	5.3	**4.8**	-	-	-	-	**4.4**	**4.1** ± 1.4
	115	3.7	3.4	3.5	3.4	**3.3**	-	-	**4.4**	**3.5** ± 1.6
	280	6.7	4.6	4.3	4.0	4.0	3.9	**3.8**	**5.9**	**3.6** ± 1.6
O_2 [%]	**85**	83	68	**60**	-	-	-	-	**56**	**55** ± 18
	115	48	43	44	42	**41**	-	-	**61**	**47** ± 20
	280	86	58	54	51	50	50	**47**	**81**	**49** ± 20
T [°C]	**85**	27.3	27.0	**27.0**	-	-	-	-	**28.1**	**30.4** ± 2.5
	115	28.5	26.8	26.7	26.5	**26.5**	-	-	**31.2**	**30.8** ± 3.1
	280	27.5	26.8	26.8	26.5	26.5	26.6	**26.4**	**32.0**	**31.3** ± 3.5

*Distinct lowering of EC throughout the year, during Sep-Dec'07 in 115 ft only **1,272** ± 173 µS/cm.

APPENDIX A3: RESULTS OF THE P-INJECTION SPIKE

Parameters\sample	HTW	85 $ft_{original}$	INJ 85-1	INJ 85-2	INJ 85-3	INJ 85-4	INJ 85-5	INJ 85-6
EC [µS/cm]	415	477	446	427	418	426	451	487
EH [mV]	182	222	217	210	215	204	214	171
pH	7.02	7.09	7.16	7.13	7.11	7.08	7.15	7.08
$O2_{conc}$ [mg/L]	8.0	6.5	6.5	7.0	6.7	6.2	6.7	5.1
$O2_{sat}$ [%]	102	83	81	84	82	75	81	65
T [°C]	27.7	27.5	25.7	24.7	26.4	25.2	25.2	27.2
Fe^{+2} [mg/L]	1.66	2.48	0.99	2.72	2.45	2.45	2.35	2.55
Fe^{+3} [mg/L]	0.80	3.01	1.42	0.48	0.60	1.39	1.51	1.75
Fe (tot) [mg/L]	2.46	4.04	2.41	3.20	3.05	3.84	3.86	4.30
Mn^{+2} [mg/L]	0.093	0.010	0.175	0.208	0.179	0.160	0.134	0.129
Mn (tot) [mg/L]	0.421	2.000	0.453	0.518	0.479	0.500	0.500	0.522
$NO3^-$ [mg/L]	1.9	2.0	1.1	1	1.1	2.5	1.2	2.3
$NO2^-$ [mg/L]	<0.005	0.057	0.013	0.015	0.078	0.008	0.006	0.037
NH_4^+ [mg/L]	0.86	2.10	2.00	2.05	1.85	2.30	1.70	1.40
S^{-2} [mg/L]	0.06	0.01	0.01	0.01	0.01	0.02	0.01	<0.01
HCO_3^- [mg/L]	217	282	273	278	271	292	285	302
H_2CO_3 [mg/L]	18	38	40	39	41	42	43	40
P(unid) [µg/L]	367	268	316	313	307	307	271	292
PO_4^{-3} [µg/L]	370	628	1,193	1,664	1,948	2,297	2,942	2,033
P(sum) [µg/L]	737	897	1,509	1,977	2,255	2,604	3,213	2,325
P(tot) [µg/L]	107	703	1,224	1,969	2,368	2,888	2,833	2,150
P(unid) [%]	50	30	21	16	14	12	8	13
PO_4^{-3} [%]	50	70	79	84	86	88	92	87
H_3AsSO_3 [µg/L]	<0.5	<0.5	1	1	<0.5	<0.5	<0.5	<0.5
Arsenite [µg/L]	30	124	66	110	69	78	4	51
Arsenate [µg/L]	40	82	63	71	114	124	189	142
As(sum) [µg/L]	69	205	129	180	184	202	193	194
As tot [µg/L]	15	203	127	184	192	208	215	203
Arsenite [%]	43	60	51	61	38	38	2	26
Arsenate [%]	57	40	49	39	62	62	98	74

APPENDIX A4: RESULTS OF THE SPEARMAN RANK CORRELATIONS

shallow aquifer – depth dependent variations: correlation between two parameters, including all results found for Ca-HCO3-type shallow aquifer groundwaters (30, 50, 70, 85, 90 ft)

single wells – seasonal changes: correlation between two parameters, regarding changes over time within the single test site wells

p +, p - = likelihood-value or significance level (interval 0.000 – 1.000), calculated during the Spearman rank correlation test, showing if a significant correlation exists between two tested parameters. The significance level during this study is set to $p < 0.05$. The symbols + or - mark the direction of the interrelationship.

p* + or **p** +** = highlighted value calculated for p when a positive significant correlation on the $p \leq 0.05$ level (*) or even the $p \leq 0.01$ (**) exists

p* – or **p** –** = highlighted value calculated for p when a negative significant correlation on the $p \leq 0.05$ level (*) or even the $p \leq 0.01$ (**) exists

		shallow aquifer wells	single wells - seasonal changes						
well name		30, 50, 70, 85, 90 ft	30 ft	50 ft	70 ft	85 ft	90 ft	115 ft	280 ft
mid screen depth ± screen length [m]		-	8.4 ± 0.8	14.5 ± 0.8	20.6 ± 0.8	25.1 ± 0.8	25.9 ± 1.5	33.5 ± 1.5	80.8 ± 4.6
P(tot)	As(tot)	0.000** +	0.000** +	0.000** +	0.000** +	0.490 +	0.000** +	0.000** -	0.336 +
	As(sum)	0.000** +	0.000** +	0.000** +	0.000** +	0.981 -	0.000** +	0.000** -	0.271 +
	Arsenite	0.000** +	0.204 +	0.059 +	0.455 +	0.072 -	0.065 +	0.002** -	0.861 +
	Arsenate	0.000** +	0.071 +	0.111 +	0.318 +	0.036* +	0.858 +	0.022* -	0.299 +
P(sum)	As(tot)	0.000** +	0.000** +	0.002** +	0.002** +	0.061 +	0.001** +	0.783 -	0.112 +
	As(sum)	0.000** +	0.000** +	0.058 +	0.000** +	0.079 +	0.000** +	0.234 +	0.066 +
	Arsenite	0.000** +	0.098 +	0.121 +	0.737 +	0.591 -	0.012* +	0.415 +	0.729 +
	Arsenate	0.000** +	0.216 +	0.077 +	0.059 +	0.056 +	0.920 +	0.058 +	0.070 +
PO4	As(tot)	0.000** +	0.000** +	0.033* +	0.019* +	0.269 +	0.001** +	0.476 -	0.106 +
	As(sum)	0.000** +	0.000** +	0.355 +	0.007** +	0.380 +	0.000** +	0.446 +	0.073 +
	Arsenite	0.000** +	0.139 +	0.126 +	0.792 +	0.218 -	0.505 +	0.582 +	0.729 +
	Arsenate	0.000** +	0.078 +	0.063 +	0.184 +	0.039* +	0.972 +	0.110 +	0.086 +
P(unid)	As(tot)	0.000** +	* temporal variation data for P(unid) probably not reliable due sensitivity variations during AEC-ICP-MS measurements						
	As(sum)	0.000** +							
	Arsenite	0.000** +							
	Arsenate	0.000** +							

		shallow aquifer wells	single wells - seasonal changes						
well name		30, 50, 70, 85, 90 ft	30 ft	50 ft	70 ft	85 ft	90 ft	115 ft	280 ft
mid screen depth ± screen length [m]		-	8.4 ± 0.8	14.5 ± 0.8	20.6 ± 0.8	25.1 ± 0.8	25.9 ± 1.5	33.5 ± 1.5	80.8 ± 4.6
Fe(tot)	As(tot)	0.000** +	0.010* -	0.061 +	0.001** +	0.721 +	0.000** +	0.208 +	0.363 -
	As(sum)	0.000** +	0.058 -	0.277 +	0.027* +	0.438 +	0.005** +	0.658 +	0.407 +
	Arsenite	0.000** +	0.791 +	0.024* +	0.329 -	0.338 +	0.018* +	0.251 -	0.422 +
	Arsenate	0.000** +	0.257 -	0.842 -	0.009** +	0.624 -	0.581 +	0.842 +	0.729 +
Fe(III)	As(tot)	0.000** +	0.422 -	0.212 -	0.759 -	0.896 +	0.000** +	0.842 +	0.079 +
	As(sum)	0.000** +	0.161 -	0.495 +	0.990 -	0.689 +	0.007** +	0.892 +	0.268 +
	Arsenite	0.000** +	0.742 +	0.269 +	0.029* -	0.669 +	0.494 +	0.477 -	0.338 +
	Arsenate	0.000** +	0.669 -	0.006** +	0.000** +	0.785 -	0.035* +	0.445 -	0.548 -
Fe(II)	As(tot)	0.000** +	0.060 -	0.030* +	0.000**+	0.841 +	0.014* +	0.008** +	0.794 +
	As(sum)	0.000** +	0.483 -	0.464 +	0.006**+	0.543 +	0.059 +	0.085 +	0.715 +
	Arsenite	0.000** +	0.971 +	0.078 +	0.841 +	0.711 +	0.025* +	0.983 +	0.926 +
	Arsenate	0.000** +	0.452 -	0.972 -	0.356 +	0.984 -	0.935 +	0.039* +	0.236 +
Mn(tot)	As(tot)	0.000** +	0.153 +	0.087 +	0.690 +	0.031* +	0.019* +	0.060 -	0.672 -
	As(sum)	0.000** +	0.080 +	0.421 +	0.465 +	0.040* +	0.005** +	0.963 +	0.582 -
	Arsenite	0.000** +	0.038* +	0.909 -	0.639 +	0.164 +	0.012 * +	0.576 +	0.673 -
	Arsenate	0.050 +	0.470 -	0.505 -	0.601 +	0.409 -	0.551 -	0.178 +	0.830 -
Mn(II)	As(tot)	0.000** +	0.092 -	0.014* +	0.401 -	0.005** +	0.576 +	0.015* -	0.279 -
	As(sum)	0.000** +	0.068 -	0.025* +	0.658 -	0.007** +	0.113 +	0.221 -	0.408 -
	Arsenite	0.000** +	0.468 +	0.433 +	0.753 +	0.004** +	0.174 +	0.639 -	0.626 +
	Arsenate	0.001** +	0.711 -	0.847 -	0.263 +	0.062 -	0.282 -	0.663 -	0.981 -
NH_4^+	As(tot)	0.000** +	0.016* +	0.454 +	0.579 +	0.148 +	0.020* +	0.848 -	0.004** +
	As(sum)	0.000** +	0.018* +	0.650 +	0.705 +	0.570 +	0.001** +	0.656 +	0.020* +
	Arsenite	0.000** +	0.920 +	0.952 -	0.861 -	0.023* +	0.189 +	0.535 +	0.658 +
	Arsenate	0.000** +	0.148 +	0.245 +	0.858 -	0.058 -	0.714 +	0.833 +	0.833 +
NO_2^-	As(tot)	0.719 -	0.264 -	0.193 +	0.178 -	0.136 +	0.371 +	0.066 -	0.431 +
	As(sum)	0.915 -	0.020* -	0.094 +	0.193 -	0.126 +	0.038* +	0.385 -	0.340 +
	Arsenite	0.067 +	0.896 +	0.968 -	0.108 +	0.062 +	0.000** +	0.334 -	0.732 +
	Arsenate	0.807 +	0.069 +	0.450 +	0.619 -	0.146 -	0.166 -	0.897 +	0.178 +
NO_3^-	As(tot)	0.487 -	0.009** +	0.954 +	0.005** +	0.787 +	0.123 +	0.524 -	0.178 +
	As(sum)	0.407 -	0.026* +	0.264 +	0.027* +	0.609 +	0.163 +	0.660 -	0.312 +
	Arsenite	0.064 +	0.841 +	0.968 -	0.108 +	0.060 +	0.001 **+	0.334 -	0.778 +
	Arsenate	0.861 -	0.157 +	0.450 +	0.619 -	0.141 -	0.260 -	0.897 –	0.160 +

		shallow aquifer wells	single wells - seasonal changes						
well name		30, 50, 70, 85, 90 ft	30 ft	50 ft	70 ft	85 ft	90 ft	115 ft	280 ft
mid screen depth ± screen length [m]		-	8.4 ± 0.8	14.5 ± 0.8	20.6 ± 0.8	25.1 ± 0.8	25.9 ± 1.5	33.5 ± 1.5	80.8 ± 4.6
SO_4^{2-}	As(tot)	0.000**-	0.001**-	0.083 +	0.779 +	0.307 -	0.114 -	0.107 -	0.965 -
	As(sum)	0.000**-	0.001**-	0.028*+	0.906 +	0.689 +	0.067 -	0.582 -	0.593 +
	Arsenite	0.000**-	0.715 -	0.141 +	0.562 +	0.703 +	0.005**-	0.291 +	0.566 +
	Arsenate	0.000**-	0.770 -	0.696 +	0.248 +	0.291 -	0.894 -	0.874 +	0.234 -
DOC	As(tot)	0.000** +	0.018* +	0.090 -	0.152 -	0.810 +	0.958 +	0.000** -	0.008** +
	As(sum)	0.000** +	0.001** +	0.536 -	0.463 -	0.791 +	0.406 +	0.004** -	0.023* +
	Arsenite	0.000** +	0.301 +	0.843 -	0.487 +	0.340 +	0.305 -	0.001** -	0.216 +
	Arsenate	0.000** +	0.535 +	0.899 -	0.858 -	0.379 -	0.462 +	0.014* -	0.257 -
TIC	As(tot)	0.000** +	0.000** -	0.179 -	0.000** -	0.358 -	0.285 +	0.000** -	0.210 +
	As(sum)	0.000** +	0.000** -	0.725 +	0.000** -	0.258 -	0.068 +	0.001** -	0.180 +
	Arsenite	0.000** +	0.433 +	0.673 +	0.684 -	0.075 -	0.637 -	0.001** -	0.624 +
	Arsenate	0.000** +	0.302 -	0.113 -	0.289-	0.692 +	0.545 -	0.000** -	0.328 -
CO_2	As(tot)	0.000** +	0.006** -	0.003** +	0.897+	0.046* +	0.150 +	0.714 +	0.075 +
	As(sum)	0.000** +	0.002** -	0.018** +	0.739 -	0.090 +	0.069 +	0.546 +	0.145 +
	Arsenite	0.001** +	0.099 -	0.371 +	0.606 +	0.191 +	0.015* +	0.435 +	0.318 +
	Arsenate	0.013** +	0.425 +	0.594 +	0.966 -	0.268 -	0.729 +	0.149 +	0.903 +
HCO_3^- (Alkal.)	As(tot)	0.000** +	0.000** -	0.228 +	0.309+	0.101 +	0.000** +	0.000** -	0.072 +
	As(sum)	0.000** +	0.000** -	0.778 +	0.794 +	0.211 +	0.000** +	0.012* -	0.182 +
	Arsenite	0.000** +	0.056 -	0.642 +	0.606 -	0.815 +	0.013 * +	0.043* -	0.157 +
	Arsenate	0.000** +	0.895 +	0.949 +	0.225 +	0.701 +	0.680 +	0.013* -	0.830 -
E_H*	As(tot)	0.000** -	* temporal variation data for redox potential E_H probably not reliable due to sampling methodology, at most it may reflect average depth dependent differences in redox potential between wells						
	As(sum)	0.000** -							
	Arsenite	0.013* -							
	Arsenate	0.005** -							